Design and Control of Resilient Micro-Inverter System

by

Jason Runge

A THESIS SUBMITTED IN PARTIALFULFILMENT OF THE REQUIRMENTS FOR THE DEGREE OF

Masters of Applied Science in Electrical and Computer Engineering

Faculty of Engineering and Applied Sciences
University of Ontario Institute of Technology
Oshawa, Ontario, Canada
February 2016

Acknowledgements

First, I would like to express my profound gratitude to my supervisor Professor Hossam Gabber for his unwavering support. I am privileged to work alongside him and his continual guidance and advice over the course of this work has been invaluable. Always a steady hand and word of encouragement have helped me push forward through the road blocks with this research.

Secondly I would like to express my gratitude and give thanks to all the people in the ESCL lab. Thank you all for your help and support.

Finally, I would like to thank my family and friends for their love, support and encouragement. They have always been there for me, and without them this work would not have been possible.

Abstract

The growing implications of climate change have created an increasing demand for clean and renewable energy sources. Solar photovoltaics (PV) are increasingly popular as an alternative energy source due to the fact that they produce clean and renewable power with zero operating emissions. However, PV industries are facing issues of unreliability and low product life spans for the connected inverters. These issues can hinder the future growth of the industry. The aim of this research was therefore to design a micro-inverter system with improved resiliency for grid connected applications. The thesis is broken into the Inverter phase and the Resiliency phase. The Inverter phase consisted of the design of two inverters: a 300W micro-inverter and a 600W inverter simulated in PSIM. The Resiliency phase focused on the application of the designed inverters into four case studies for improving the resiliency of a PV system. It was found that placing an extra micro-inverter in parallel to the overall system was the most cost effective design with a high efficiency.

Keywords: Micro-Inverter; Micro-Inverter system, Resiliency; Key Performance Indicators; Per Unit Key Performance Indicators, Dual Mode Inverter.

Table of Contents

Acknowledgements i

Abstract ii

List of Figures ix

List of Tables xii

List of Abbreviations and Acronyms xiii

Nomenclature xv

Chapter 1: Overview 1

1.1 Introduction 1

1.1.1 Solar Sector Growth 1

1.1.2 Solar in Canada 2

1.2 Problem Statement 4

1.3 Research Objectives 4

1.4 Project Organization 5

1.5 Design Requirements of Micro-inverter 6

1.6 Design Requirements of Control System 6

Chapter 2: Literature Review 7

2.1 History of the Inverter 7

2.2 Micro-Inverter History 7

2.2.1 Evolution of PV Inverters 7

2.2.2 Single Stage Inverters 8

2.2.3 Two Stage Inverters 9

2.3 Inverter Overview 10

2.3.1 Overview 10

2.3.2 Inverter Classifications 11

2.4 Inverter Control Strategies 11

2.5 Grid Synchronisation - Phase Locked Loop 12

2.6 Key Performance Indicators Background Theory 14
2.6.1 Introduction 14
2.6.2 Performance KPI 15
2.6.3 Economic KPI 16
2.6.4 Per-Unit KPI 17
Chapter 3: Thesis Framework and Methodology 21
3.1 Thesis Framework 21
3.1.1 Data Collection 22
3.1.2 Design of a 300W inverter 22
3.1.3 Design of a 600W inverter 22
3.1.4 Inverters Analysis 22
3.1.5 Development of Micro-Inverter System 22
3.1.6 Development of Micro-Inverter System Performance Criteria 23
3.1.7 Design of the Resiliency Controller 23
3.1.8 Design of Resiliency Cases 23
3.1.9 Analysis of Case 23
3.2 Methodology 24
3.2.1 Inverter Design Methodology 24
3.2.2 Resiliency Case Design Methodology 25
3.2.3 Resiliency Evaluation Methodology 26
Chapter 4: Single Phase Inverter Circuit Design 28
4.1 Circuit Block Overview 28
4.2 Solar Panel Used 28
4.2.1 Governing Equations 30
4.3 DC-DC Converter Sub-circuit Design 31
4.3.1 Introduction DC-DC Converters 31
4.3.2 Boost Converter Need 31

4.3.3 Modes of Operation 33
4.3.4 Governing Equations 34
4.3.5 PSIM MODEL 36
4.4 DC Link 37
4.4.1 Purpose 37
4.4.2 Power Decoupling 37
4.4.3 2nd Order Harmonics 38
4.4.4 Sizing 38
4.5 Inverter Topology Sub-circuit Design 40
4.5.1 Inverter Operation Introduction 40
4.5.2 PSIM MODEL 41
4.6 SPWM Design 42
4.6.1 Overview 42
4.6.2 SPWM 42
4.6.3 PSIM MODEL 42
4.7 Filter Sub-circuit Design 43
4.7.1 Overview 43
4.7.2 Inverter Need 43
4.7.3 Topologies 44
4.7.4 Governing Equations 45
4.7.5 PSIM MODEL 47
4.8 Over/Under Voltage Protection Sub-circuit Design 48
4.9 Maximum Power Point Tracking Control Loop Design 50
4.9.1 Purpose 50
4.9.2 Choice in Method 51
4.9.3 PSIM Model 51
4.10 Grid Synchronisation -Phase Locked Control Loop Design 53

4.10.1 Overview 53
4.10.2 Operational Theory 53
4.10.3 PSIM MODEL 54
4.10.4 PSIM MODEL with SPWM 55
4.11 300W Overall Circuit Design 56
4.11.1 PSIM Circuit Design 56
4.11.2 Components 56
4.11.3 Results 58
4.12 600W Overall Circuit Design 63
4.12.1 Circuit Design 64
4.12.2 Components 64
4.12.3 Results 65
4.13 Inverter Analysis KPI 68
4.13.1 300W 68
4.13.2 600W 69
Chapter 5: Micro-Inverter System Resiliency Designs 71
5.1 Case 0: Micro-Inverter System 71
5.2 Resiliency Methodologies 72
5.2.1 Need 72
5.2.2 Assumptions 72
5.3 Resiliency Controller Design 73
5.3.1 Resiliency Controller Requirements 73
5.3.2 Resiliency Controller Circuit Design 73
5.4 Simulation Faults 74
5.5 Case 1: Two 300W Inverters Paired Inside Single Inverter Unit 75
5.5.1 Overview Block Diagram of 1.2kW system 75
5.5.2 Operational Theory Single 300W Inverter 75

5.5.3 Circuit Design 77
5.5.4 Results 77
5.6 Case 2: Extra 300W Micro-inverter in Parallel to Micro-Inverters 82
5.6.1 Overview Circuit Block Diagram of 1.2 kW Inverter 82
5.6.2 Operational Theory for 600W system 83
5.6.3 Circuit Design 83
5.6.4 Results 85
5.7 Case 3: Back up 600W inverter inside Paired Micro-Inverters 90
5.7.1 Overview Circuit Block Diagram of 1.2kW system 90
5.7.2 Operational Theory for 600W system 90
5.7.3 Circuit Design 91
5.7.4 Results 92
5.8 Case 4: Dual Mode Inverters 97
5.8.1 Overview Circuit Block Diagram of 1.2kW system 97
5.8.2 Operational Theory for 600W System 98
5.8.3 Dual Mode Inverter Design 99
5.8.4 Circuit Design 103
5.8.5 Results 103
Chapter 6: Results 109
6.1 Motivation 109
6.2 Assigning Weights 109
6.3 Summary of Resiliency KPU 109
6.4 Calculating and Mapping of PU-KPI 111
6.4.1 Resiliency Power Coverage 112
6.4.2 Efficiencies 112
6.4.3 Response Time 113
6.4.4 THD 113

6.4.5 Economics 114
6.5 Governing Equation and Design Choice 115
Chapter 7: Applications 116
7.1 Micro Energy Grid 116
7.2 Solar Panel Windows 117
Chapter 8: Conclusions and Future Work 119
8.1 Motivation 119
8.2 Summary and Conclusions 119
8.3 Innovative Contributions for the Thesis Work 120
8.3.1 Literature Review 120
8.3.2 Inverter Design 120
8.3.3 Micro-Inverter System 120
8.4 Future Work 121
8.4.1 Experimental Design within MEG 121
8.4.2 Reliability improvements to micro-inverter 121
8.4.3 KPI Improvements 121
Bibliography 122

List of Figures

Figure 1-1: PV Worldwide Installed Capacity [1] 1
Figure 1-2: Projected PV Worldwide Capacity [1] 2
Figure 1-3: Trend for PV Installations across Canada [2] 3
Figure 1-4: Provincial Install PV Power 2014 [4] 3
Figure 2-1: First Generation PV Systems 8
Figure 2-2: Two Stage Inverter 9
Figure 2-3: Inverter Block Diagram 10
Figure 2-4 Inverter Control Strategies 12
Figure 2-5: PLL Overview [27] 13
Figure 2-6: KPI Overview 14
Figure 3-1: Thesis Framework 21
Figure 3-2: Inverter Methodology 24
Figure 3-3: Resiliency Case Design Methodology 25
Figure 3-4: Evaluation Methodology 26
Figure 4-1: Inverter Overview 28
Figure 4-2: Solar Panel Data Ecilpsall NRG72 [38] 29
Figure 4-3: I-V Curve NRG72 300M Solar Panel [37] 30
Figure 4-4: Boost Converter Initial Start Up 32
Figure 4-5: Boost Converter Switch Mode 32
Figure 4-6: Boost Converter Closed Switch Mode 33
Figure 4-7: Modes of Operation Boost Converter 34
Figure 4-8: Boost Converter Feedback 35
Figure 4-9: Boost PWM generated 36
Figure 4-10: PSIM Boost Converter Design 36
Figure 4-11: H-Bridge 40
Figure 4-12: H-bridge Operation 41
Figure 4-13: PSIM Model H-Bridge 42
Figure 4-14: SPWM PSIM MODEL 43
Figure 4-15 Filter Model 45
Figure 4-16 Iterative Filter Design [48] 47
Figure 4-17: PSIM LCL Filter 47
Figure 4-18: Frequency Analysis of Filter 48

Figure 4-19: Over-Voltage Protection Circuit 49
Figure 4-20: Over-Voltage Protection Working 49
Figure 4-21 PSIM's MPPT Model 52
Figure 4-22: PLL Mathematical Model as [33], [34] 54
Figure 4-23: PSIM PLL Model 55
Figure 4-24: PSIM PLL Model with SPWM 55
Figure 4-25: 300W Micro-Inverter PSIM Model 56
Figure 4-26: 300W Micro-inverter Solar Panel Input 58
Figure 4-27: 300W Boost Converter 59
Figure 4-28: 300W Boost Converter Switching Loss 59
Figure 4-29: DC Link Voltage 60
Figure 4-30: 300W Inverter SPWM 60
Figure 4-31: SPWM with reduced firing rate 61
Figure 4-32: 300W Inverter Output 62
Figure 4-33: Transient Phase Synchronization 62
Figure 4-34: 300W Inverter Voltage Control 63
Figure 4-35: 600W Inverter Design 64
Figure 4-36: 600W Inverter Solar Panel Output 66
Figure 4-37: 600W Boost Converter 66
Figure 4-38: 600W Boost Converter Switching losses 67
Figure 4-39: 600W DC Link Voltage 67
Figure 4-40: 600W Inverter Output 68
Figure 5-1: Micro Inverter System Design [56] 71
Figure 5-2: Control Circuit for Resiliency 73
Figure 5-3 PSIM Fault 74
Figure 5-4: Case 1 Overview 75
Figure 5-5: Case 1 Operational Theory 76
Figure 5-6: Case 1 PSIM Model 77
Figure 5-7: Case 1 Results for system working under normal operation 78
Figure 5-8: Case 1 Micro-inverter 1 Failure 79
Figure 5-9: Case 1 System Output 80
Figure 5-10: Case 2 Overview 82
Figure 5-11: Case 2 Operational Theory 83
Figure 5-12: Case 2 PSIM Model 84

Figure 5-13: Case 2 Results for system working under normal operation 85
Figure 5-14: Case 2 Micro-inverter 1 Failure 86
Figure 5-15: Case 2 Micro-inverter 2 Failure 87
Figure 5-16: Case 2 Switching time 88
Figure 5-17: Overview Case 3 90
Figure 5-18: Case 3 Operational Theory 91
Figure 5-19: Case 3 PSIM Model 92
Figure 5-20: Case 3 Normal Operation 93
Figure 5-21: Case 3 Micro-inverter 1 Failure 94
Figure 5-22: Case 3 Micro-inverter 2 Failure 94
Figure 5-23: Case 3 Control Time 95
Figure 5-24: Case 4: Overview 97
Figure 5-25: Case 4: Operational Theory 98
Figure 5-26: Case 4 Boost Converter 99
Figure 5-27: Case 4 H-Bridge 100
Figure 5-28: Case 4 Filter 100
Figure 5-29: Case 4 PSIM Model 103
Figure 5-30: Case 4 Normal Operation 104
Figure 5-31: Case 4 Inverter 1 Failure 105
Figure 5-32: Case 4 Inverter 2 Failure 106
Figure 5-33: Case 4 Control Time 107
Figure 6-1: KPI Efficiency vs. Case 110
Figure 6-2: KPI PP vs. Case 110
Figure 6-3: PU-KPI Resiliency Power Coverage 112
Figure 6-4: PU-KPI Efficiency 112
Figure 6-5: PU-KPI Response time 113
Figure 6-6: PU-KPI THD 114
Figure 6-7: PU-KPI Economics 114
Figure 7-1: MEG 116
Figure 7-2: Building in Toronto 117

List of Tables

Table 4-1: Filter Topologies Advantages and Drawbacks 44
Table 4-2: 300W Inverter Bill of Materials [55] [56] 57
Table 4-3: 600W Inverter Bill of Materials [55], [56] 65
Table 4-4: KPI Analysis 300W micro-inverter 69
Table 4-5: Micro-inverters in Marketplace 69
Table 4-6: KPI Analysis 600W inverter 70
Table 4-7: Comparison of 600W Inverters 70
Table 5-1: Case 1 Extra Components [55] [56] 80
Table 5-2: Case 1 KPI 81
Table 5-3: Case 2 Extra Components [55] [56] 89
Table 5-4: Case 2 KPI 89
Table 5-5: Case 3 Extra Components [55] [56] 96
Table 5-6: Case 3 KPI 96
Table 5-7: Dual Mode Inverter Components [55] [56] 102
Table 5-8: Case 4 Extra Components [55] [56] 107
Table 5-9: Case 4 KPI 108
Table 6-1: Weights 109
Table 6-2: KPI Summary Table 111
Table 6-3: PU-KPI Summation 115

List of Abbreviations and Acronyms

Acronym	Definition
MEG	Micro-energy-grid
mΩ	milli Ohms
µF	micro Farad
AC	Alternating Current
AWG	American Wire Gauge
CAN	Canadian Dollar
CSI	Current source Inverter
D	Change rate of the errors
DC	Direct Current
ESR	Equivalent series resistance
I	Integral past value errors
I	Current in Direct Current
IC	Incremental Conductance MPPT method
IEEE	Institute of Electrical and Electronics Engineers
IEEE - 1547	Standard for Interconnecting Distributed Resources with Electric Power Systems
Irms	Current in Alternating Current expressed as Root Means Square
KPI	Key Performance Indicators
kW	Kilo watts
MG	Micro-grid
mH	milli Henry
MPPT	Maximum power point tracking
ms	milliseconds
P	Present value errors
P	Power
P&O	Perturb and Observe MPPT method
PI	Proportional Integral Controller
PID	Proportional, Integral and Derivative Controller
PLL	Phase Locked Loop
PSIM	Powersim
PU-KPI	Per Unit KPI
PV	Photovoltaic Solar
PWM	Pulse Width Modulation
PP	Payback Period
SPWM	Sine Pulse Width Modulation
THD	Total Harmonic Distortions

V	Voltage in Direct Current
VCO	Voltage Controlled Oscillator
Vrms	Voltage in Alternating Current expressed as Root Means Square
VSI	Voltage source Inverter
W	Watts

Nomenclature

Symbol	Definition
η	Efficiency
P_{out}	Power output to micro-inverter
P_{in}	Power input to micro-inverter
$P_{Loss\ DC\ Link}$	Power losses in the DC link
$P_{loss\ boost\ converter}$	Power losses in the boost converter
$P_{loss\ H\text{-}Bridge}$	Power losses in the H-bridge
$P_{loss\ filter}$	Power Losses in the filter
$t_{v\text{-}response}$	Length of time above/below the IEEE standard
$t_{v\text{-}stopped}$	Time over/under voltage stopped
$t_{v\text{-}started}$	Time over/under voltage started
Initial Cost	Initial cost for the inverter
System Cost	Initial cost for the micro-inverter system
$Income_{yearly}$	Yearly income generated from the micro-inverter/system
PVP	Photovoltaic potential
PP	Payback Period
j	The number of PU-KPI
n	Total number of PU-KPI
a_j	Weighting factor assigned to PU-KPI
T_{respon}	Total length of time for resiliency measures to be deployed
$T_{res\ deploy}$	Time at which resiliency measure was deployed
$T_{failure\ detected}$	Time at which failure was detected
$I_L(0)$	Initial inductor current in boost converter
V_{in}	Voltage applied to inductor in boost converter
$i_L(t)$	Current through inductor in the boost converter
V_0	Voltage output boost converter
D	Duty cycle of boost converter
ΔV_0	Output voltage ripple of the boost converter
L_{min}	Minimum inductance for boost converter (continuous to discontinuous mode)
C	Capacitor for boost converter
f	Switching frequency for boost converter
L_{op}	Operational lifetime
$L_{op}(0)$	Specified operational lifetime at hotspot temperature
T_h	Operating temperature
ΔT	Change in temperature
$v_g(t)$	Grid voltage (2nd Order Harmonics)
$\hat{V}_g$	Amplitude of grid current
ω_g	Grid angular frequency
$i_g(t)$	Grid current
$\hat{I}_g$	Amplitude of grid current
ϕ	Phase angle of grid current
$P_{out}(t)$	Instantaneous Power output from the grid
S	Apparent power

I_{dc}	DC component of voltage applied to DC Link
$i_{dc,ripple}(t)$	AC component of voltage applied to DC Link
C_{decoup}	Capacitor DC link size
ω_{res}	Filter resonant frequency
L	Total Filter Inductance
V_{dc}	Voltage DC link
I_{rated}	Rated utility is current
Δ_{ripple}	Maximum ripple percentage (5-25%)
f_s	Switching frequency of SPWM
m_a	Modulation index
a	Inductance index
σ	Switching harmonic current attenuation ratio
Δ_{ripple}	Maximum ripple magnitude percentage
V_{rated}	Rated utility voltage
ω_0	Utility angular frequency
C_f	Capacitor for inverter output filter
R_3	Damping resistor for inverter output filter
v_{in}	Input sine wave to PLL
U_M	Amplitude of input sine wave to PLL
v_{sync}	Output synchronized wave to PLL
$PU\_KPI_{Resnse\ Time}$	Ratio of IEEE standards for clearing to the Micro-inverter system
$PU\_KPI_{Res\ Power\ Coverage}$	Ratio of resiliency measure to cover power output
$PU\_KPI_{E\ N\ to\ F}$	Ratio of maximum efficiency under normal operation to operation under fault
$PU\_KPI_{E\ Case\ to\ Case}$	Ratio of maximum efficiency from system with no resiliency measures to system with resiliency measure deployed
PU_KPI_{THD}	Ratio of THD under normal operation to THD operation under fault
$PU\_KPI_{THD\ Case\ to\ Case}$	Ratio of THD from system with no resiliency measures to system with resiliency measure deployed
$PU\_KPI_{Initial\ Cost}$	Ratio of Initial Cost for system with no resiliency measures to system with resiliency measure deployed
PU_KPI_{PP}	Ratio of PP from system with no resiliency measures to system with resiliency measure deployed

Chapter 1: Overview

1.1 Introduction

There is a growing demand for renewable energy systems based on the mounting effects of global climate change. Solar energy generation, specifically photovoltaic (PV) is an attractive option because it diversifies the energy generation portfolio and exhibits no emissions during operation. The following section outlines an overview of the current trends of PV in the worldwide and Canadian market.

1.1.1 **Solar Sector Growth**

The increasing evidence and effects of climate change have created a rising demand for cleaner, greener and more renewable sources of energy generation. This demand was created in order to offset and reduce the reduction of greenhouse gas emissions caused by traditional energy generation sources, such as fossil fuels. PV energy generation is one of the most promising emerging technologies which has seen a significant emergence worldwide over the past decade.

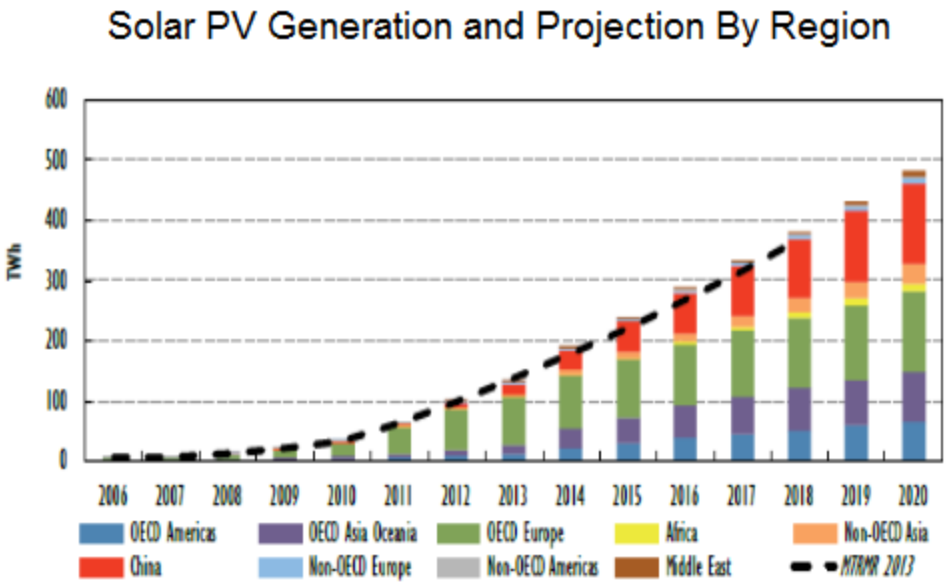

Figure 1-1: PV Worldwide Installed Capacity [1]

Figure 1-1 shows the cumulative worldwide installed capacity for PV in TWh from the International Energy Agency (IEA). Europe, Asia-Pacific, and North America have significantly increased their generation capacities of PV since 2005.

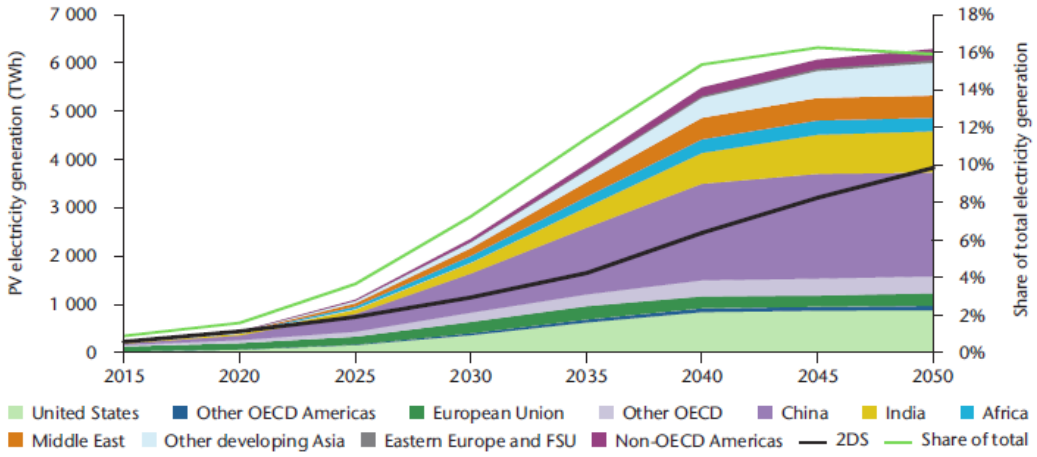

Figure 1-2: Projected PV Worldwide Capacity [1]

Figure 1-2 depicts the projections made by the IEA for the worldwide installed PV capacity from 2015 to 2050. The industry is projected to have continued growth over the next few decades. The growth is expected to increase drastically in 2025, specifically in China and India with significant increases also seen in the Middle East and the United States. This increasing trend is attributed to the falling costs of PV panels, inverters, increasing system efficiency, and the increasing energy demand. In mature PV markets competition is already quite competitive. However, the increasing trends are backed by government legislation and subsidies. With this support, the PV market will see the continued increase of PV electricity generation capacity.

1.1.2 **Solar in Canada**

In Canada, solar PV has become one of the more favorable renewable energy technologies due to its social, economic, legislative, and incentive factors. This includes the federal, provincial and municipal plans to reduce carbon emissions output. Government incentives and rebates programs have made purchasing and installing PV systems economically affordable which has contributed significantly to its gain in deployment.

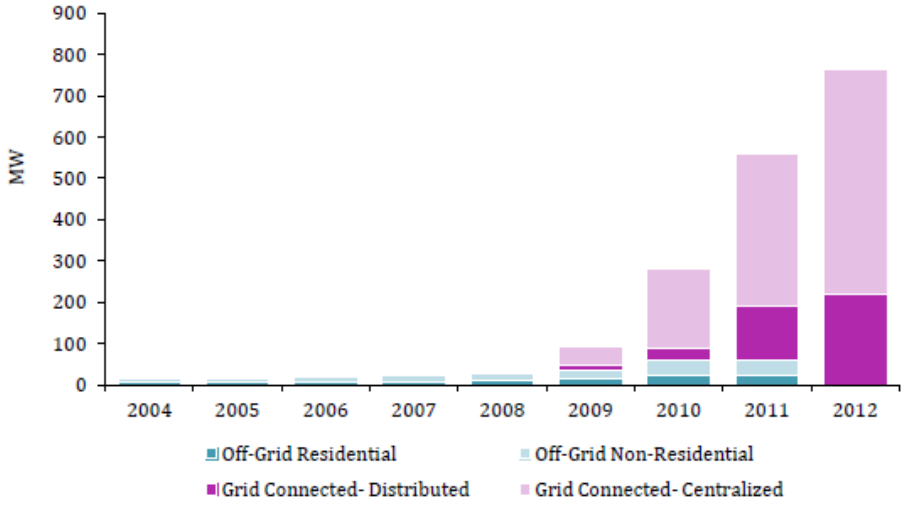

Figure 1-3: Trend for PV Installations across Canada [2]

Since 2009, Canada's PV installations has been increasing steadily every year. This was largely a result of the provinces beginning to implement programs and incentives starting from 2008/2009. These programs, made PV economically viable for citizens. For example, in 2008 the Ontario's government launched its incentive and feed-in-tariff program aimed at the increase of the provinces' generation capacities for renewable energy sources [3]. As a result of these government incentive programs, the PV deployment has gradually been increasing across all of Canada.

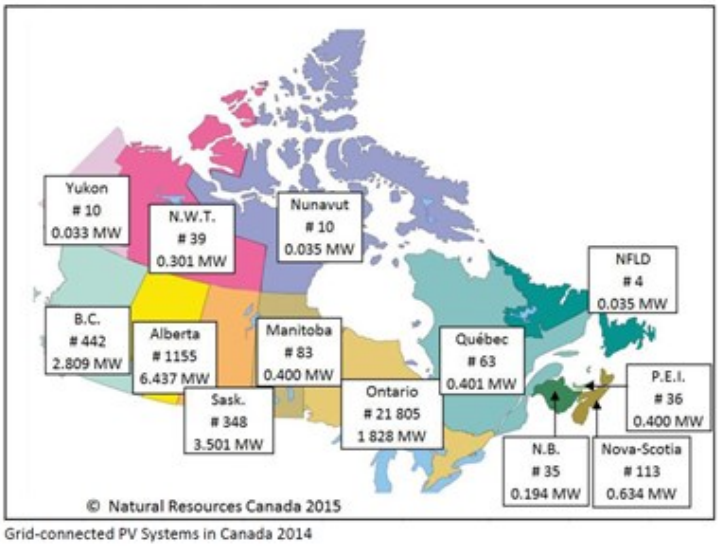

Figure 1-4: Provincial Install PV Power 2014 [4]

Figure 1-4 depicts the installed PV capacity throughout the Canadian Provinces and Territories for 2014. The largest outputs come from Alberta, Saskatchewan, British Columbia and Ontario. In 2013, the Ontario provincial government announced its long term energy plan. It stated that the provincial government will target to deploy 50MW/year for the micro-fit program [3]. It was also stated the Ontario government will target to reach an overall goal of 3% of its total capacity in Ontario from solar PV [3], from the current installed capacity of approximately 1% [3]. Therefore, it can be expected that the trend of Figure 1-3 will continue to increase as provinces continue to back PV incentives programs.

1.2 Problem Statement

A key factor in the long term success of the PV industry is the confidence in the reliability of the system [5]. For PV systems, the two largest expenses are attributed to the costs of the inverters and the solar panels. Inverter prices have been dropping by about 10% for every doubling of cumulative production, while PV modules have been dropping by about 20% for the same amount [5].

The reliability and low product life spans have remained issues to date within the industry. For a PV system, inverters are the most common cause of failure in the field [5], [6]**.** These issues have the potential to damage the reputation of the entire industry and could possibly hinder the future growth of the industry. Despite this, the industry's main focus has been on lowering the price the inverters and improving their overall efficiency [5]**.** Given this focus, the long term reliability and resiliency of an inverter system has not yet been fully developed. The United States Department of Energy (DOE) is currently working with Sandia National Laboratories in the development of accelerated inverter testing protocols and standards for reliability. Unfortunately, to date no standards for inverter reliability exist [5] and system resiliency is rarely discussed at all.

This indicates a growing need for the development of reliable inverters and resilient inverter systems. Enhancing the robustness and performance of PV systems will aid and support the continued penetration of solar energy into the electricity grid and will lead to the overall success of the industry [6].

1.3 Research Objectives

The target of this thesis is to design a micro-inverter system with improved resiliency. To achieve such goal, the following objectives are identified:

- Design micro-inverter
- Design of the micro-inverter system
- Design and evaluate control mechanisms for resilient micro inverter systems
- Evaluate micro-inverter system resiliency strategies

The detailed tasks of this thesis are as follows:

- Design of a 300W micro-inverter
- Design of a 600W inverter
- Evaluation of inverters
- Design of the micro-inverter system
- Development of the micro-inverter system performance criteria
- Design of a resiliency controller for micro-inverter systems
- Development and design resiliency case studies
- Evaluation of resiliency control strategies using performance criteria

1.4 Project Organization

The following section organizes the main topics of this thesis and provides on overview of each chapter.

Chapter 1 provides an overview for the thesis with the current state of the industry, problem statement, research objectives, and design requirements.

Chapter 2 provides a brief background of the single phase grid connected inverter. A literature review is completed on the PV inverter, PV system configurations, traditional control strategies, and system evaluation metrics.

Chapter 3 provides the thesis framework along with the design methodologies used.

Chapter 4 provides the design of the inverters sub-circuits and control circuits. In addition it shows the final design for the 300W micro-inverter and the 600W inverter along with an analysis of both inverters.

Chapter 5 first describes the base micro-inverter system. The resiliency controller and simulation faults are then described. Following this, the chapter then explores the different resiliency methodologies through case studies.

Chapter 6 provides the overall results for the different resiliency strategies. These result are then applied to the proposed evaluation method to identify the best resiliency strategy.

Chapter 7 demonstrates several industry applications to resilient inverters.

Chapter 8 provides the conclusion and recommendations for the thesis. In addition, the highlights and contributions of this thesis are listed.

1.5 Design Requirements of Micro-inverter

In order to begin, the design requirements are first listed for the micro-inverter. These requirement consists of both customer and engineering requirements.

- Must be able to handle up to 300W loads
- 20-50 VDC input
- Output 120Vrms, 60 Hz single phase power
- Grid Connected capability
- Over and Under Voltage Protection
- Must have a THD of $< 5\%$
- Overall DC-AC efficiency of greater than 95%

1.6 Design Requirements of Control System

Secondly, the requirements for the micro-inverter system are listed below. As with Section 1.5, these are also a combination of both customer and engineering requirements.

- Ability to recognize fault in an inverter system
- Ability to reconfigure inverter and/or the system design in the event of an inverter fault
- Lowest Cost
- High efficiency
- Quick response time.
- Complies with grid standards

Chapter 2: Literature Review

This chapter provides an overview for an inverter. First, the general history of inverters is provided along with the industry history for PV. Next, an overview of the inverter is provided along with traditional control strategies and grid synchronisation techniques. This chapter ends with the description of the performance measurement tools used to evaluate the inverters and the micro-inverter system.

2.1 History of the Inverter

In essence, inverters are electronic devices which convert direct current (DC) into alternating current (AC) [7]. There are many different types and applications for inverters from single phase types feeding off grid appliances, to polyphase (multiple phases) and motor drives, etc.

No one knows the exact origins of the word inverter with absolute certainty. David Prince is the person who is most likely credited with coining the term [8]. In 1925, Prince published an article in the GE review titled "The Inverter" [8] . In this article, Prince explained how he took the rectifier circuit and inverted it, taking in DC current and outputting AC current. By 1936, Princes' term inverter had spread throughout the world and became a term that is still commonly usage [8]. Originally, rotary converters were manufactured until the 1950's which would transform the DC into AC, these were commonly referred to as "inverter rotaries" [7]. However in the 1950's, semiconductor technology began to emerge and quickly replaced the inverter rotaries. Today, the IEEE defines inverters as "a machine, device, or system that changes direct-current power to alternating-current power" [7].

As stated above, the IEEE classifies inverters as a broad range of devices that converters DC to AC. As a result of this board range, there are many different classifications of inverters and inverter designs. The evolution of PV inverters will be further discussed in the next section which provides an overview of a sub-section within this board range.

2.2 Micro-Inverter History

2.2.1 Evolution of PV Inverters

In order to connect a PV unit to the grid, a system is needed in order to convert the DC power generated from the solar panel into AC. Typically inverters are categorized based on their number of power stages and source types [9]. First generation PV systems used a single centralized inverter configuration with a single power stage. More recently, industry focus has shifted to using smaller decentralized inverters with multiple power stages. A general summary of the evolution of PV systems and their configurations are described in [10].

2.2.2 **Single Stage Inverters**

First generation grid connected PV systems commonly dominated the market place in the past [10]. This generation of inverters are commonly referred to as centralized single stage inverters [10]. These systems normally consisted of a single power stage (the inverter) and had the solar panels modules oriented into a series string configuration as shown in Figure 2-1 below.

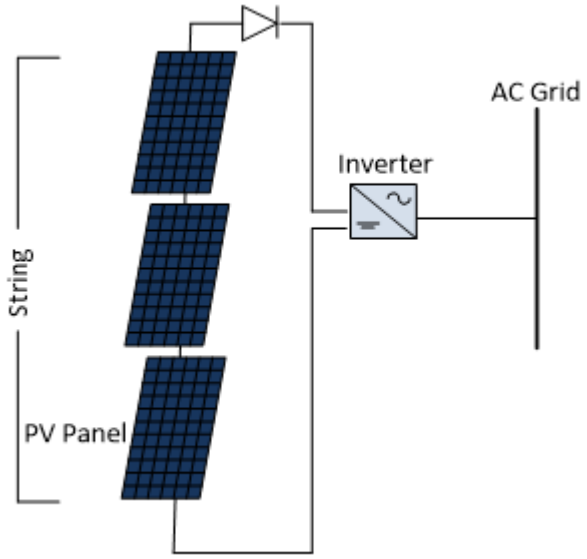

Figure 2-1: First Generation PV Systems

In order for this system to work, the PV panels were arranged in a series connection along with a string diode to protect the panels from back-current. Multiple panels were needed to be placed in strings in order to increase the voltage to appropriate high levels for grid connection. Several strings could then be placed in parallel with one another to reach the desired power output levels, not exceeding inverter power limitations. Maximum Power Point Techniques (MPPT) later became incorporated into the design in order to maximize solar output. Unfortunately, this generation of system suffered from many drawbacks: high current DC cables were needed, reduced efficiency of overall system due to single panel, overall system efficiency loss due to degradation factors, efficiency losses due to string diodes, power losses due to a centralized MPPT, and large harmonics [10]. One of the most significant problems was the need to have many PV panels in a single series string in order to reach the required voltage levels. For example, in order to meet European standards approximately 16 PV panels needed to be connected in a series string (using 45V per panel to reach 720Vrms) [10]. This made the systems expensive with many different ways for the efficiency to be decreased. For instance, if shading occurred on a single panel within the string then the

entire systems output would be reduced to that of the shaded PV panel, reducing the entire system's efficiency. Another example is when a manufacturing defect occurred in a solar panel which would limit the current of the overall system and again result in a lower efficiency.

2.2.3 **Two Stage Inverters**

In order to improve the efficiency of the overall system, a second generation of systems began to emerge. These are known as two stage inverter systems and consist of putting an extra power stage before the inverter stage. Furthermore, the solar power modules are oriented into a parallel configuration rather than string. The additional power stage within the circuit consists of a DC/DC converter implemented in order to amplify the voltage for the inverter power stage. There are many benefits to this topology, such as improved systems efficiency, lower THD, and a reduction in circuit size by removal of bulk transformers [10]. This configuration allows MMPT to be added to each panel for optimization of output power. Overall system efficiency is improved as shading or manufacturing defects of a single panel no longer restrict the output of other solar panels in the system. Figure 2-2 shows two ways the additional power stage can be integrated into the overall circuit design for second generation systems.

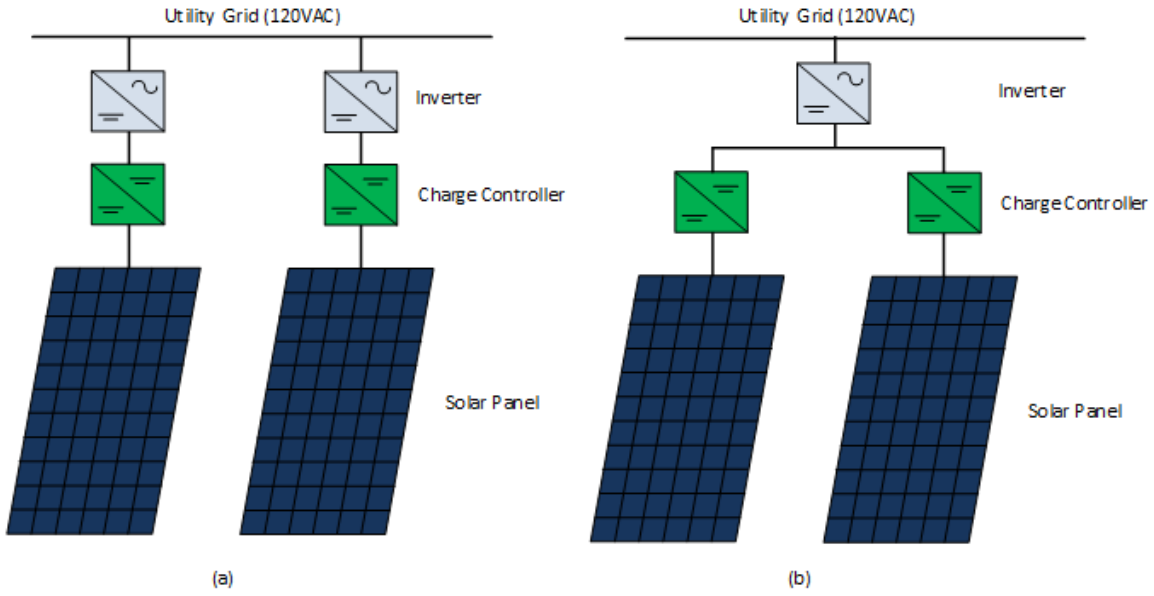

Figure 2-2: Two Stage Inverter

Figure 2-2 (a) shows each solar module with its own dual power stages. Figure 2-2 (b) shows each solar panel being given its own primary power stage and at the second power stage they are coupled together.

For the purposes of this thesis, the two stage inverter is being used with both (a) and (b) explored as ways to increase the resiliency of the overall system.

2.3 Inverter Overview

2.3.1 **Overview**

Grid connected inverters need control systems in order to synchronize voltage and current outputs to that of the grid. In addition, control systems are needed in order to ensure that correct voltages are fed into the grid complying with IEEE standards and regulations. IEEE standard 1547 provides the requirements for distributed energy systems and states that distributed sources (such as PV) must be within the tolerance of 120Vrms <|5%| along with <5% THD [11]. The challenges in connecting to the grid are ensuring that the outputs are synchronized and with low Total Harmonic Distortions (THD's). The problem is that at times, the grid current can fluctuate in non-linear manners. There are many reasons why this may happen, an example of this is a non-linear load such as rectifier circuit being attached/disconnected to the grid. In addition to the having to synchronise to a non-linear output, the input source also behaves non-linearly. The sources for inverters, PV, are often changing in non-linear manners due to weather conditions: temperature, cloud cover, time of year, angle, etc. [7].

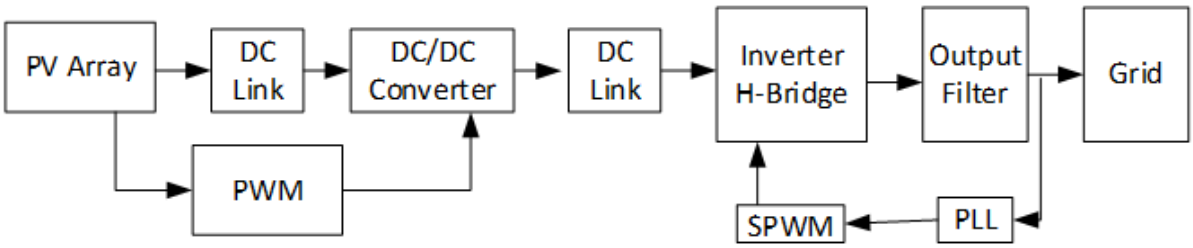

Figure 2-3: Inverter Block Diagram

Figure 2-3 above shows a block diagram for a typical micro-inverter system. A few of the essential control loops for the circuit as also shown in the figure. Inverter control loops are not limited to the ones shown above and there exist a variety of other loops as well which can apply for such things as output filter control, output current control, power factor correction control and many others. The control loops indicated in the above figure are used for couple of reasons. First, to ensure that the output regulations are being met. Secondly, to have the system outputting as much power to the grid as possible.

Traditionally PD, PI, and PID controllers have been the most popular types of controllers used in power electronics. But in recent years, non-linear controllers have become increasingly popular as they are allowing systems to become more intelligent, improved performance characteristics and becoming

economically feasible. A fuzzy logic controller is an example of a type of nonlinear controller which has become successfully integrated with the inverter; their studies have shown many benefits for enhancing performance characteristics over a wide range of inverter applications [12], [13], [14], [15], [16], [17], [18], [19], [20].

2.3.2 **Inverter Classifications**

There are many ways to classify inverters. These can be based on a variety of things from output power, size, topologies, control structures, types, and applications. Of all the different classifications, usually the type of inverter is first used in order to classify inverters. This refers to the type of input power sources for the inverter, which then reflects to the type of components used in the inverter. Since practical sources for electronics (batteries, solar panels, etc.) can provide either a constant current or a constant voltage, inverters are typically classified into which source is supplying the power. This then breaks the inverters into two main classification types: the voltage source inverter (VSI) and the current source inverter (CSI) [21] [22]. For the case of this work, solar panels are being used. Therefore the micro-inverter designed is a voltage source inverter.

A second important classification for inverters relates to the power output of the device. Typically inverters are defined according to the follows classification:

Large: >100kW
Medium: 100kW to 10kW
Small: 10kW<

Typically, micro-inverters are a sub classification of the small inverter classification and range in output power of 100W to 350W. This is the typical range of output power for a single solar panel module.

2.4 Inverter Control Strategies

Traditionally, inverters are controlled by a Pulse Width Modulation (PWM) strategy [23]. PWM involves the turning of switches on and off multiple times per half cycle in order to produce a periodic output waveform. PWM strategies are not limited solely to inverters and are widely utilised throughout a variety of applications. This is due to their effectiveness and low THD outputs, reduced power losses, and ease of generation and deployment [23].

Present day available PWM schemes can be broadly classified into either: Sinusoidal PWM (SPWM) and non-sinusoidal PWM. If switching losses are not a major concern (a few kHz is acceptable), then SPWM methods and offshoots are very effective at controlling the inverter [24]. This is because the generated harmonics are beyond the bandwidth of the system and therefore are not dissipating a significant amount of power losses [24]. However, at higher switching frequencies other methods such as space-vector

technique or selective harmonic elimination technique are more beneficial. For the purposes of this design, lower switching frequencies will be used and therefore SPWM will be implemented.

In SPWM, two signals are compared against one another. A modulating reference (sinusoidal) signal and a carrier wave (triangular) signal. Pulses are generated by comparing the two different signals against one another, and then used to trigger the switches within the inverter power stage. The width of each pulse can be varied in portion to the amplitude of the sine wave. The frequency and phase of the reference signal determines the inverter's output frequency and phase.

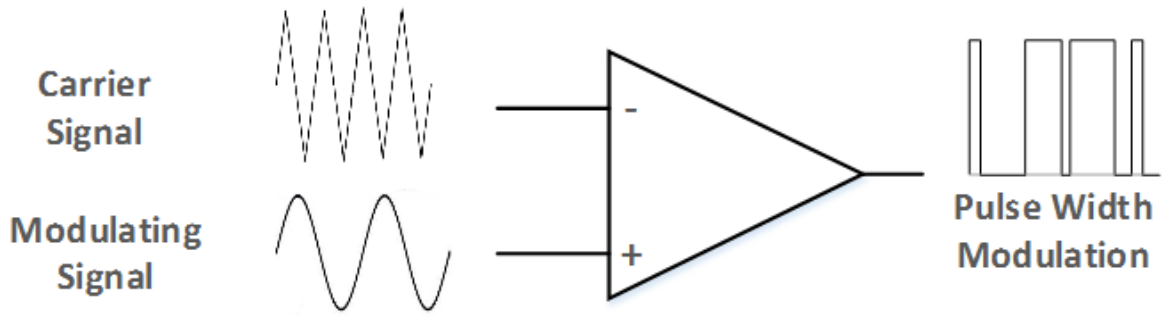

Figure 2-4 Inverter Control Strategies

Figure 2-4 above shows the general graphical representation of the SPWM technique. Of SPWM, there are two main types: unipolar and bipolar. Bipolar switching is simple to use and implement. In addition, it has low distortions and switching losses [25]. Unipolar, is more complex to implement, however it has reduced switching losses and generates less EMI.

2.5 Grid Synchronisation - Phase Locked Loop

In order to synchronize with the grid, a specialized control system is needed. A phase locked loop (PLL) is a control system that was originally published by Appleton in 1923 and Bellescize in 1932 [26]. The original concept was designed to be used for radio signals. However, the control system quickly became popular and spread to a variety of industries and applications: communication systems, motor controls, inverters, clocks, multiprocessors, et cetera.

In brief, a phase lock loop is a closed loop feedback system which generates an output signal in relation to the frequency and phase of the inputted reference signal. This is done by raising or lowering the frequency of the voltage controlled oscillator within the circuit.

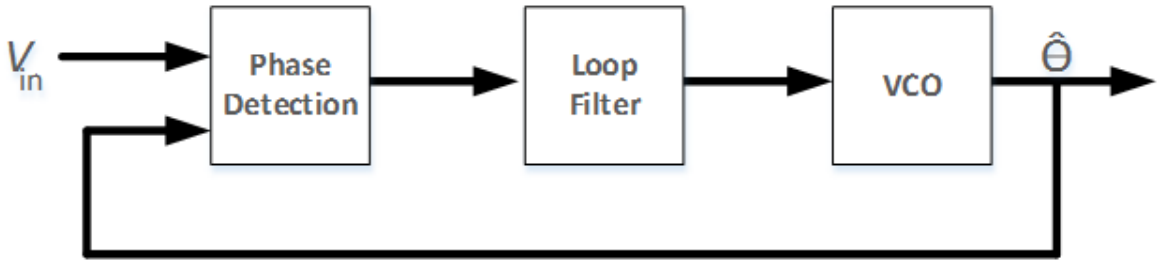

Figure 2-5: PLL Overview [27]

Figure 2-5 provides and overview for the PLL system. The system consists of a phase detector, loop filter, and a voltage controlled oscillator. The phase detector detects the phase difference between the oscillator and the input reference signal that indicates the error. In order to avoid high transient fluctuations and noise, a loop filter is added to help remove them. The signal then is outputted to the voltage controlled oscillator and it adjusts the output accordingly. The negative feedback forces the error signal to approach zero, indicating that the output and reference signal are both locked with each other [27]. In some topologies, feedback terms are added in order to help synchronisation speed, improve immunity to noise and enhance other performance characteristics. For instance, the inclusion of a Kalman filter into the overall structure which reduced the response time [28], or the application of fuzzy logic which reduce the overshoot [29].

The conventional method of synchronisation is to duplicate the grid voltage so that the reference signal has the same phase as the grid. Typically, there are two main types of PLL for single phase inverters: stationary frame and synchronous frame [30]. For stationary frame PLL, the input reference signal is only the grid voltage and it does not require additional signals. This methods employs a sinusoidal multiplier phase detector, then loop filter and VCO [30]. Extra feedback terms have been deployed to this method in order to help improve the systems synchronisation speed and its immunity to noise [30].

Synchronous frame phase lock loop (SRF-PLL) is another method used. Arguably, this is method is the most widely used way for connecting three phase inverter systems. This is due to simple and robust structure which can estimate phase angle and frequency of a balanced three phase system with minimal steady state errors [31], [26]. This method can be applied within a single phase system, although an additional reference signal is needed. This signal is an orthogonal version of the reference signal. In order to obtain this second orthogonal signal, two general methods are used. The first method generates the orthogonal signal directly from the input signal. The second method generates the orthogonal signal using the phase angle information

and applies an inverse transform. Despite the different methods for SRF-PLL, it was found that they all converge to the same one point even with different internal structures [32].

This thesis uses a low complexity PLL method based of mathematical modeling as proposed by Antchev, Pandiev, Petkova, Stoimenov, and Tomova [33], [34]. This method is based on trigonometric transformations – sine and cosine in a phase detector block. The grid synchronizer is easy to implement, provides a quick response time and is easy to deploy to digital programmable devices. Further explanation of this PLL and its integration into the overall design will be discussed in section 4.10.

2.6 Key Performance Indicators Background Theory

2.6.1 Introduction

Key Performance Indicators, or KPI, are a performance measurement tool used throughout a wide variety of fields. Essentially, KPI are used to evaluate the effectiveness/in-effectiveness of something by providing a uniform platform. KPI were used in this thesis to evaluate the inverters and the micro-inverter systems.

As the main evaluation tool, KPIs play an important role in the component level design all the way to the full system design. There are typically four main categories of KPIs: Economic, Environmental, Safety and Performance. For this thesis, only two main categories were explored, Performance and Economic KPI.

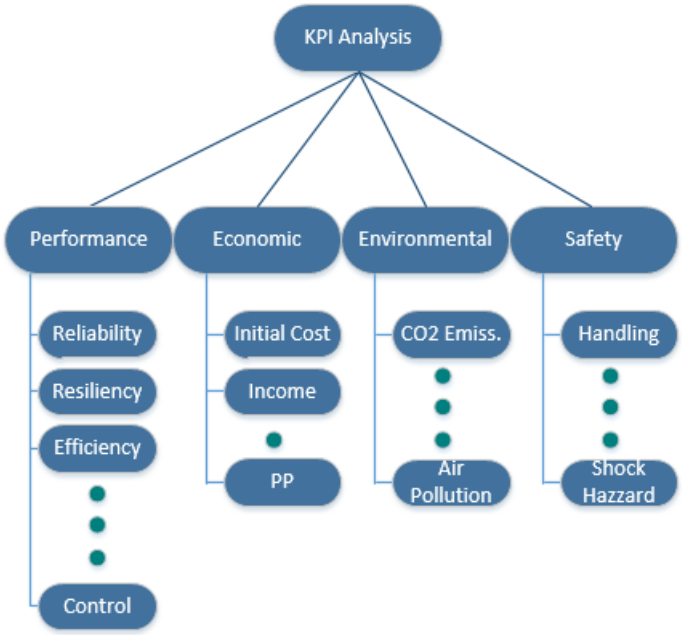

Figure 2-6: KPI Overview

In addition to providing the platform to gauge the effectiveness of different inverter designs, the KPI also allowed a feedback mechanism during the design process. For example, a requirement for the micro-inverter was to have an efficiency greater than 95%. When designing the 300W micro-inverters, the efficiency was evaluated for each design case. If the efficiency was above the requirement, then the micro-inverter design met the specific requirement criteria and the next KPI was evaluated. Otherwise, further iterations were done until it had met the requirement.

2.6.2 **Performance KPI**

2.6.2.1 Peak Operational Efficiency

System efficiency is one of the most important parameters for the design and analysis. It is used in order to quantify the effectiveness of the micro-inverter in converting the DC power generated by the solar panel to AC grid output.

$$\boldsymbol{\eta = \frac{P_{out}}{P_{in}} * 100} \qquad \textbf{2-1}$$

In the case of the Inverter design,

$$\boldsymbol{\eta = \frac{P_{in} - \sum P_{losses}}{P_{in}} * 100} \qquad \textbf{2-2}$$

$$\boldsymbol{\eta = \frac{P_{in} - (\sum P_{loss\ DC\ link} + \sum P_{loss\ boost\ converter} + \sum P_{loss\ DC\ link_2} + \sum P_{loss\ H-Bridge} + \sum P_{loss\ filter})}{P_{in}} * 100} \qquad \textbf{2-3}$$

Each power loss will be examined further in the Chapter 4, for now it is an introduction to the specific governing equations which make up the KPI for efficiency. For the system design shown in Chapter 5, power loses differs by the addition of extra power losses (depending on which case). These power loses are associated with Mosfets and relays added in order to control power flow.

2.6.2.2 Peak Operating THD

Total Harmonic Distortions is the measurement of the harmonic distortion present within a signal. This is another vital KPI for the inverter system as there is a regulation in order to ensure that the any generator connecting to the grid supplies synchronised low distortion voltages. IEEE standard 1547 (Standard for Interconnecting Distributed Resources with Electric Power Systems) [11] requires that the maximum allowable THD from a distributed technology be less than 5%. As such, no inverter system would be allowed to connect to the distribution grid without having a THD off less than 5%.

$$\boldsymbol{THD = \frac{\sqrt{V_{k2}^2 + V_{k3}^3 + V_{k4}^2 + \cdots + V_{kn}^2}}{V_{fund}} * 100} \qquad \textbf{2-4}$$

2.6.2.3 Over/ Under Voltage Response Times

IEEE standard 1547 requires that the voltage supplied to the grid from a distributed source must be within tolerance of +/- 5% of grid voltage. In addition the standard states a response time/clearing time of less than 160ms [11] if greater than tolerance has been detected. As such, it is requirement of final inverter circuit to have a control system in place which can detect both too much voltage (over the limit) and too little voltage (under limit). This is meant to protect the grid as well as the inverter itself.

$$\boldsymbol{T_{respon}\ (ms) = T_{res\ deploy} - T_{failure\ detected}} \quad \textbf{2-5}$$

The response time is defined as the time the voltage distortion was stopped (through disengaging the inverter from the grid) subtracted from the time started the distortion started. This can be seen in equation 2-5 above.

2.6.2.4 Maximum Synchronisation Time

This KPI as refers to the maximum amount of time needed for the inverter to synchronise with the grid (reference voltage).

2.6.3 Economic KPI

Economic indicators are an essential tool for evaluating if a project/design is economically feasible. As such assessing a few key indicators for the project are presented.

2.6.3.1 Initial Cost of the Inverter

The first KPI related to economics, is the overall cost of the inverter. This is strictly for each inverter individually and is cost of each of the components (shipping costs are not included in the calculation). In order to account for any unknowns which may result in additional costs, the recommended practice of adding 15% contingency cost to the estimate for components was adopted.

$$\boldsymbol{Initial\ Cost}\ (\$) = \boldsymbol{\sum Components * 0.15 + \sum Components} \quad \textbf{2-6}$$

2.6.3.2 Overall Cost for 1.2kW system

This KPI refers to the initial cost for the entire 1.2kW system. This would include four 300W inverters, 4 solar panels, 2 roof mounts (2 solar panels per single mount), plus extra components needed. This does not include labor and installation costs as these costs vary not only from geographical local, but also contractor.

$$\boldsymbol{System\ Cost = \sum Components\ cost} \quad \textbf{2-7}$$

$$\boldsymbol{System\ Cost}\ (\$) = \boldsymbol{\sum inverter + \sum solar\ panels + + \sum mounts + \sum extra} \quad \textbf{2-8}$$

2.6.3.3 Estimated Yearly Income

The KPI refers to the expected annual income for a 1.2kW system located in Toronto Ontario Canada. In order to calculate this, data was collected from Government of Canada webpage which shows the PV potential and insulation (kWh/kW) level (monthly) across Canada [35], [4]. In addition, the assumption was made (section 5.2) that this system would connect to the grid, and therefore would qualify for Ontario's microFIT program with a rooftop deployment of 0.294$/kWh [36].

$$\boldsymbol{Income_{yearly}}\left(\frac{\$}{year}\right) = \sum_{1}^{12} \boldsymbol{PVP} * \boldsymbol{Inverter}\ \textbf{System Output}\ \boldsymbol{Power} * \boldsymbol{microfit\ cost} \qquad \textbf{2-9}$$

2.6.3.4 Estimate Payback Period

Payback period is the final economic KPI assessment used. This refers to how long a period of time (in years) before the initial cost of the system has been recuperated.

$$\boldsymbol{PP}\ (\boldsymbol{years}) = \frac{\boldsymbol{Initial\ System\ Cost}\ (\$)}{\boldsymbol{Income_{yearly}}\ (\frac{\$}{year})} \qquad \textbf{2-10}$$

In order to calculate this, a few assumptions needed to be made. The assumptions used for this calculation were: 1.2kW system, system deployed to Toronto, Ontario, solar irradiance values for Toronto apply, and the system qualifies for microFIT. In addition, it was assumed that the prices for the microFIT would remain at current levels throughout the products duration. It should be noted that all prices within this thesis (parts, calculations, rates) as calculated in Canadian dollars.

2.6.4 **Per-Unit KPI**

Resiliency is defined "as the ability of a system to recover from a failure" [37]. It is an important parameter and exploring different resiliency designs is the main focus of this thesis. However resiliency methods for single phase grid connected micro-inverters systems is a novel idea and as such no standard exists to evaluate different micro-inverter systems against one another. Therefore this thesis proposes to use KPI in order to help evaluate different micro-inverter systems.

A problem arises however when trying to summarize the KPI in order to evaluate a system as a whole. It can be seen above that the KPI's have different units depending on the performance characteristic in question: examples initial cost ($), payback period (years), resiliency time (ms), etc. While KPI provides a useful method to compare and contrast individual characteristics, it provides a problem when looking to summarize all the characteristics and evaluate the system as a whole. In order to overcome this problem, a novel method was designed based off of turning the KPI into unit less values.

2.6.4.1 Governing KPI Analysis Equation

In order to assess the overall system, all KPI are converted into per unit (non-dimensional) values. These values, can then be multiplied by a weighting factor.

$$\boldsymbol{KPI_{resiliency}} = \sum_{j=1}^{n} \boldsymbol{a_j} * \boldsymbol{PU\ KPI_j} \quad \textbf{2-11}$$

Where j = the number of KPI, n = total number of KPI, a_j = weighting factor assigned, $PU\ KPI_j$ = the specific value from the per unit KPI calculation.

In essence, the larger the outcome summation, the better the system. For each case study, the PU-KPI values were calculated. These PU-KPI have two different categories. The first category, is for comparing a system with resiliency deployed against the base Case 0. The second category shows the performance changes between modes of operation within a specific case study. Meaning the deviation of performance from operating normally to when the system is operating under fault. All PU-KPI fit into the two different categories, which allow for unit less values to be created.

Each PU-KPI are then multiplied by its associated weighting factor, whose values are determined based on the stakeholder's requirements. The higher emphasis a stakeholder requires on specifics performance criteria, the higher the weight attached to that specific PU-KPI. Upon completing the PU-KPI table, each PU-KPI value for the specific case is then summed. The case which has received the highest final score shows the best method to achieve resiliency for the stakeholder based on their overall system requirements

2.6.4.2 Per Unit Resiliency Response time

As stated previously, IEEE standard 1547 states that a disconnection of a distributed source must occur within 160ms of failure occurring [11]. Therefore, using the response time KPI and the IEEE standard, a PU-KPI measurement is created.

$$\boldsymbol{PU\_KPI_{response\ time}} = \frac{\boldsymbol{IEEE\ fault\ clearing\ standard}}{\boldsymbol{T_{res\ deploy} - T_{failure\ detected}}} = \frac{\boldsymbol{160ms}}{\boldsymbol{T_{res\ deploy} - T_{failure\ detected}}} \quad \textbf{2-12}$$

This KPI is normalized into a ratio which effectively describes how fast/slow the resiliency scenario detects failure, disconnects the failed inverter from grid, re-directs power flow and resynchronizes to the grid. Essentially this PU-KPI show a ratio of resiliency response time to the IEEE standard 1547.

2.6.4.3 Per Unit Resiliency Power Coverage

This KPI provides a measure of how much power of the resiliency scenario can cover when compared to the total system.

$$PU\_KPI_{Res\ Power\ coverage} = \frac{Power\ Output\ (W)_{system\ under\ fault}}{Power\ Output\ (W)_{system\ normal\ operation}} \quad \textbf{2-13}$$

To illustrate with an example, say there is have a system of 1.2kW. This consists of four 300W micro-inverters. We have one single redundancy micro-inverter of 300W. Now given the event that the entire 1.2kW system goes offline, the resiliency scenario can therefore output 300W/1200W or 1/4. Recalling large the result, the better, a system with 1200W resiliency capability equals 1.2kW/1.2kW = 1.

2.6.4.4 Per Unit Efficiency Normal operation to Resiliency operation

This KPI provides a measure of how the efficiency deviates from the normal operating case to operating under fault.

$$PU\_KPI_{E\ N\ to\ F} = \frac{Efficiency_{\ system\ under\ fault}}{Efficiency_{\ system\ normal\ operation}} \quad \textbf{2-14}$$

This helps system designers figure out how the system efficiency changes from the normal operating condition to operating under fault. In certain applications, achieving a max efficiency may be an important factor.

2.6.4.5 Per Unit Efficiency Case to Case

This provides a measure of how the efficiency deviates from Case 0 (no resiliency scenario deployed) to Case j (resiliency strategies deployed).

$$PU\_KPI_{E\ Case\ to\ Case} = \frac{Efficiency_{\ system\ Case\ j}}{Efficiency_{\ system\ Case\ 0}} \quad \textbf{2-15}$$

2.6.4.6 Per Unit THD Normal Operation to Resiliency Operation

This KPI is needed in order to measure the THD when comparing normal operation to the resiliency operation of the system.

$$PU\_KPI_{THD} = \frac{THD_{normal\ operation}}{THD_{under\ fault}} \quad \textbf{2-16}$$

Extra relays and Mosfets included in the case studies introduce new resistances into the system. These resistance can have an effect on the output filter and therefore have an effect on the THD of the system. As such it is necessary to check the THD for all cases to makes sur it has met the standard, and how it deviates from the normal THD operation.

2.6.4.7 Per Unit THD Case to Case

This is a measure of how the THD deviates from Case 0 (no resiliency scenario deployed) to the Case j, operating under normal operating conditions.

$$PU\_KPI_{THD\ \ Case\ to\ Case} = \frac{THD_{\ case\ 0}}{THD_{\ casej}} \quad \textbf{2-17}$$

2.6.4.8 Per Unit Initial Cost

To see the deviation from the original initial cost of the system (one without any resiliency scenario) to the one with resiliency scenarios deployed, the following per PU-KPI was created.

$$PU\_KPI_{Initial\ Cost} = \frac{Initial\ Cost_{\ no\ resiliency\ case}}{Initial\ Cost_{resiliency\ case}} \quad \textbf{2-18}$$

The initial cost of the system (will be less, as there as less components) is divided by the initial cost of the system with no resiliency added. This effectively shows how many times most expensive the resiliency cases are versus the initial cost.

2.6.4.9 Per Unit Payback Period

The final PU-KPI for the resiliency scenario is the PP KPI. This can be seen in the equation 2-18 below.

$$PU\_KPI_{PP} = \frac{PP_{\ no\ reilsnecy\ case}}{PP_{\ resiliency\ case}} \quad \textbf{2-19}$$

Chapter 3: Thesis Framework and Methodology

In this chapter, the research framework and methodologies are presented. The research was conducted to achieve the objective in two phases. The first being is inverter phase, and constitutes the design of inverters. The second is the resiliency phase, and is meant to: design, analyze, and evaluate the resiliency case studies for a micro-inverter system.

3.1 Thesis Framework

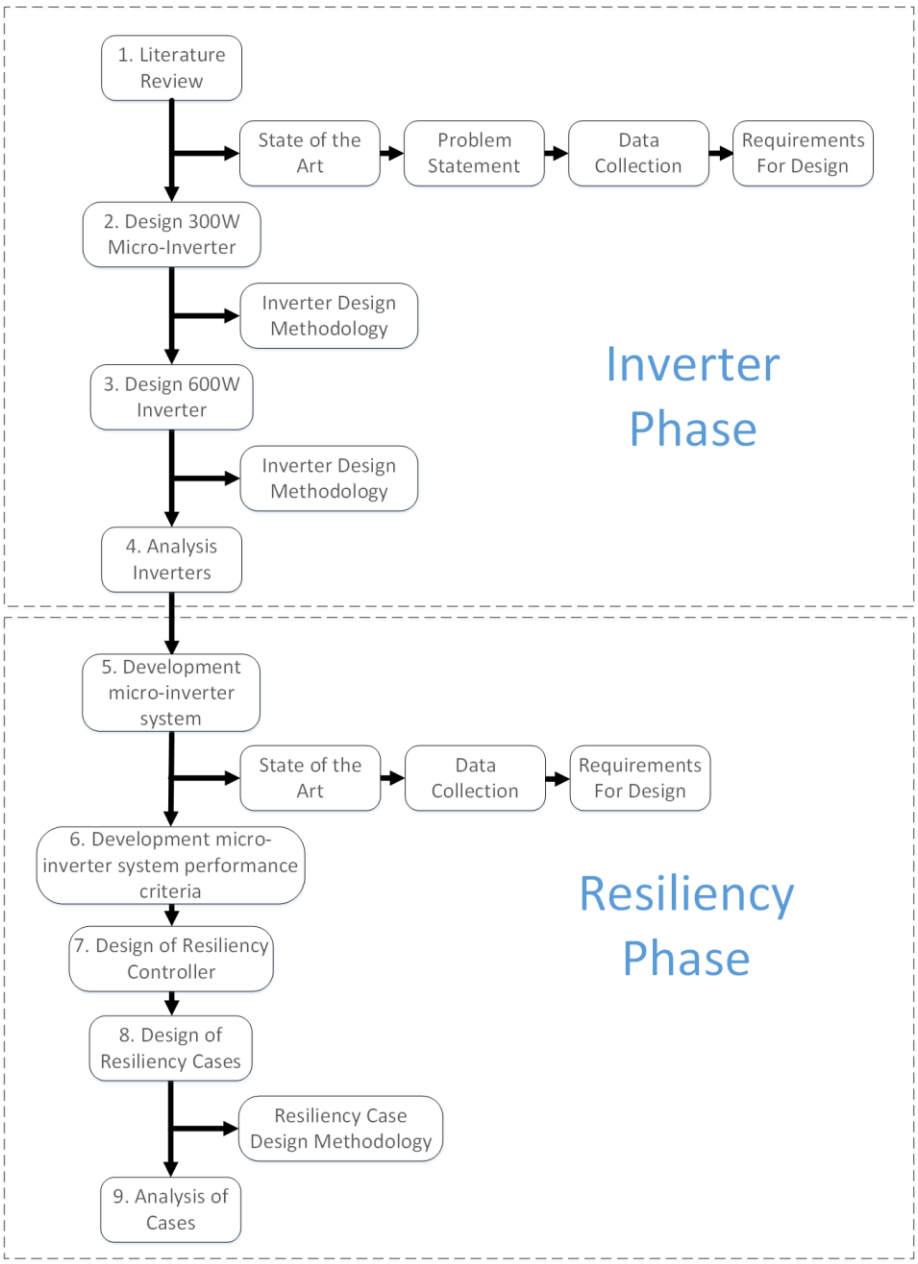

Figure 3-1: Thesis Framework

Figure 3-1 shows the thesis framework steps taken in order to complete the research objective. The framework includes, data collection, design of inverters (both a 300W and 600W), analysis of the inverters, development of a micro-inverter system PU-KPI criterion, design of a resiliency controller, case study design and analysis. Each of the steps of Figure 3-1 are explained below.

3.1.1 **Data Collection**

In this step, the problem statement was identified, necessary background data was collected, design requirements are collected and any other background information needed. Examples of some of the data collected includes such things as solar irradiance in Toronto, microfit rates, and KPI for inverters.

3.1.2 **Design of a 300W inverter**

In the following step, a single phase synchronized 300W micro-inverter was designed. A design methodology was used in order to design the inverters in as realistic way as possible while meeting with output standards. This methodology will be shown further in section 3.2.1.

3.1.3 **Design of a 600W inverter**

In order to evaluate some resiliency strategies initially hypothesized, a 600W inverter was needed. Therefore this step consisted of designing a 600W single phase grid connected inverter. The same design methodology was applied for this design as the micro-inverter which is shown in section 3.2.1.

3.1.4 **Inverters Analysis**

Following the inverter designs, a full analysis was conducted. This analysis was strictly a performance analysis in order to ensure that the inverters designed met with grid standards as well as stakeholder requirements. A preliminary comparison was also done with market available inverters of similar power rating.

3.1.5 **Development of Micro-Inverter System**

In order to test different resiliency cases/scenarios, a standard platform was needed. This platform is the Case 0, or scenario without any resiliency measures applied to it. Each of the case studies would take Case 0, and then modify upon it in order to test out that specific resiliency method. In order to create this base system a further literature review and data collection was needed. This literature review included obtaining such things as: average residential PV system size (kW), average spacing between solar panels, methods to arrange panels on roof, cost of roof mounts, etc.

3.1.6 **Development of Micro-Inverter System Performance Criteria**

After the design for the micro-inverter system was achieved, performance criteria method was created in order to effectively evaluate the difference resiliency cases. This evaluation was then used to compare the different cases against one another based on unit less PU-KPI values.

3.1.7 **Design of the Resiliency Controller**

In order to deploy the resiliency case, a controller was needed. This controller had to monitor micro-inverters output, identify error/fault occurrence and then provide the corrective action to redirect power flow based on fault occurrence. A controller was not commercially available and had to be designed to satisfy this need. In addition, this controller needed to be easily integrated into both hardware and simulation.

3.1.8 **Design of Resiliency Cases**

For this step, four hypothesized cases were designed, simulated and evaluated. The cases were designed, built and simulated in PSIM software in order to increase the systems resiliency. Similar to the Inverter design, a methodology was used to aid with the design of each case study and to iterate upon them in order to ensure the results of the system met with grid standards. This methodology will be shown in section 3.2.2 below.

3.1.9 **Analysis of Case**

As stated above, during the design of each resiliency case, some performance criteria were included and evaluated upon in order to ensure that system output met grid standards. However, since this was an iterative process; a full in depth analysis was not done in order to conserve time and effort. Upon completion of all the case studies, the full in analysis was then performed utilizing the proposed evaluation method to identify the best method for increasing micro-inverter system resiliency.

3.2 Methodology

This section demonstrates the methodologies used for the design of inverter and case studies. Use of a good design methodology ensures that objectives remain clear and crisp, although the methods to achieve those objectives can be varied. An example that occurred during the design work was the modification of the output filter for the inverter. Originally an LC was desired; however, this was modified to LCL during the design process after it was found to have better performance when integrated with the control systems.

3.2.1 **Inverter Design Methodology**

The inverter design methodology described in this section depicts the iterative method used. This process was continued until satisfactory results were achieved, and the requirements had been met.

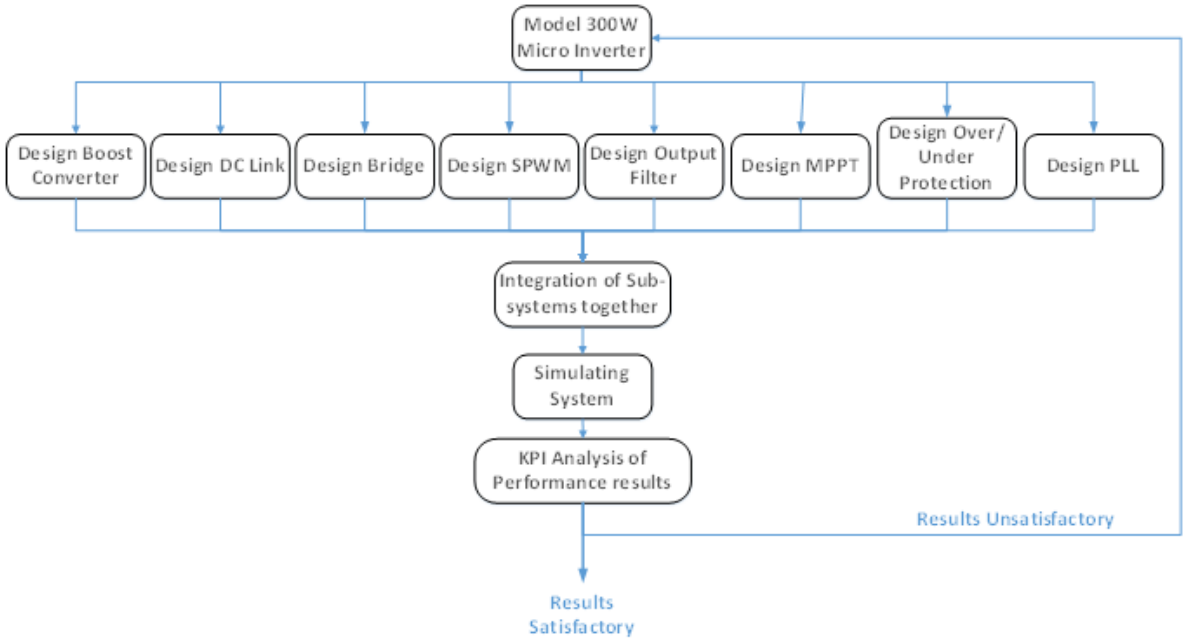

Figure 3-2: Inverter Methodology

Figure 3-2 above shows the inverter design methodology used to design both the 300W micro-inverter and the 600W inverter. The process starts with the model of the inverter and identification of its major sub-circuits. A literature review was done of each of the components, governing equations identified and values were calculated based off of those equations.

Each sub-circuit was designed with its own PSIM simulation during its initial design phase. First, the calculated values were used in the simulation in order to ensure that PSIM was operating as expected and the results followed along with governing theory. After the design of each of the sub-circuits had been

accomplished, each were integrated into an overall PSIM model. One by one the new sub-circuits were added into an overall design; each time added, the overall simulation was re-run ensuring expected results.

Finally, upon completion of all the sub-circuits into the overall design. Digikey and Mouser was then used to modify the calculated component values with components readily available in the market. During this part, the internal resistances for each of the components were taken from its datasheet and included into the overall design. Thus, the overall circuit was designed using real value components to ensure a realistic simulation as possible. In some cases, iterations were needed to be re-done and new parts had to be found as the system needed to be tuned until results met both stakeholder and engineering requirements.

3.2.2 **Resiliency Case Design Methodology**

The following methodology was used in order to design each of the resiliency scenarios cases for the thesis.

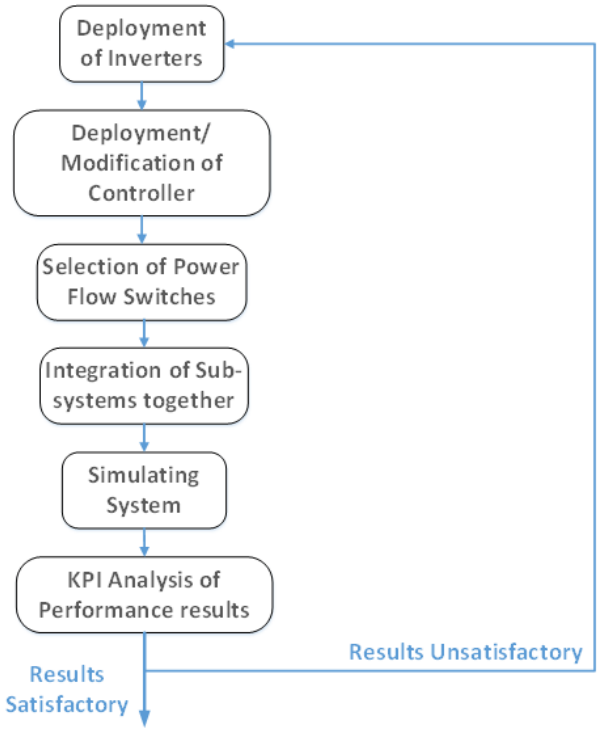

Figure 3-3: Resiliency Case Design Methodology

Figure 3-3 above shows the methodology used to design, simulate and provide a small analysis for each of the resiliency case studies. The methodology starts with opening a new PSIM model and deploying the 300W micro-inverters and 600W inverter if needed. After successfully deployed, the resiliency controller was then included into the control blocks of the inverters.

The next portion constitutes the selection of power switches in order to control and direct power flow within the system. One of the primary goals for the resiliency methods was to try and achieve a high efficiency. Therefore, switches were selected in order to try and minimize the power losses due to the internal resistances.

After the switches were selected and the controller deployed, the simulation was run in PSIM. The results of the system were analyzed to ensure all the IEEE standards (phase locked, voltage difference, THD,) had been met. The feedback portion of the figure demonstrates the need for iterations in order to ensure standards were met. Upon successful completion of meeting the requirement, then the simulation was saved and the next case study would being

3.2.3 **Resiliency Evaluation Methodology**

The following section provides the steps used for the proposed evaluation methodology.

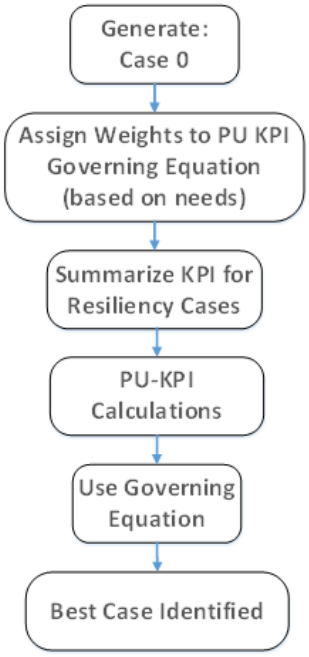

Figure 3-4: Evaluation Methodology

Figure 3-4 shows the methodology used in order to evaluate the different resiliency cases for the thesis. First, the Case 0 is generated. This refers to the general case without any resiliency measure shown in section 5.1. After this step is completed, weights are assigned to the governing equation shown in equation 2-12 of Chapter 2. These weight are based on stakeholder requirements and range from a value of 1 to 5.

For example, one person deploying a system with resiliency might have an emphases for PP, and as such attach a higher weight to it. Recall, for the equations, the larger the final score the more suitable the choice.

After the weights are chosen, the KPI for all the case studies are summarized and put into a table. For the purposes of this thesis, this includes Case 0 to Case 4. These are done in order to organize the KPI and get the results ready for the PU-KPI evaluation method. It should be noted, that all the simulations have already been successfully completed, meeting the system design requirements.

The next step refers to calculating the PU-KPI from the summary table of KPI. Using equations 2-12 to 2-19, the results of the different systems are standardised. Taking the results of the PU analysis; the values are then multiplied by the specific weights. The results for each case are then summed and the case which has the highest value is the best case. This process will be shown in Chapter 6 of the thesis.

Chapter 4: Single Phase Inverter Circuit Design

The following chapter provides an overview of the Inverter phase of the thesis. First, an overview is provided for each sub-circuit. This summarizes the background information, the governing equations and the PSIM model. Next, the design for the 300W is shown along with its results. This is followed by the 600W inverter and its results. The chapter concludes with a KPI analysis of both inverters.

4.1 Circuit Block Overview

The chapter begins by providing an overview of the inverter and the sub-circuits which constitute it.

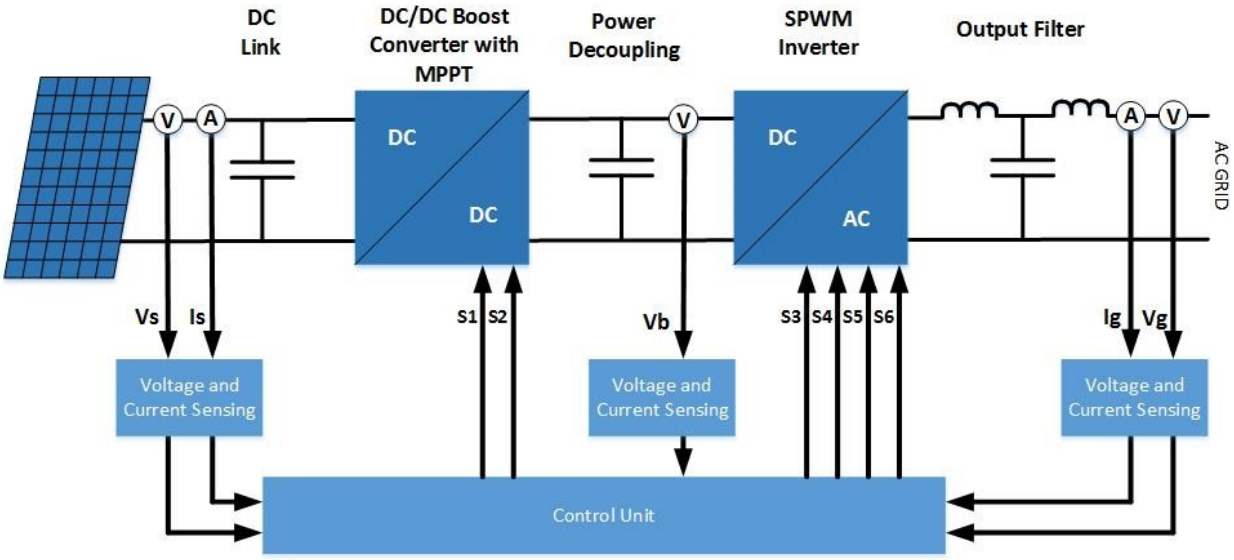

Figure 4-1: Inverter Overview

Figure 4-1 above provides an overview of the sub-circuits and each will be elaborated on it in own sub-section. This figure was provided as an introductory schematic in order for the reader to have an idea of the overall picture and how the components all relate to one another before proceeding into the detailed design.

4.2 Solar Panel Used

Beginning with the solar panel, a local manufacture of monocrystalline panels was chosen. This was decided in order to utilize local components; thus, saving on shipping costs and ease in customer service. The photovoltaic company chosen was Ecilpsall Solar located in Toronto and the NRG72-300M (300W) was chosen from their product line.

Electrical Data

Type		NRG72 300M	NRG72 305M	NRG72 310M	NRG72 315M	NRG72 320M	NRG72 325M
Rated Maximum Power at STC - Pmax(W)		300W	305W	310W	315W	320W	325W
Maximum Power Voltage - Vmp(V)		36.54	36.69	36.78	36.88	36.97	37.22
Maximum Power Current - Imp(A)		8.22	8.32	8.43	8.51	8.66	8.73
Open Circuit Voltage - Voc(V)		44.87	44.99	45.12	45.28	45.39	45.60
Short Circuit Current - Isc(A)		8.73	8.84	8.92	8.95	8.97	8.98
Operating Temperature		-40 to +85°C					
Max System Voltage		1000V (IEC) / 600V (UL)					
Fuse rating		15A					
Power Tolerance		0 to 5W					
Temperature Coefficients	Pmax	-0.438%/°C					
	Voc	-0.341%/°C					
	Isc	0.047%/°C					

Figure 4-2: Solar Panel Data Ecilpsall NRG72 [38]

Figure 4-2 above, shows the figure and data of the NRG72-300M solar panel taken from the manufactures product manual. The picture of the solar panel can be seen on the left hand side of Figure 4-2. The right hand side of Figure 4-2 provides the specifications of the solar panel. These specification are needed as the first step in the design. For example, the nominal voltage and nominal current are taken to be used for the design of the first power stage.

In addition, the datasheet provides the limits for the circuit. This is necessary in order to size components above these limits to provide a good safety margin in the design. For example, the open circuit voltage for the solar panel is 44.87V [38]. Therefore the first DC link capacitor was sized with a voltage rating higher than 45V (160V) in order to ensure it can operate safely within the design parameters for the circuit. This was a practice carried throughout the design phase and for every component chosen.

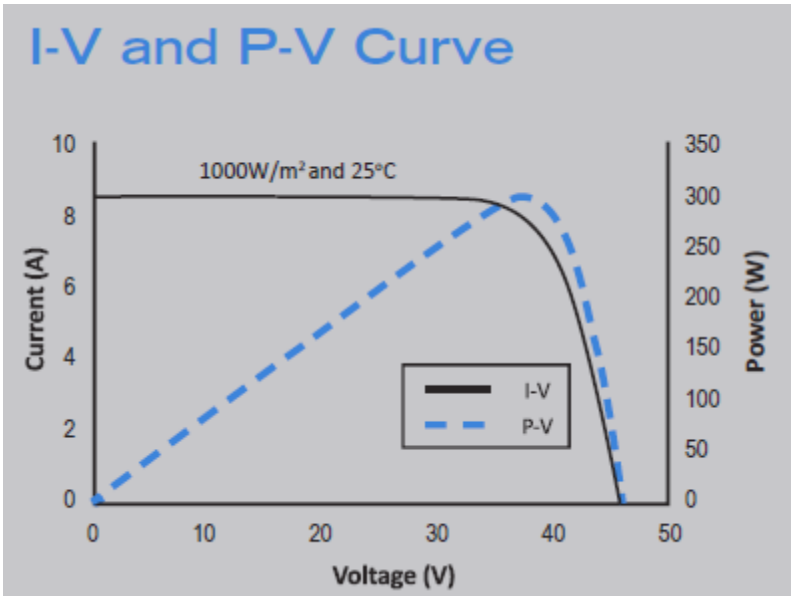

Figure 4-3: I-V Curve NRG72 300M Solar Panel [37]

Figure 4-3 above provides the I-V curve for the NRG72 300M solar panel. Within the figure, the maximum power point can be seen occurring at approximately 36V and 8.2A. Using this data the next sub-circuit can be designed.

4.2.1 **Governing Equations**

The following section outlines the mathematical formulas for photovoltaic module used within PSIM software.

$$\boldsymbol{I_d = I_0\,[\exp\left(\frac{V_d}{V_T}\right) - 1\,]} \qquad \textbf{4-1}$$

$$\boldsymbol{V_T = \frac{kT}{q} * nI * Ncell} \qquad \textbf{4-2}$$

Where: I_d = = diode current (A), V_d = diode voltage (V), I_0 = diode saturation current (A), nI = diode ideality factor, a number close to 1.0, k = Boltzman constant = 1.3806e-23 J.K-1, q = electron charge = 1.6022e-19 C, T = cell temperature (K), *Ncell* = number of cells connected in series.

Matlab software contains a database with known solar panels and manufacturers, Ecilpsall solar panels among them. This data was transferred from Matlab into the PSIM solar module and the crossed referenced with datasheet to ensure specifications of the solar panel were correct.

4.3 DC-DC Converter Sub-circuit Design

The DC-DC converter provides the first power stage within the inverter circuit design. The following section will outline the necessary background information regarding the converter, modes of operation, the governing equations and the PSIM model designed.

4.3.1 **Introduction DC-DC Converters**

DC-DC converters play a significant part in power electronics circuits [39]. Essential they are electrical circuits which transfer energy from a DC source to a DC load. Some converters increase the voltage from the source to the load or 'boost' it, these are called boost converters. Other converters lower the voltage from the source to the load and are known as buck converters. Finally, there exists some converters which can perform both capabilities (lowering and increasing the voltage) and are typically known as buck-boost converters. Within each classification, there exist several different sub-methods to achieve the desired DC-DC conversion. Each method has its own advantages and disadvantages. The DC-DC converter is an essential part of the micro-inverter circuit as it necessary to boost the low DC voltage generated by the solar panel(s) to appropriate levels for grid connection. In they also provide a means for maximum power to be extract from the solar panel.

4.3.2 **Boost Converter Need**

A boost converter is a DC-DC converter which increases the output voltage from the source and applies it to the load. Each boost converter will typically have at least two semiconductors and at least one energy storage element. Boost converters have many applications throughout industry, from such things as batteries, rectifiers, DC generators and inverters. A brief overview of the operational theory for the boost converter is covered in the sub-sections below.

4.3.2.1 Initial Start Up

During the initial start-up, the inductor is connected to ground. Current starts to flow, and the magnetic fields begins to build in the inductor storing energy. In the rest of the circuit no current is flowing; assuming the capacitor has no initial/stored energy within it.

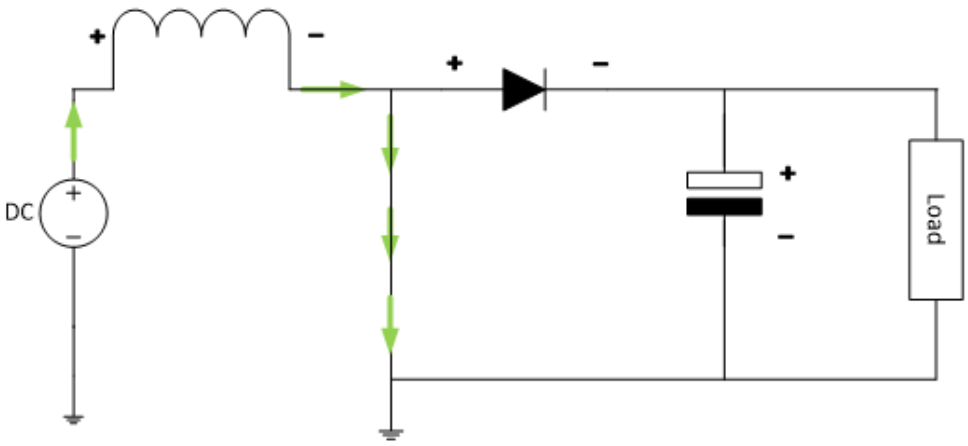

Figure 4-4: Boost Converter Initial Start Up

Figure 4-4 above shows the path of current flow during the initial start-up as indicated by the green arrows. The diode is reverse biased in this scenario; thus preventing the current from flowing into the rest of the circuit.

4.3.2.2 Switch Open Mode

Next, the switch connecting the inductor to ground is opened. As the switch is now open, the sudden drop in current produces a back e.m.f. in the inductor with the opposite polarity. The polarity of the inductor is now in the same direction as the voltage source. The diode is now forward biased and current begins to flow through it and the high voltage is applied to the load. The capacitor begins to store a charge across it.

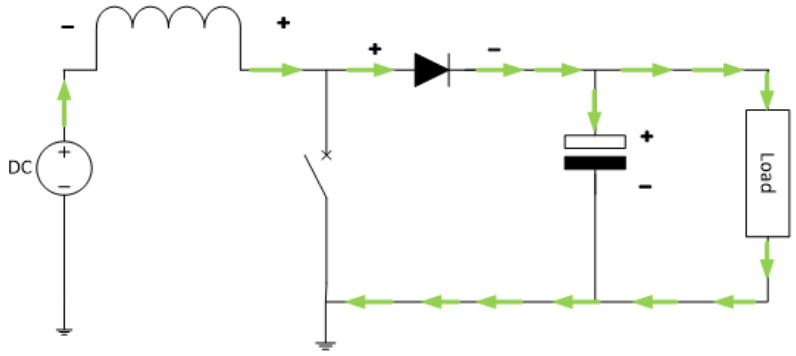

Figure 4-5: Boost Converter Switch Mode

The Figure 4-5 above shows the circuits operation when the open switch has occurred. Current flow is shown by the green arrows. As the voltage begins to decrease, the energy stored in the inductor begins to discharge and the magnetic field begins to collapse.

4.3.2.3 Closed Switch Mode

The next stage is the closed switch operation again. Recall that this occurs, the inductor is connected to ground and the magnetic field begins to build. During this stage, the capacitor now begins to discharge is stored energy inside it.

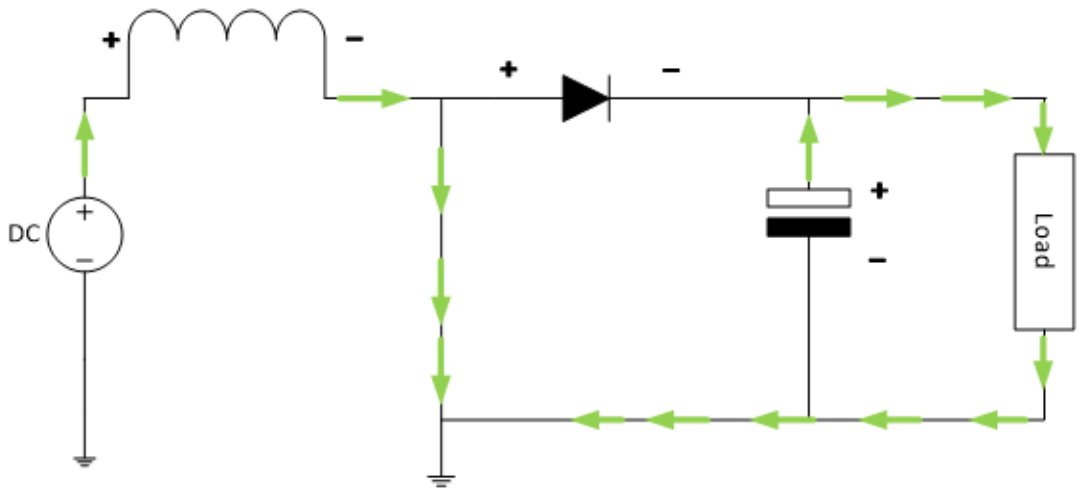

Figure 4-6: Boost Converter Closed Switch Mode

Figure 4-6 above shows the boost converter during the operation of the closed switch and non-initial state. The green arrows indicated the conventional current flow in the circuit. It can been seen in the figure the charging of the inductor is done with isolation from the load by means of the diode. In addition the discharging capacitor current can be seen in the right hand side of the circuit. Under steady state operations, the inductor pulsates on and off, producing a higher voltage which is periodically applied to the load. Under steady state, the capacitor also acts to smooth out and stabilize the voltage across the load during on/off times of the inductor.

4.3.3 **Modes of Operation**

For a boost converter, there are two basic modes of operation: continuous condition mode and discontinuous conduction mode [39], [7]**.** The main parameters for governing which mode of operation used are: inductance, duty cycle, time on and resistance. If the inductance is reduced from a high initial value; the valley current will decay and finally become zero at the end of the duty cycle. When this happens the boost

converter has reached the discontinuous mode. The value of the inductance at this point is found through equation (4-7) below it is known as the critical value of the system.

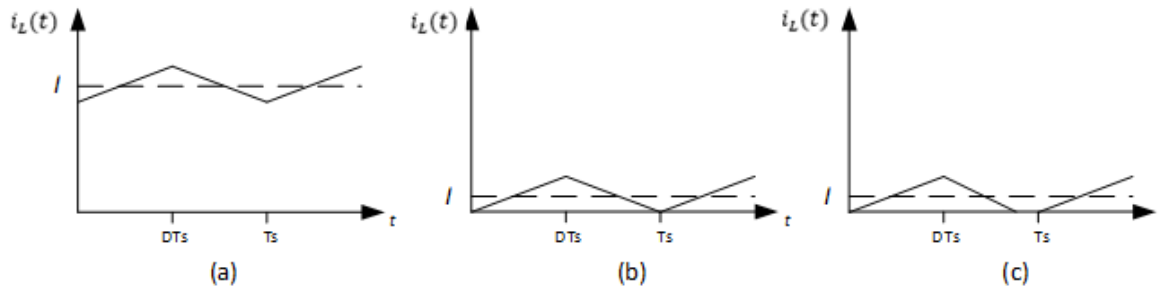

Figure 4-7: Modes of Operation Boost Converter

Shown graphically in Figure 4-7(a) is the operation of a boost converter during continuous conduction mode. The current through the inductor, represented by $i_L(t)$, fluctuates and never reaches zero during the operation as the switch pulsates on/off. The average output current to the load, *I*, is shown through the horizontal line. Figure 4-7(b) shows the current in the circuit, as the inductance value is lowered to the critical value. At which point, the current in the circuit reaches back down to zero at the end of the duty cycle. Finally, if the inductance value is lowered further the current reaches zero, before the end of the duty cycle. This is known as discontinuous conduction mode and can be seen in Figure 4-7(c). Each mode of operation has their own advantages and disadvantages. For the purposes of this research, the circuit designed is operating in continuous conduction mode as this requires smaller inductors than discontinuous conduction mode for same power output.

4.3.4 **Governing Equations**

The following section outlines the governing equations for a boost converter operating in continuous conduction mode [39]:

4.3.4.1 Operation

At charging interval,

$$i_L(t) = \frac{1}{L} V_{in}\, t + I_L(0) \qquad 0 \leq t < DT \qquad \textbf{4-3}$$

Where; $I_L(0) = initial\ inductor\ curent\ at\ t = 0$, $V_{in} = voltage\ across\ inductor$, $i_L(t) =$ current through $inductor$

When switch is turned off at $t = DT$, the inductor voltage becomes,

$$\boldsymbol{i_L(t) = \frac{1}{L}\,(V_{in} - V_o)(t - DT) + I_L\,(DT)} \qquad \textbf{DT≤t<T} \qquad \textbf{4-4}$$

Evaluating 4-3 - 4-4 such that during steady state operation, the net change of current between the on/off state must equal zero:

$$\boldsymbol{\frac{1}{L}\,V_{in}\,DT - \frac{1}{L}\,(V_{in} - V_o)(1 - D)T = 0} \qquad \textbf{4-5}$$

Solving we obtain,

$$\boldsymbol{\frac{V_0}{V_{in}} = \frac{1}{1-D}} \qquad \textbf{4-6}$$

There is minimum critical value of inductance, such that anything above would be in continuous conduction mode and anything below would be in discontinuous conduction mode.

$$\boldsymbol{L_{min} = \frac{RT\,(1-D)^2 D}{2}} \qquad \textbf{4-7}$$

Output ripple for the Boost converter is given by the following equation,

$$\boldsymbol{\frac{\Delta V_0}{V_0} = \frac{D}{RCf}} \qquad \textbf{4-8}$$

4.3.4.2 Control Theory

In order to control the boost converter and provide a constant output voltage under fluctuating input conditions, a feedback control system is needed. Output voltage can be maintained by regulating the duty cycle applied to the switches in the circuit. This method can be used to maintain a consistent voltage output across the DC capacitor and h-bridge for the inverter.

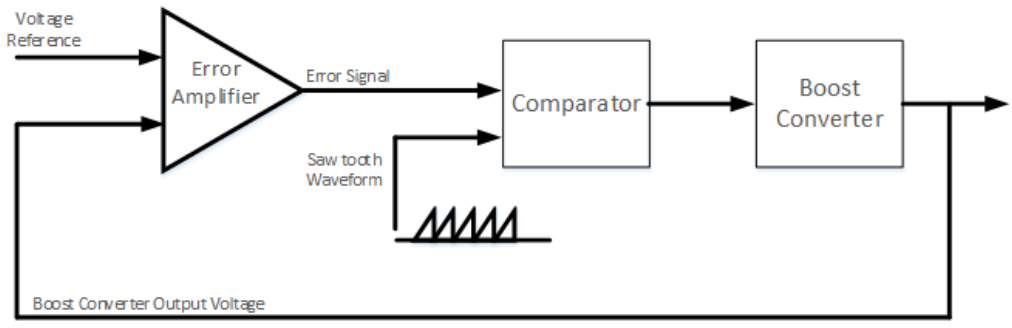

Figure 4-8: Boost Converter Feedback

Figure 4-8 above shows the feedback controller for a boost converter [9]. The error signal comes from the subtraction of the output voltage from the boost converter to the reference voltage. The output error signal is then sent to a comparator, which adjusts the PWM duty cycle. The adjustment are made by a comparison of the error signal with a saw tooth signal. The output pulses of the comparator are then sent to trigger the Mosfets of the boost converter. Additional P, I, D terms are often placed in the error signal in order to help improve the control circuits design and operation. Fuzzy Logic controllers for DC converter are also gaining popularity due to their ability to increase the overall performance of the converters [18], [19].

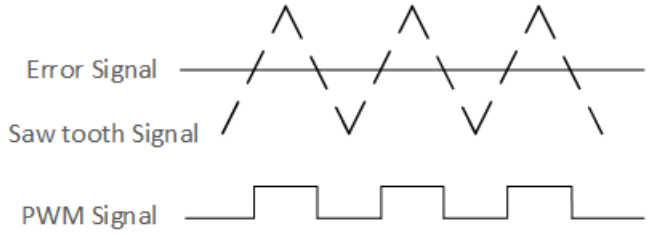

Figure 4-9: Boost PWM generated

Figure 4-9 above demonstrates how the comparator outputs the PWM signal based off of the input error signal and saw tooth signal. The error signal is adjusting to greater/lesser values resulting in longer/shorter pulse widths applied to the gates of the switches.

4.3.5 **PSIM MODEL**

The following section shows the boost converter circuit designed and implemented in PSIM.

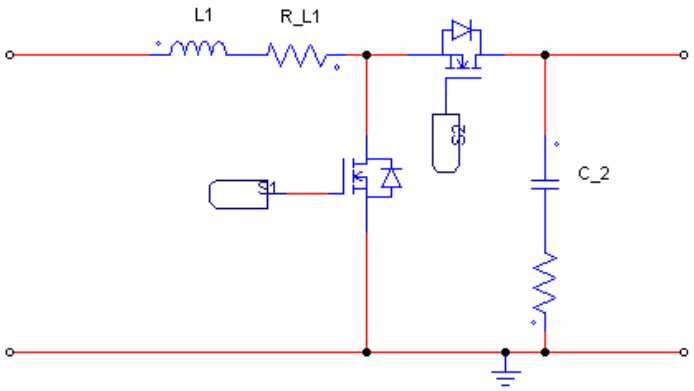

Figure 4-10: PSIM Boost Converter Design

Figure 4-10 above differs from Figure 4-4 by the addition of two resistors, replacement of a Mosfets instead of and ideal switch, and replacement Mosfet instead of a diode. In order to simulate an inverter as close as possible; real life values for components were chosen. As such, the resistances were added from the datasheets for the inductor and capacitor. The same is true for the N-channel Mosfets, however no resistors was added to the circuit design because the component within PSIM allows for the internal resistance to be included directly. Values for all the components will be displayed in sections 4.11 and 4.12 which go over the specific design examples for a 300W and 600W inverter.

4.4 DC Link

4.4.1 **Purpose**

There are of two different DC-Link capacitors within the micro-inverter design. The first connecting the solar panel to the boost converter, and the second connecting the boost converter to the h-bridge. The purpose of these components is to act as an intermediate device between power systems input and outputs. Effectively, they are there in order to help maintain a constant supply. DC links are used in a wide variety of application ranging from AC-DC converter, wind power generation, power supplies, motor controllers, battery systems, UPS system and inverters. In VSI, capacitors are used in order to help stabilize and provide constant amount of voltage (to both stages of the inverter). For CSI, inductors are typically used.

4.4.2 **Power Decoupling**

Power decoupling is used to decouple one part of the electric circuit to another. That is, it is meant to reduce noise and distortions in the circuit caused by various elements. Normally power decoupling is achieved by means of an electrolytic capacitor. This is because of their significantly lower costs when compared to other types of capacitors such as film, aluminium, etc. Unfortunately the use of electrolytic capacitors has also been one of the main reasons for inverter failures within the field.

Inverter warranties tend come with an average of 3-5 years, while PV modules come with a warranty of approximately 20 years [5]. Little information has been published from companies regarding the failure modes of the inverters; however, the US DOE at a workshop for solar agreed the most urgent problem facing the inverters is the DC-bus capacitor linking [5]. In addition, a lot of research has also shown the capacitor to be the main reason for failure.

Typically, in most commercial inverters the DC capacitor is an electrolytic type due to economic advantages which have contributed to the short life expectancy of the inverter. This is because these capacitors tend to the have a significantly reduced life expectancy when operating under fluctuating temperatures [10]. Inverters are usually exposed to the outside environment, and as such the lifetime expectancy of the inverter drastically reduces according to the following equation [10]:

$$L_{op} = L_{op}(0) * 2^{\frac{T_0 - T_h}{\Delta T}} \quad \textbf{4-9}$$

Where L_{op} is the operational lifetime, $L_{op}\ (0)$ is the specified operational lifetime at hotspot temperature T_0 which can be taken from the datasheet, T_h is the operating temperature and ΔT is the degree that would results in half the operational life, this is also found within the data sheet. The typical $L_{op}\ (0)$ is approximately between 3,000 to 6,000 hours at 85^0C [10] for electrolytic capacitors. As such, the DC link capacitor has typically been the main limiting factor in commercialized inverters.

Film capacitors are a clear alternative to electrolytic as they offer a wider temperature range and can with stand high voltage levels with a relatively small size [40]. The trade-off however is that they are significantly more expensive. Film capacitors can easily be in excess of four times as expensive as an electrolytic capacitor for the same farad. As such there is a difficult balance to be struck. Small capacitance would be more economical, however would weaken the power decoupling between the boost converter and inverter power stage. This weakening can contribute to an overall loss in efficiency [40].

4.4.3 2nd Order Harmonics

For PV inverter applications there are typically two factors which can cause undesirable voltage fluctuations across the DC bus. These fluctuations are undesirable as then can reduce the efficiency by causing the MPPT to be stuck in a local maximum power point rather than the overall maximum power point.

The first cause for a DC fluctuation across the bus is a result of a rapid change in the input power supplied. However, due to the nature of the sun and MPPT controllers which help regulate the DC voltage, this is not the primary concern which can reduce the efficiency.

The major concern which can cause fluctuations in the DC-bus voltage is the double line frequency ripple across the capacitor [41] , [42]. This occurs as a result of the pulsating output power downstream of the inverter. In order to minimize the 2nd order harmonics appearing across the DC-Link capacitor, a significantly large DC-Link capacitor is needed. However, if using film capacitors, the balance must be stuck due to their high cost.

4.4.4 Sizing

As a result of the pulsating output power from of the inverter (downstream), an AC signal occurs on the input side of the inverter stage (upstream). These harmonics pulsate at twice the frequency of the output and are known as second order harmonics. These harmonics can penetrate into the front end of the DC-DC boost converter which can reduce the overall efficiency of the inverter unless otherwise managed.

Assume the grid current and voltage are:

$$v_g(t) = \hat{V}_g \cos(\omega_g t) \quad \textbf{4-10}$$

$$i_g(t) = \hat{I}_g \cos(\omega_g t - \phi) \quad \textbf{4-11}$$

Instantaneous Power output from the grid is therefore,

$$P_{out}(t) = \hat{V}_g I_g \cos(\omega_g t)\widehat{\cos}(\omega_g t - \phi) = V_g^{rms} I_g^{rms} cos\phi + V_g^{rms} I_g^{rms} \cos(2\omega_g t - \phi) \quad \textbf{4-12}$$

Written another way,

$$P_{out}(t) = Scos\phi + S\cos(2\omega_g t - \phi) \quad \textbf{4-13}$$

Where S is the apparent power (VA). Assume (I) instantaneous power output from the inverter is equal to the instantaneous power input to the inverter. (II) DC-link voltage on the input has a nominal voltage of V_{dc}

Therefore,

$$P_{in}(t) \cong P_{out}(t) \quad \textbf{4-14}$$

$$V_{dc} * i_{dc}(t) = Scos\phi + S\cos(2\omega_g t - \phi) \quad \textbf{4-15}$$

Now assume the DC capacitance filters out the high switching frequency components in the DC current$i_{dc}(t)$, which can be separated into the DC component I_{dc} and an AC component $i_{dc,ripple}(t)$

$$V_{dc} * i_{dc,ripple}(t) = S\cos(2\omega_g t - \phi) \quad \textbf{4-16}$$

Rearranging yields,

$$i_{dc,ripple}(t) = \frac{S}{V_{dc}}\cos(2\omega_g t - \phi) = \hat{I}_{dc,ripple}\ \cos(2\omega_g t - \phi) \quad \textbf{4-17}$$

The capacitance can then be obtained given the magnitude of the maximum ripple voltage [43] :

$$C = \frac{S}{2*\pi*f*V_{dc}*\Delta V_{DC}} \quad \textbf{4-18}$$

Several solutions have been proposed to help solve the issue of large capacitors in single phase inverters. A few of these include; fly back converters for additional power decoupling, push pull types [44] and the use of proportional resonant controllers [45]. Each has its own advantages and drawbacks.

4.5 Inverter Topology Sub-circuit Design

The inverter circuit provides the second power stage within the overall circuit design. As with the first power stage, the following section will outline the necessary background information and the PSIM model.

4.5.1 Inverter Operation Introduction

Inverters are a sub-classification of the Power Electronics field [7, 39]. The IEEE definition of an inverter is "a machine, device or system that changes direct-current to alternating current" [8]. While this is broad classification, it helps to get a firm understanding. Inverters convert DC into AC. There are many different applications (grid connected/off grid), topologies of inverters, power stages, and firing circuits for inverters. While the classification of all these is beyond the scope of thesis, it is good to known and be aware of the basics. A full bridge (full AC) inverter, in its simplest form can be seen in the Figure 4-11 below.

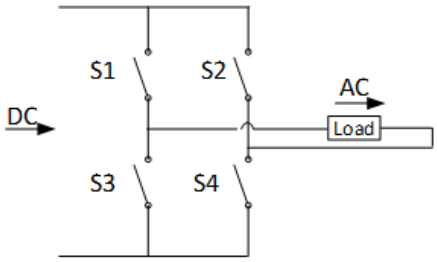

Figure 4-11: H-Bridge

Figure 4-11 shows one of the simplest AC inverter designs. The inverter is called an H-Bridge inverter as the switches are configured to look like an 'H' with the middle bar being the grid/load. This is an inverter in the ideal sense. Typically instead of ideal switches, FETs, transistors, etc. are often used, all of which exhibit some losses into the system.

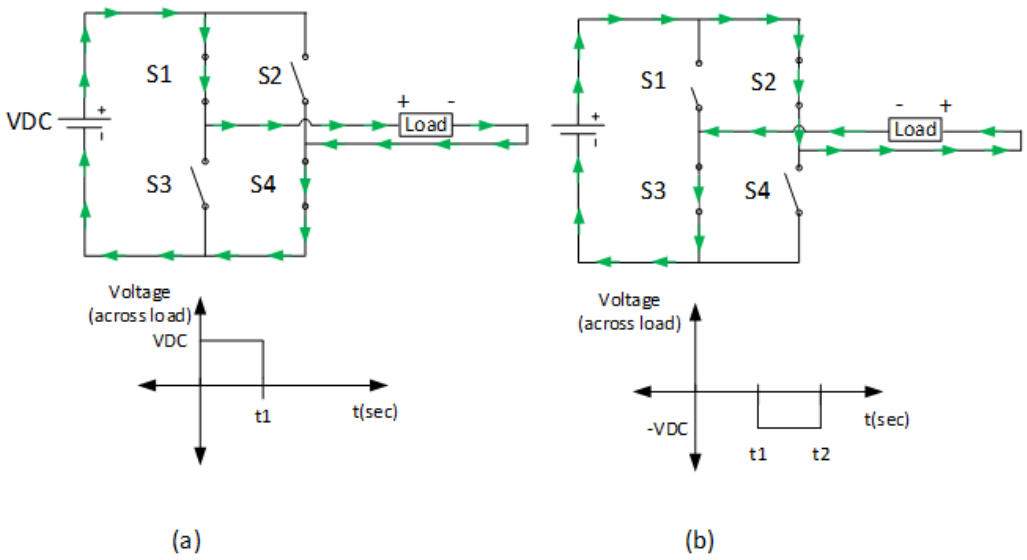

Figure 4-12: H-bridge Operation

In order for the system to generate AC voltage, first switches S1 and S4 are trigged to close. This allows a voltage to be applied to the load and current flows through. Since ideal case, the ideal switches are used which exhibit no internal resistances and the voltage applied to the load is equal that of the source. This occurs until t1 as seen in Figure 4-12a. At a certain period of time t1, switches S1 and S4 are re-opened. Thus the voltage is removed and current stops flowing. At this time, switches S2 and S3 are then closed. Therefore the voltage polarity across the load changes and current flows in the opposite direction. This occurs until another point in time, t2. At this time S2 and S3 are reopened, while S1 and S4 are re-closed and the process continues. Combining these two cases creates a square wave output across the load. While, the square wave generation is seldom used as most electronic devices cannot operate using this method [39, 7], it is useful and provides a basic understanding of how the inverter operates. Different firing schemes can be used in order to have the inverter output a sinusoidal wave and will be discussed in section 4.6.

4.5.2 **PSIM MODEL**

For this design, a full h-bridge inverter was chosen in order to simplify the overall design of the micro-inverter.

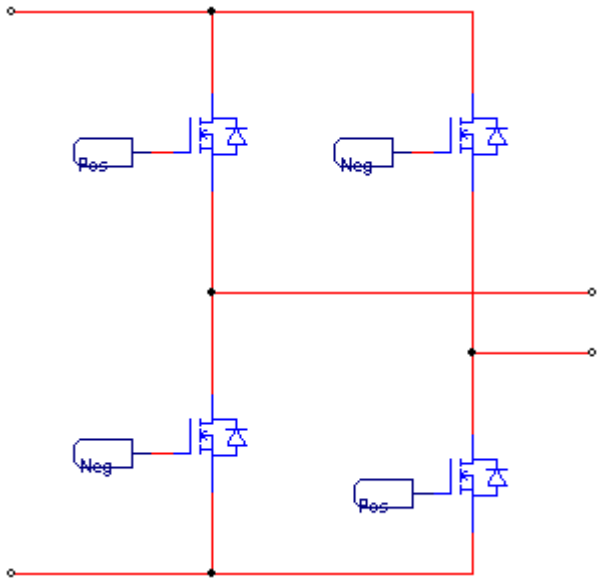

Figure 4-13: PSIM Model H-Bridge

The two wires on the far left hand side of Figure 4-13 are the connections to the positive and negative high voltage DC rails. The two wires on the bottom are the connections to the SPWM sub-circuits. Finally the two on the right hand side are the output of to the load.

4.6 SPWM Design

4.6.1 **Overview**

In order to trigger the Mosfets for an H-bridge configuration, a method is needed. Varying the duty cycle for the pulses being applied the Mosfets allows for a pure sine wave to be obtained with addition of a filter. The pattern at which the pulses can vary depending on which method being used. However they all can be implemented easily within a digital micro-controller, analog circuitry, or FPGA as seen in [46].

4.6.2 **SPWM**

SPWM switching is a widely used method for triggering inverters due to its simplicity, effectiveness and overall performance characteristics. In order for it to operate, upper and lower switches in the same inverter leg (S1 and S4, then S2 and S3) are turned on while the others are turned off. Because of this, only two reference signals were chosen: a reference modulating sine wave v_m (to be linked with the PLL and discussed in section 3.10) and a triangular carrier wave v_{cr}.

4.6.3 **PSIM MODEL**

The firing circuits for inverters vary depending on the semiconductors used as well as the desired output. For instance, square wave inverters can be triggered with 555 timer circuits or by the use of more specialized

integrated circuits (ICs). For the chosen inverter design, using a sine pulse width modulation circuit was chosen. This can be seen in the Figure 4-14 below.

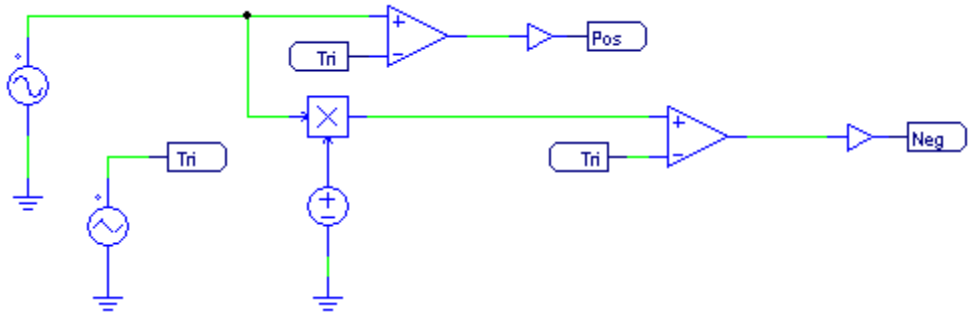

Figure 4-14: SPWM PSIM MODEL

The Figure 4-14 above shows the circuitry utilised for the trigerring circuit. Two signals are generated and compared to one another. The first is a sine wave genertor, represented by the source of the far left hand side of Figure 4-14. The second source is a triangluar wave generator shown in the bottom left hand corner of Figure 4-14. The triangluar wave is operating with a peak-to peak voltage of 10V and 20kHz. The sine wave generator is operating at the desired 60Hz frequency. The output of these two signals are sent to the comparator and trigered for every positive cycle. A pulse is created when the output of the sine wave is greater than that of the triangular wave for a positive cycle. This effectivly tirggers the gates of the inverters in switches Q1 and Q3, allowing current to flow in that direction of the inverter. In order for current to flow in the other direction of the inverter, Q2 and Q4 gates need to be triggered. This is accomplished by inverting the sine wave and comparing it with a second comparator cicuit.

4.7 Filter Sub-circuit Design

4.7.1 **Overview**

Filters are essential parts of most electronic circuits and controls systems as they play a vital role in a variety of circuits and applications [47] . In circuit theory, a filter is a device that can attenuate the amplitude of a signal with respect to is frequency. In the ideal case, a filter will change the relative amplitude of various frequency components while not adding new frequencies to the input signal. Filters are often used in electronic circuits to emphasise certain frequencies of an input signal while rejecting the other frequencies.

4.7.2 **Inverter Need**

With respect to the inverter, filters provide a fundamental tool necessary to connect to the grid and meet the government standards. IEEE 1574 which states that inverters must have a THD of less than 5% [11].

In order to convert the SPWM signal into a pure since wave, a filter is needed to tune out all the high frequency pulses resulting from the switching and let a 60Hz signal pass.

4.7.3 **Topologies**

There are many different types of filters used for single phase inverters. Each type has its own benefits and drawbacks. Below is a table, completed from a literature review which outlines a few of the benefits and drawbacks of the three major types of filters, the L-filter, LC-filter and LCL-filter.

Filter Type	**Benefits**	**Drawbacks**	**References**
L– Filter	- Low cost - Simple to use	- Voltage drop across the inductor makes a poor system dynamics and consequently a long response time - Low attenuation - High inductance value - Switching frequency of the inverter must have a high value in order to sufficiently attenuate the harmonics - Since low attenuation of the inverter, a shunt element is needed to further attenuate the switching frequency components	[48]
LC-Filter	- Suited to configuration where the load impedance across the capacitor is relatively high at and above the switch frequency. - Higher attenuation	- Very high capacitance is not recommended, since the system may face in rush current - High reactive current fed on capacitor at the fundamental frequency.	[48]
LCL-Filter	- Better attenuation yet still at inverter switching frequency - Better decoupling between the filter and grid impedance - Low ripple current distortion across the grid side inductor since the current ripple Is reduced by the capacitor	- Third order equation, more difficult - More components - Has to consider various constraints, such as resonance phenomenon, the current ripple through inductors, total impedance of the filter, current harmonics attenuation at switching frequency	[48], [49]

Table 4-1: Filter Topologies Advantages and Drawbacks

Table 4-1 above shows the benefits and drawbacks for single phase inverter filters obtained through the literature review. The literature review was done on the most common three types; however, other methods of filters such as the LLCL filter [50] exist but are not as common. Originally it was planned to use an LC filter, this was revised as it was not as effective and required larger value components. This was then modified to an LCL filter during design phase for the inverters as it had smaller values, better attenuation and low ripple current distortions.

4.7.4 **Governing Equations**

The following section outlines the filters governing equations and process to iterate to the correct component values.

4.7.4.1 Transfer function

The following section outlines the transfer function for the inverter filter.

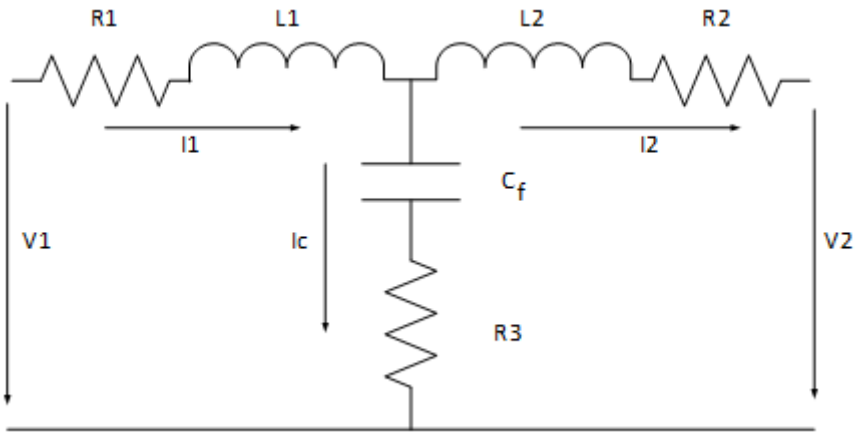

Figure 4-15 Filter Model

Figure 4-15 above shows the model of the LCL filter, and below shows the transfer function derived.

$$\boldsymbol{G(s) = \frac{i_2(s)}{v_1(s)} = \frac{R_3C_fs+1}{L_1L_2C_fs^3+(L_1+L_2)R_3C_fs^2+(L_1+L_2)s}} \quad \textbf{4-19}$$

4.7.4.2 Equations

The following section outlines the formulas used to calculate the values for the LCL filter as proposed by [48] [49]:

The resonant frequency is,

$$\boldsymbol{\omega_{res} = \sqrt{\frac{L_1+L_2}{L_1L_2C_f}}} \quad \textbf{4-20}$$

Total Filter Inductance calculation is given by,

$$\boldsymbol{L = \frac{V_{dc}}{4\, I_{rated}\Delta_{ripple}f_s}\,(1-m_a)m_a} \quad \textbf{4-21}$$

Where $I_{rated}$the rated utility is current, Δ_{ripple} is the maximum ripple percentage (5-25%), V_{dc} = voltage DC link, f_s is the switching frequency, m_a is the modulation index [48] [49].

By adding a second inductor, the inductor is divided into two parts based on the following equation.

$$\boldsymbol{L_1 = aL_2} \quad \textbf{4-22}$$

Where a (a≥1) is the inductance index calculated using the switching harmonic current attenuation ratio below:

$$\boldsymbol{\sigma = \frac{i_2}{i_1} = \frac{(1+a)r}{a(1-r)-r}} \quad \textbf{4-23}$$

Where,

$$\boldsymbol{r = \frac{1}{L_2 C_f \omega_{sw}^2}} \quad \textbf{4-24}$$

In addition,

$$\boldsymbol{\frac{r}{1+a} = \frac{\Delta_{ripple} V_{rated} \omega_0}{2\pi^2 V_{dc} f_{sw} a}} \quad \textbf{4-25}$$

Where Δ_{ripple} is maximum ripple magnitude percentage (5%-25%) [48] [49], V_{rated} is the rated utility voltage, a is the reactive power factor, ω_0 is the utility frequency.

Filter capacitance can be found through the following equation,

$$\boldsymbol{C_f = \frac{Q_{re}}{\omega_0 V_{rated}^2} = \frac{a\, P_{rated}}{\omega_0 V_{rated}^2}} \quad \textbf{4-26}$$

Finally the damping resistor can be found from the following formula,

$$\boldsymbol{R_3 = \frac{1}{3\omega_{res} C_f}} \quad \textbf{4-27}$$

4.7.4.3 Procedure

The following provides the iterative procedure for selecting component values for the LCL filter. This procedure utilizes formulas 4-19 - 4-27.

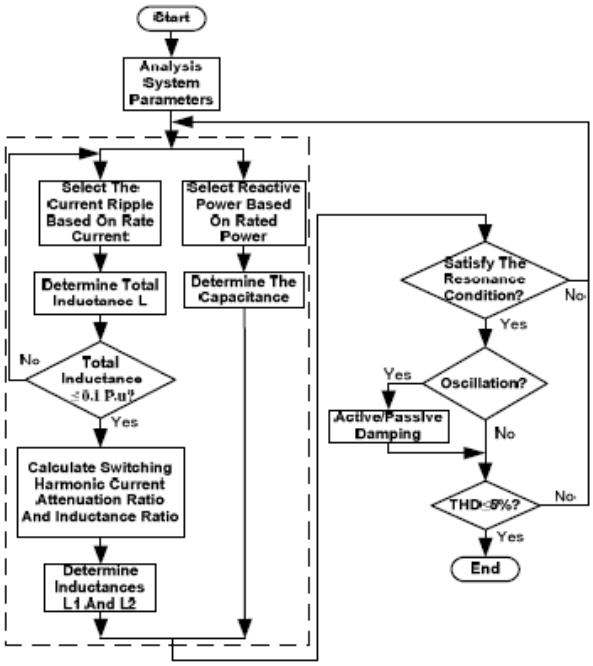

Figure 4-16 Iterative Filter Design [48]

The following procedure is outlined in [47] as a method to first calculate and then manually converge onto the appropriate values for the filter. This iterative process was used for the selection of the filter components for both designs.

4.7.5 **PSIM MODEL**

The following is the PSIM filter model created for the inverters. Similar to the other PSIM models, the internal resistances were included.

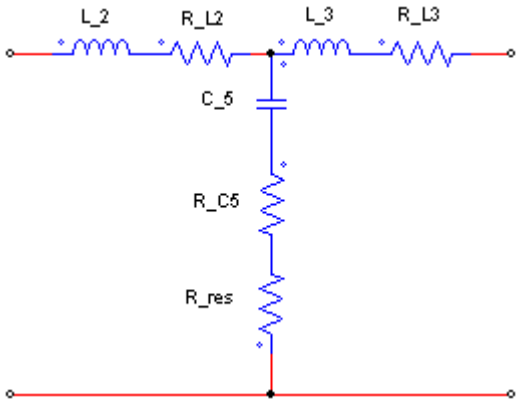

Figure 4-17: PSIM LCL Filter

This filter was chosen and designed such that a 60Hz signal can pass through effectively and higher frequencies are attenuated. In addition to functioning values, sizes were chosen than can be easily acquired from manufacturers and are readily available for purchase.

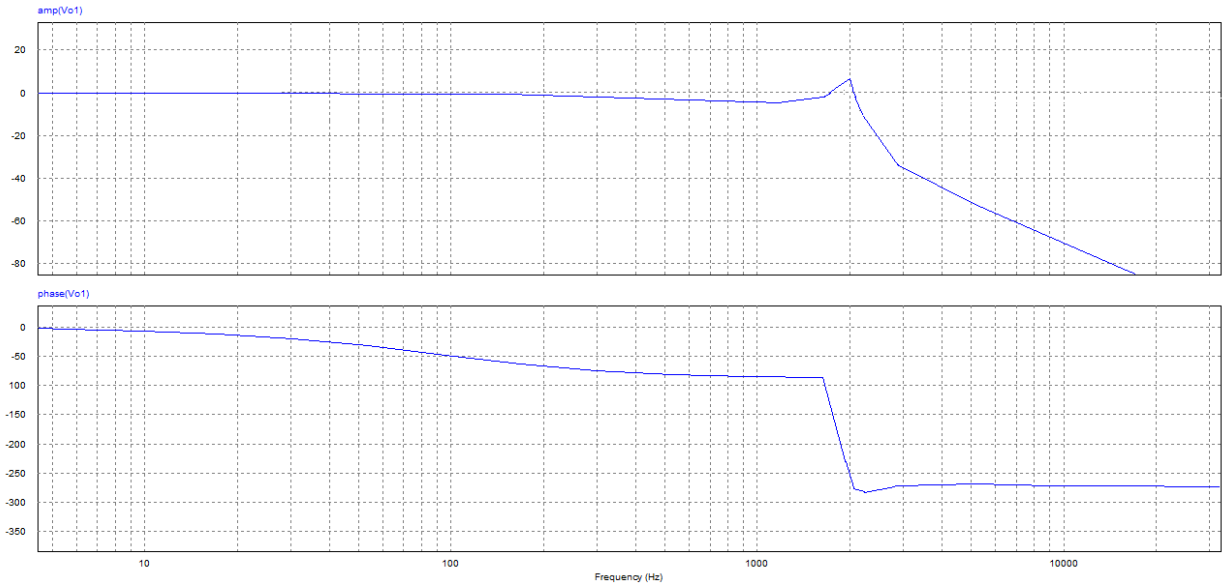

Figure 4-18: Frequency Analysis of Filter

Figure 4-18 above shows the frequency analysis of the filter for the 300W micro-inverter. It can be seen that for the current (top graph) is low pass filter which passes the 60Hz and regrets the high order frequencies. This filter helps smooth out and turn the SPWM into a sinusoidal signal and helps reduce harmonics in the output. It also follows the same trend as shown in by [48] [49].

4.8 Over/Under Voltage Protection Sub-circuit Design

IEEE Standard 1547 states that the output voltage and THD from a distributed generation source must be <5% [11]. Therefore a controller in needed in order to provide a failsafe in case the difference exceeds 5%. This control circuit was designed in order to meet that need. The control circuit turns on (outputs high) if the voltage difference between the inverter and grid greater than 5% for 1ms. This time (1ms) can easily be modified if desired to increase/decrease the time response.

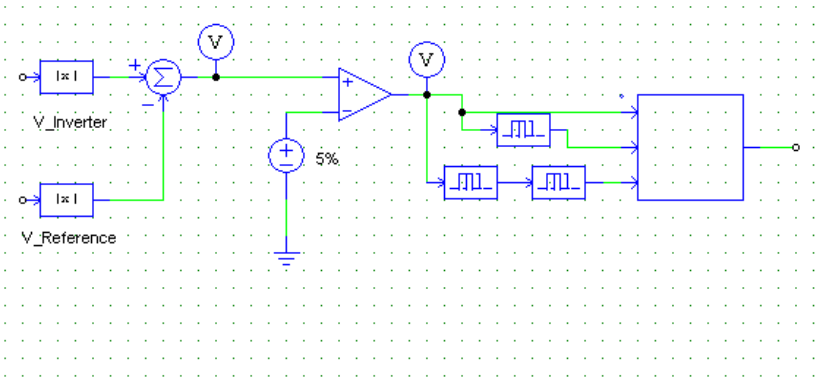

Figure 4-19: Over-Voltage Protection Circuit

Figure 4-19 above shows the over voltage protection scheme. The inverter voltage reference is taken at the output of the Mosfets and then compared to the grid reference voltage. Both signals are turned into absolute values in order to check for all positive and negative portions of the cycle. An error signal is created from the subtraction the two signals against each other. This error signal is then sent to a comparator, which compares the results to a reference value of 5% of 120Vrms. The output of the comparator is then sent to the C-Block module in PSIM. The block contains the programming logic for the controller. Two of the error signals are sent to time delay blocks before the C-block. The time delays work as a signal storage section, taking previous values in order to see how long the pulse (over threshold voltage) has been on for. They are set to a value of 0.00055seconds each. The C-Block is monitoring the three input values from the error signal. If all three signal inputs to the block are high, then the C-Block outputs a digital high in order to shut down the inverter and disconnect it from the grid.

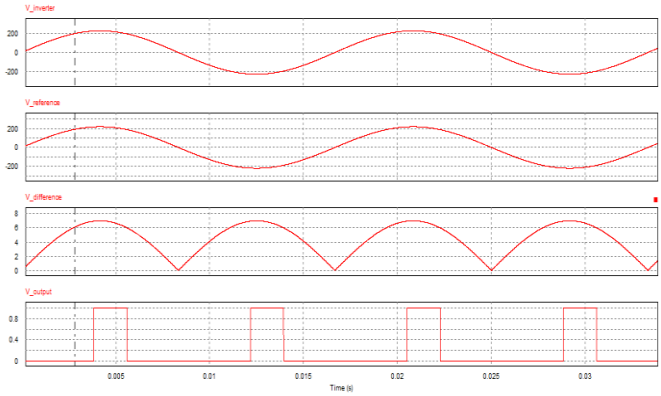

Figure 4-20: Over-Voltage Protection Working

Figure 4-20 above, shows the outputs of the over/under voltage protection sub-circuit. The top most graph shows a signal representing the inverter voltage signal. The second from the top shows a signal representing the reference signal. The third from the bottom shows the difference between the two signals. Finally the bottom most circuit shows the output of the controller sub-circuit. It can be seen from the bottom most figure, that the output turns high after approximately 1ms, the counter being started at the time position of the vertical line on all four figures.

4.9 Maximum Power Point Tracking Control Loop Design

4.9.1 **Purpose**

Maximum power point tracking is a term used for techniques deployed to PV in order to extract the maximum power output available from the solar panels. The need for MPPT arises as solar cell V-I characteristics are nonlinear and can fluctuate from environmental conditions. Despite this, there is a specific point (Maximum Power Point or MPP) at which the maximum power of the solar panel can be extracted at the current environmental conditions. Consequently at this specific point, the maximum output can be sent to the grid. While this MPP is not known, it can be found with the application of MPPT techniques.

There are many different of MPPT techniques and methods, a few of the most notable are: fixed duty cycle, P&O, IC, constant voltage, fractional open-circuit voltage, modified open circuit voltage, pilot cell, fuzzy logic, and neural networks [51]. Two of the most commonly used are briefly described below.

1) Perturbation and Observation (P&O)

For this method, the controller adjusts the voltage by a small increment, after it has, it then measures the output power from the solar panel. If the power increases, the controller adjust the voltage again as to keep moving in that direction. The controller will keep making adjustments this direction until the power output no longer increases in value. Then is will move in the opposite direction. This is known as perturb and observe and is arguable one of the most common methods due to: its ease of implementation, high and quick tracking capabilities. A drawback of this method however is that when shadows occur onto a solar panel, several peaks may occur. This can then cause the Perturbation and Observation method to become stationary around a local maximum which might not be the actual maximum output power achievable. In addition it can produce small oscillations in the output power around the maximum point as it is continually searching by increasing or decreasing the voltage. This tendency makes it oscillate around the MPP. These oscillations can be minimized be reducing the step size; however this results in a longer time need to locate the MPP. Despite this drawback, this remains one of, if not the most popular methods for MPPT [52].

2) Incremental Conductance (IC)

Incremental conductance is another popular technique used for MPPT. This method measures the incremental changes in PV current and voltage (similar to P&O) to predict the effecting change. The algorithm is based off of the equation

$$\left(\frac{dI_{pv}}{dV_{pv}}\right) + \left(\frac{I_{pv}}{V_{pv}}\right) = 0$$

Where $I_{pv,}\, V_{pv}$ are the solar panel current and voltage. It can be verified that the system is currently to the right hand side of the maximum power point, if $dI_{pv}/dV_{pv} + I_{pv}/V_{pv} < 0$. In addition, if $dI_{pv}/dV_{pv} + I_{pv}/V_{pv} > 0$ then the system is operating on the left hand side of the MPP. This is the founding theory behind the incremental conductance MPPT algorithm. When both vales are the same, the maximum power point has been reached. The algorithm then holds the value here and repeats the process. This algorithm responds quicker than the P&O method, however it comes at a drawback of requiring higher computation power. In addition, this method can also produce oscillations around the MPP as it continually is assessing and responding.

4.9.2 **Choice in Method**

For the purposes of this thesis, the P&O method was utilised. The reason for this are, firstly PSIM has a pre-existing control circuit designed which can be used, second this method is easy to implement and deploy to hardware as shown in [52] [53]. Finally this method was chosen because it has the highest amount of energy transfer among all the different algorithms (Constant Voltage Method, Incremental Method, Short Circuit Method, Open Voltage) [54]. Taking this all into account, the P&O method was the preferred method to be used.

4.9.3 **PSIM Model**

The following section shows the pre-existing MPPT P&O method available within PSIM.

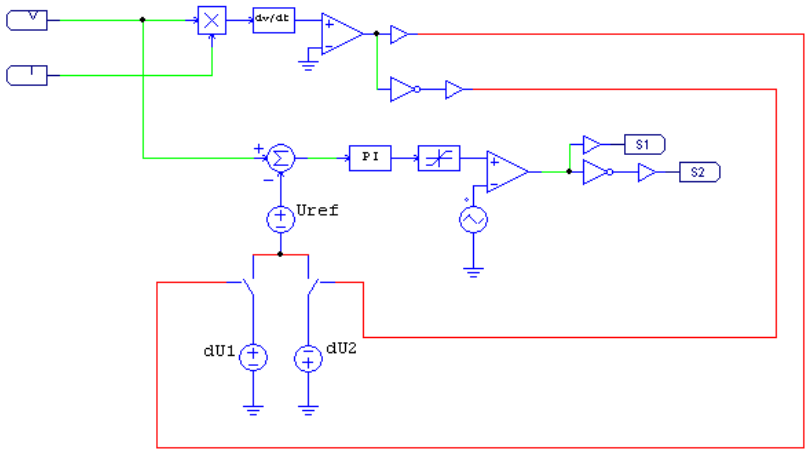

Figure 4-21 PSIM's MPPT Model

Figure 4-21 above shows the PSIM MPPT model incorporated into the design of the overall inverter. The PSIM model samples the voltage and current, takes the derivative and compares the results to zero. If the result if above zero, the system will trigger the dU1 switch to close, thereby increasing the voltage reference. If the result is below zero, then the inverse dU2 switch is triggered and the reference decreases in voltage. The error signal between the voltage and voltage reference is then sent to a PI controller and comparator as per the control theory explain in the boost converter section.

4.10 Grid Synchronisation -Phase Locked Control Loop Design

4.10.1 **Overview**

As covered in section 2.5, PLL are a critical control systems for grid connected micro-inverters as they are needed in order to synchronise with the grid voltage. For the purposes of this design, a PLL based off of trigonometric transformations was used. This design was originally proposed by [33], [34]. The advantages of this PLL is its insensibility to changes of amplitude in the input signal after synchronisation has occurred, reduced settling time for frequency changes, reduced settling time for phase changes and ease of implementation into hardware and software [33], [34].

4.10.2 **Operational Theory**

As stated above, one of the major advantageous of this proposed PLL is it insensibility to changes in the input after synchronisation has occurred. This is because most often disturbances have a short duration and usually consist of incrementing or decreasing the voltage.

The assumption for this method is that,

$$v_{in} = U_M \sin v$$

$$v_{sync} = \sin \hat{v}$$

With this in mind, then the operation of the proposed PLL is based open the following mathematical equations [33], [34]:

$$\boldsymbol{U_M \sin v \,.\cos \hat{v} = U_M \frac{1}{2}[\sin(v - \hat{v}) + \sin(v + \hat{v})]} \quad \textbf{4-28}$$

$$\boldsymbol{-U_M \cos v \,.\sin \hat{v} = -U_M \frac{1}{2}[\sin(v - \hat{v}) + \sin(v + \hat{v})]} \quad \textbf{4-29}$$

After summing equation 3-26 and 3-27 the basic trigonometric relations can be obtained,

$$\boldsymbol{U_M \sin v \,.\cos \hat{v} - U_M \cos v \sin \hat{v} = U_M \sin(v - \hat{v})} \quad \textbf{4-30}$$

Equation 4-30 is incorporated into the standard PLL model as shown in Figure 4-22 below:

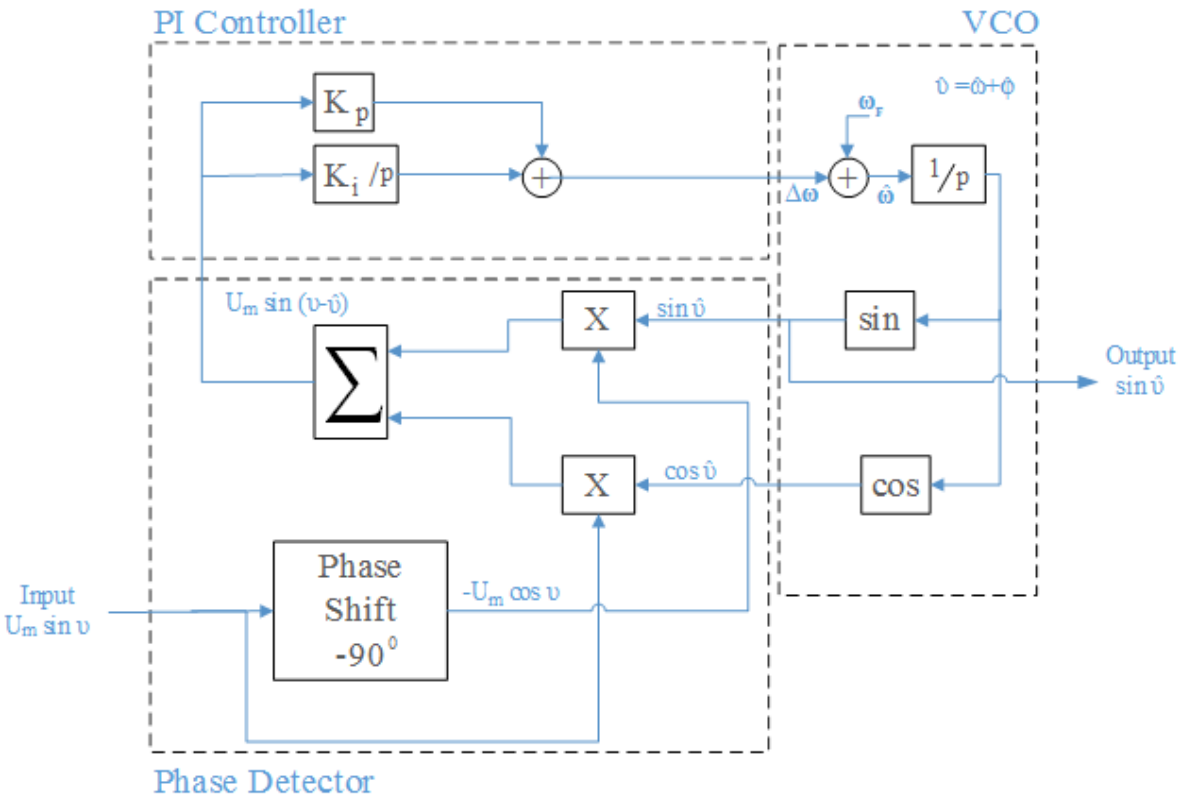

Figure 4-22: PLL Mathematical Model as [33], [34]

The operating principle is such that the right hand side of equation 4-30 is used as an error signal for the closed loop PLL. This signal is then sent to the PI controller which then changes the values of the input signal to the VCO. This process continues until the phase difference and frequency between the input and output signal goes to zero. After which, the PI controller is equal to zero and the steady state operation has been reached.

4.10.3 **PSIM MODEL**

In order to simulate the PLL a model was created in PSIM according to the equations and methods proposed in [33] [34].

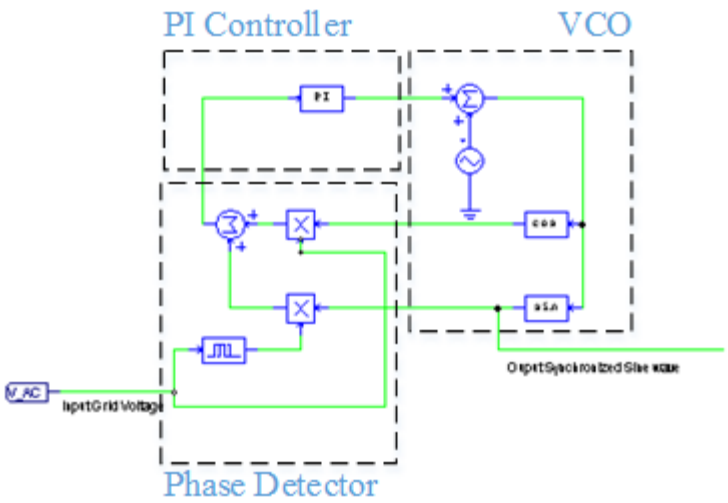

Figure 4-23: PSIM PLL Model

Figure 4-23 shows the components of the PLL built in PSIM. The simulation model contains: a summer block, PI block, multipliers, sine wave, cosine wave, and a time delay block. The time delay is acting as a phase shifter and generates a cosine wave feeding into cosine multiplier. The multipliers are the right hand side of equation 4-30 and then feed into a PI block. This block preforms the operation of being the PI regulator in the PLL. The output of the PI is then fed into the VCO portion which outputs a sine wave. In addition the output sine wave is also fed back to the beginning in order to compare with the input reference signal.

4.10.4 **PSIM MODEL with SPWM**

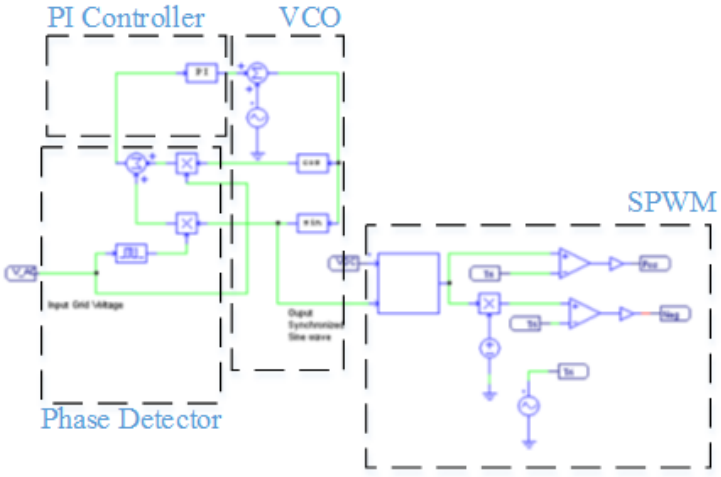

Figure 4-24: PSIM PLL Model with SPWM

The following Figure 4-24 shows how the PLL is integrated into the overall circuit and connected to the SPWM. The output of the PLL is a sine wave synchronised to the input signal (voltage source from the grid) and this is used as the reference sine wave signal for the SPWM sub-circuit. Outputs for the SPWM are then sent to the triggers of the Mosfets in the inverter power stage.

4.11 300W Overall Circuit Design

The following section outlines the overall 300W micro-inverter designed in PSIM. First the PSIM design is shown, this is then followed by the bill of materials, and the simulation results.

4.11.1 **PSIM Circuit Design**

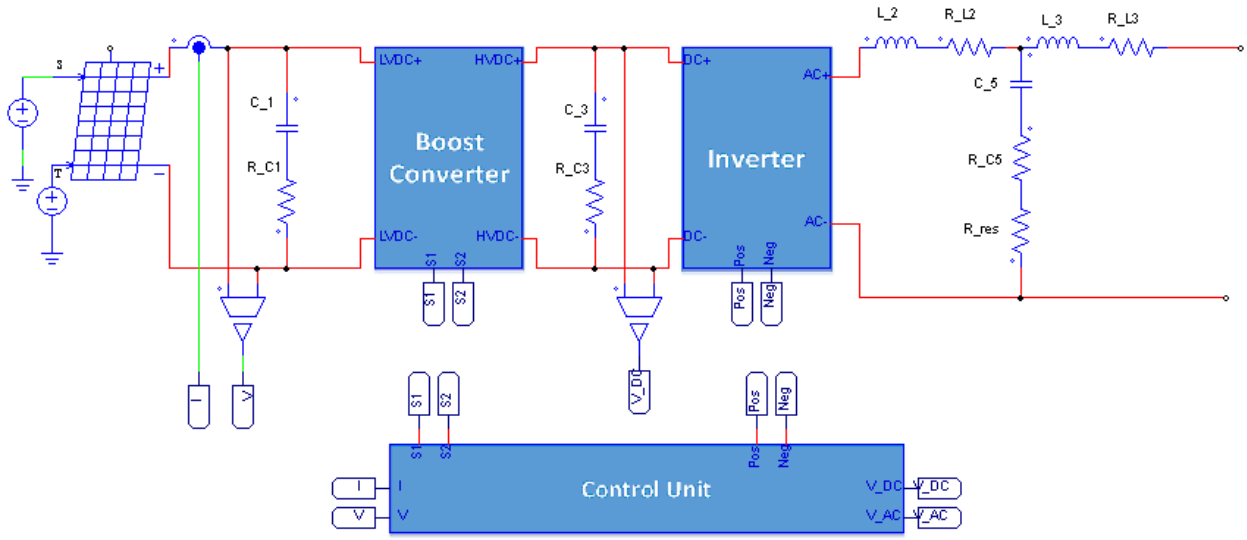

Figure 4-25: 300W Micro-Inverter PSIM Model

Figure 4-25 provides the overall circuit design for the 300W inverter in PSIM. Starting from left to right it can be seen the solar panel is followed by the first DC link. Next is the first power stage, followed by the second DC link. Next is the second power stage which contains the H-bridge inverter sub-circuit as shown in section 4.5. Last on the far right hand side is the output LCL filter. The blue square on the bottom shows the inverters control circuit unit. This unit contains the control circuits shown in sub-sections 4.8 to 4.10 within it.

4.11.2 **Components**

The following section lists the components needed in order to construct the design of the 300W micro-inverter.

Circuit ID Number	Component Description	Operating Conditions	Component Values	Manufacturer	Maximum Conditions	Amount needed	Cost per unit ($CAN)
C_1	DC link capacitor	0-46V 0-62.8mA	4.7µF	Panasonic ECA2CM4R7	0-160V 0-78mA (9.1mΩ)	1	0.49
L_1	Boost inductor	0-210V 0-8.3A	9mH	Wurth Elektronik	0-250V 0-13A (15mΩ)	1	34.98
C_2	Boost Capacitor	0-210V 0-6A	10mF	Electronicon E50.R29-505NTO	600VDC 100A (0.72mΩ)	2	70.65
S1-S6	Boost + Inverter N-Channel Mosfets	0-195V 0-8.5A	N/A	Sanken SKP253VR	250V 21A (95mΩ)	6	2.425
C_3	DC link capacitor (high voltage)	0-210V 0-6A	5mF	Electronicon E50.R29-505NTO	600VDC 100A (0.72mΩ)	1	70.65
L_2	Filter inductor	0-400V 0-7.5A	390µH	J.W.Miller 1140-391K-RC	0-9A (0.082Ω)	1	10.82
L_3	Filter Inductor	0-120V 0-3.48A	100mH	Hammond 195T5	0-5ADC (0.64Ω)	1	135.44
C_4	Filter Capacitor	0-205V 0-5A	18.3µF	TDK B32794D3205 (3.3µF)	300Vrms 630VDC (ESR 9.7mΩ)	1	1.45
C_4	Filter Capacitor	0-205V 0-5A	18.3µF	TDK B32794D2156 (15µF)	250Vrms 700VDC (ESR 3.1mΩ)	1	6.67
R_res	Filter resistance	0-11V 0-5A	2Ω	Bourns PWR263S-20	2Ω 20W	1	3.51
Control Chip	MPPT + PLL chip	0 - 42V 0-8.73A 120V AC 2.5A AC	N/A	Texas Instruments TMS320 F28027-FPTQ	-0.3-4.6V	1	16.43
Current Sensor (boost)	Boost Converter	0 - 42V 0-8.73A	N/A	Allegro MicroSystems ACS712 ELCTR-20A	20Arms (100mV/A)	1	2.69
Current Sensor	PLL	120V AC 2.5A AC	N/A	Honeywell CSLA2CD	72 Arms (32.7mV/N)	1	37.03
						Total	476.01
Extras and Reserve	PCB, wires, resistors, heat sink. Etc.)						+15%
						Estimated Total	547.42

Table 4-2: 300W Inverter Bill of Materials [55] [56]

Table 4-2 provides each of the components part number, specifications, operating condition and unit cost. All components can be found directly from the Mouser and Digikey websites [55], [56]. In order to estimate the unknown costs for the project, an extra 15% was assumed and added to the total as a cost contingency. This brought the total cost of the micro-inverter to $547.42. This value is high, however this is for two main reasons, unit prices were used and components were not quoted for bulk purchase. Secondly the cost contingency added for the estimate.

4.11.3 **Results**

The following section outlines the simulation results for the 300W micro-inverter.

4.11.3.1 Steady State Operation

The first section depicts the steady state operation of the micro-inverter.

4.11.3.1.1 Solar Panel Input

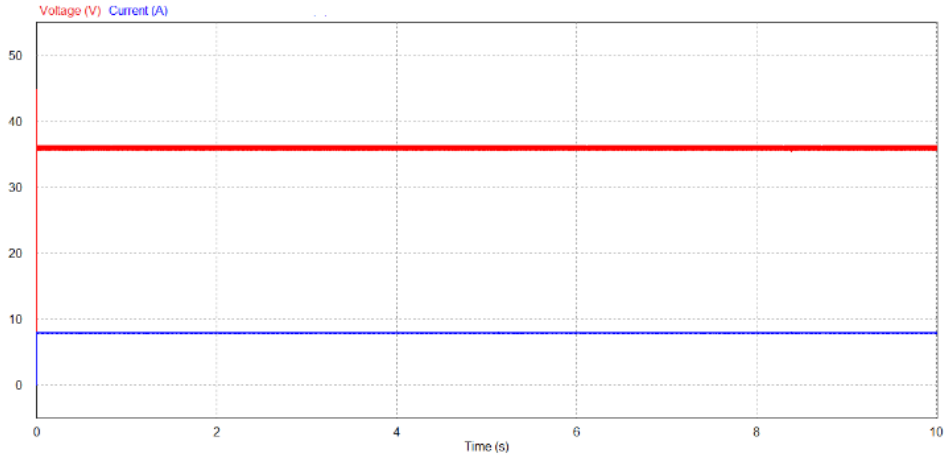

Figure 4-26: 300W Micro-inverter Solar Panel Input

Figure 4-26 shows the output of the solar panel, or input into the inverter. It be seen that the MPPT is working by keeping the voltage around 36V and 8A. The thick red line represents the voltage (top) and blue current (lower). From the figure it can be seen the MPPT is oscillating from the P&O method with minor changes in voltage. These oscillations occur with a peak to peak of approximately +/- 0.5V. The voltage noise can be reduced further, however this would come at a cost of increasing the input filter capacitance and therefore increasing the cost of the overall design.

4.11.3.1.2 Boost Converter

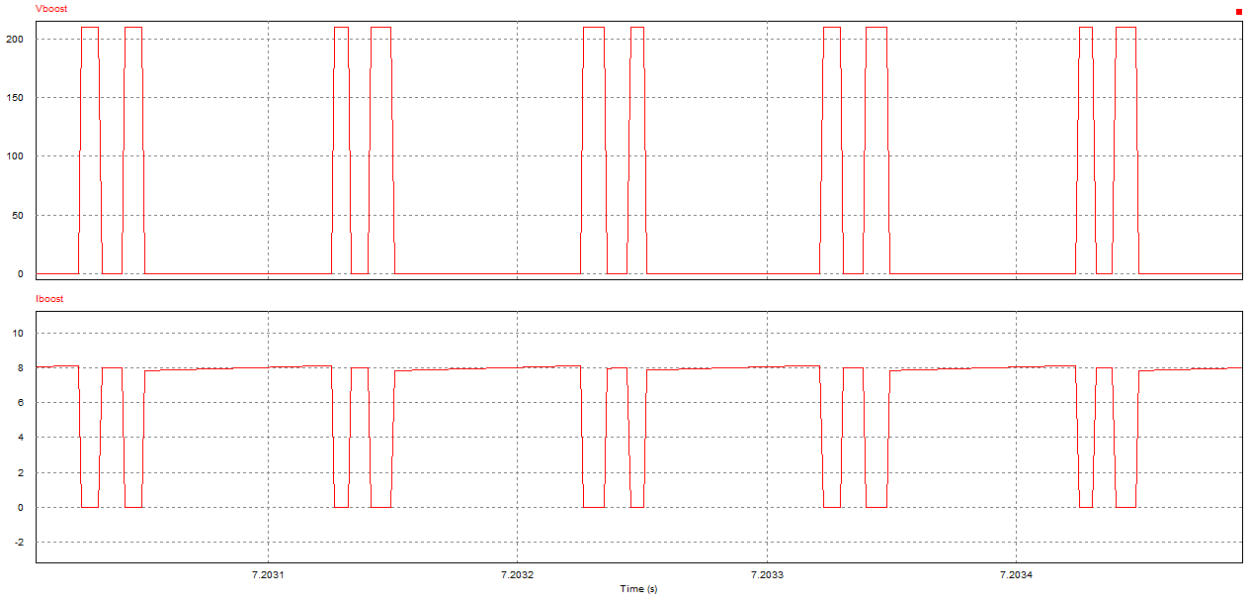

Figure 4-27: 300W Boost Converter

The following Figure 4-27 shows the results of the boost converter. The voltage (top) shows the results of the output voltage (from the inductor). The current (bottom) shows the current passing through the Mosfet which is pulsated on/off – shorting the inductor to ground. In addition to the losses in the internal resistances, there is some switching losses with the circuit.

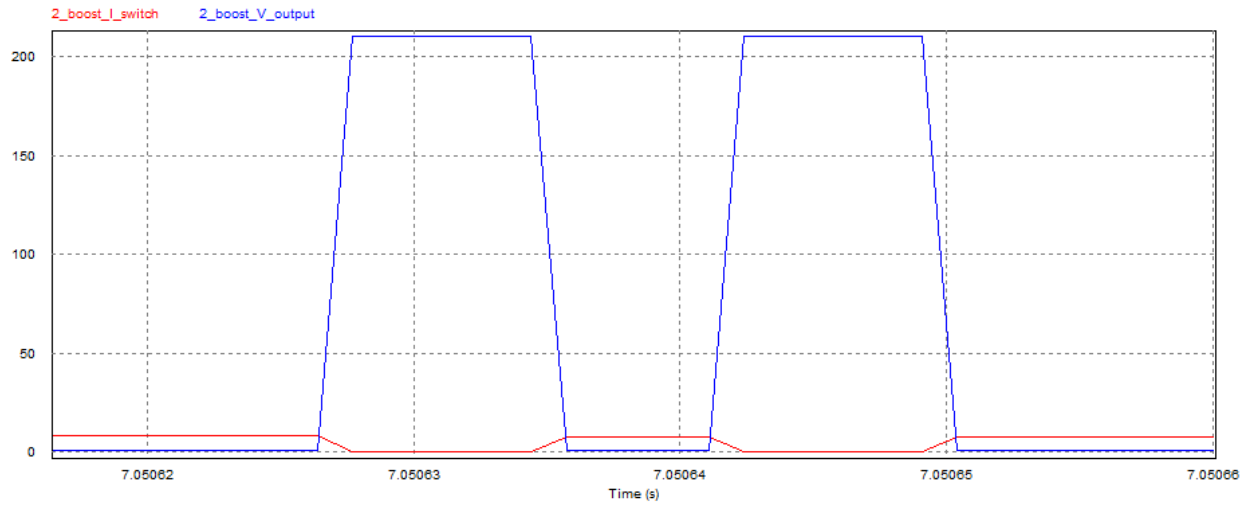

Figure 4-28: 300W Boost Converter Switching Loss

Figure 4-28 provides the overlapping of voltage and current and constitutes the switching losses of the boost converter. They contribute to a loss of approximately 4W in the overall circuit.

4.11.3.1.3 DC Link Voltage

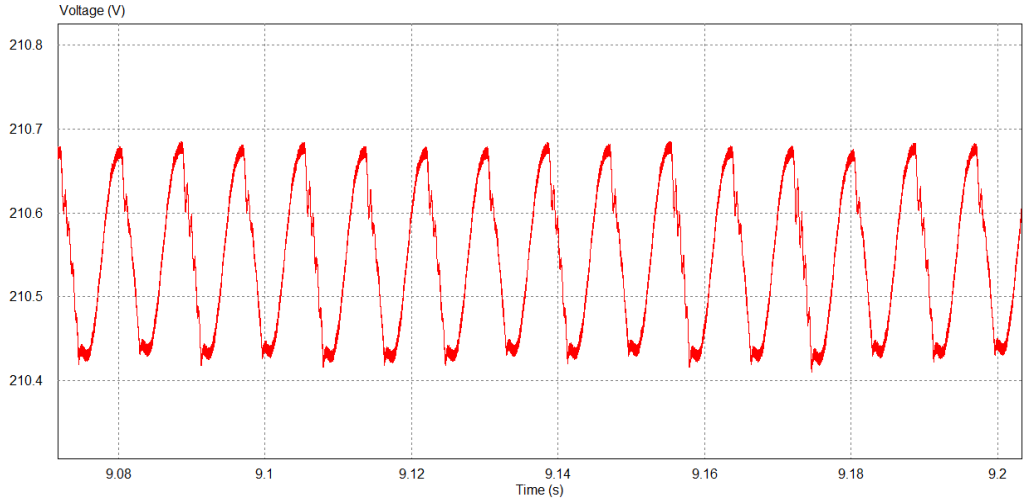

Figure 4-29: DC Link Voltage

Figure 4-29 shows the voltage across the DC link connecting both power stages together. The pulsating is due to the 2nd order harmonics of the circuit. However to minimize the harmonics, a little larger capacitor was used. The fluctuations can be seen to be around +/- 0.5V.

4.11.3.1.4 SPWM Firing Circuit

The following Figure 4-30 shows the results for the SPWM firing circuit integrated together with the PLL.

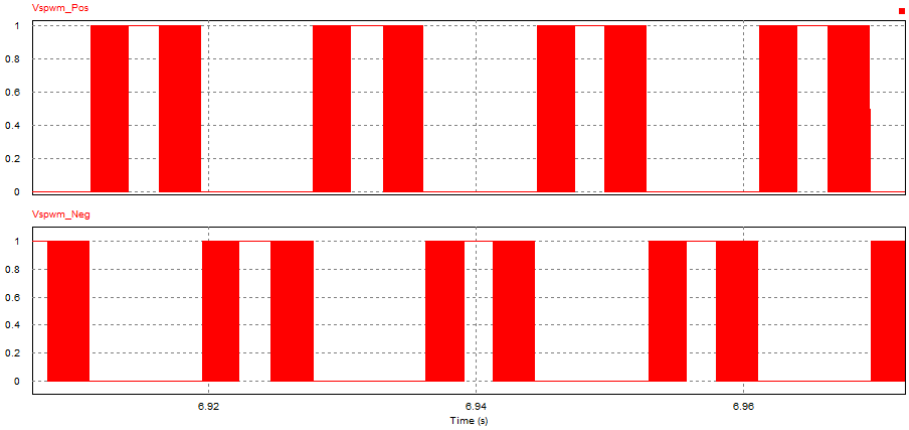

Figure 4-30: 300W Inverter SPWM

The top graph shows the results for the positive cycle (S1 and S4), while the bottom figure shows the results of the negative cycle (S2 and S3). The large red figures on the sides correspond to the fast firing rates of the circuit and consists a multitude of high frequency pulses.

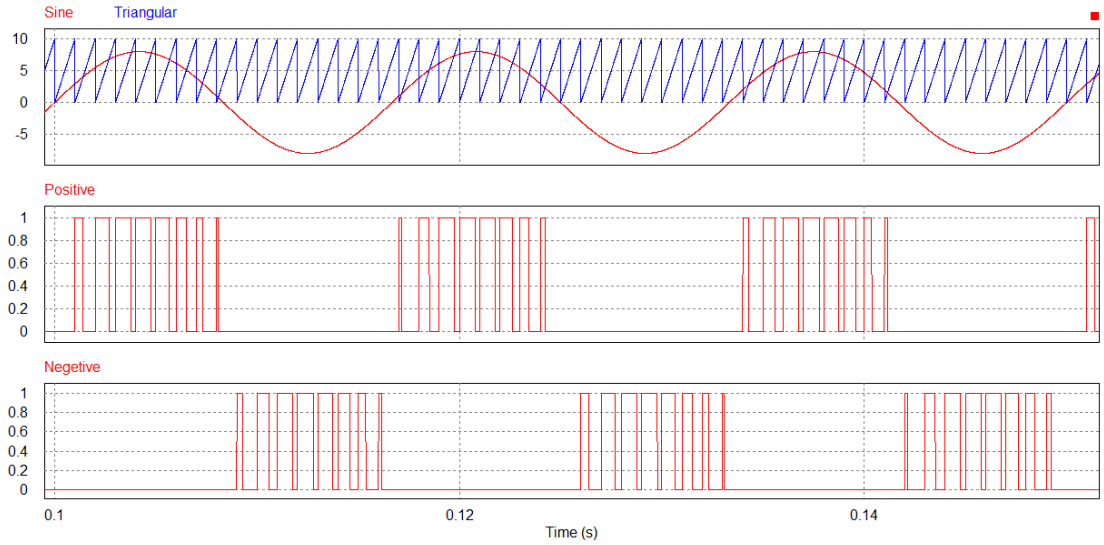

Figure 4-31: SPWM with reduced firing rate

In order to better depict what is occurring within the SPWM model designed, the triangular duty cycle was reduced. Reducing the duty cycle of the triangular wave generator from the normal operating value of 20 kHz down to 1 kHz, the following Figure 4-31 can be obtained. The modulating frequency of the input signals is 0.8 and this remains consistent during normal both simulations. The top most graph shows the inputs to the SPWM. The middle graphs show the output of the SPWM sent to trigger Mosfets S1 and S4 for every positive portion of the reference sine wave. The bottom most figure shows the output of the SPWM sent to trigger Mosfets S2 and S3 for every negative portion of the reference sine wave.

4.11.3.1.5 Inverter Output

Finally the output results of the micro-inverter are shown for steady state operation. This can be seen in the figure below.

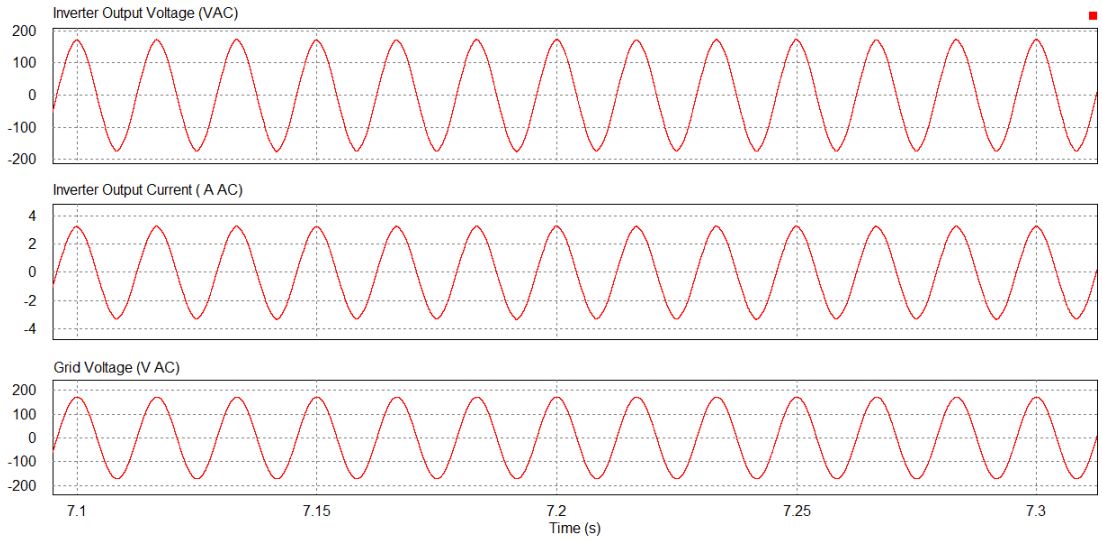

Figure 4-32: 300W Inverter Output

The top most figure of Figure 4-32 shows the micro-inverter output voltage. The middle graphs shows the output current of the inverter system and the bottom most figure shows the grid reference voltage. It can be seen in the figure that synchronisation has taken place and the system is working in unison. The RMS for the grid is 120Vrms, inverter output is 120.1Vrms and 2.27Arms.

4.11.3.2 Transient Operation

The following section demonstrates the transient operations of the designed micro-inverter.

4.11.3.2.1 Phase Synchronization

The first transient scenario to be shown is a phase difference between the grid reference and inverter output.

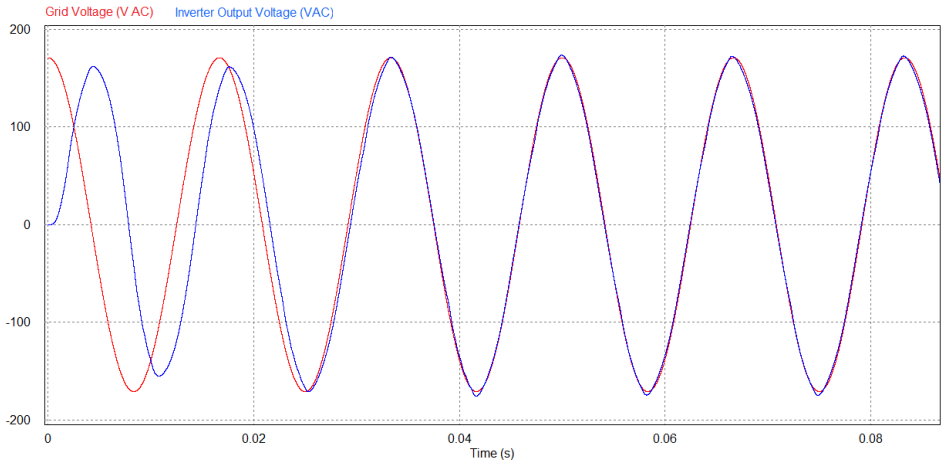

Figure 4-33: Transient Phase Synchronization

Figure 4-33 above shows the PLL operating. A phase difference of 60degrees is given between the grid reference and the inverter. The synchronization of the two voltages can be seen above. Further explanation of the response time will be shown in section 4.13 KPI analysis.

4.11.3.2.2 Voltage Control (Upon Start Up)

The following section shows the voltage control for the inverter.

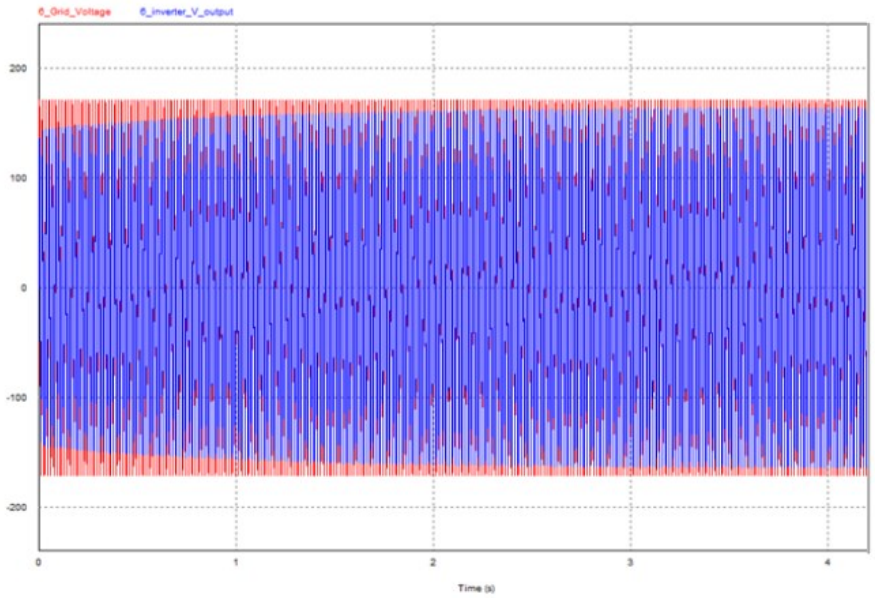

Figure 4-34: 300W Inverter Voltage Control

Figure 4-34 above shows the voltage control for the inverter circuit. The inverter was given an initial condition below the normal operation in order to show the control system responding. For the sake of this simulation, the over/under voltage protection circuit was disabled to ensure that the voltage change can be seen fully and not disengaged before steady state has been reached. The red graph shows the grid voltage while the blue show the inverter voltage. It can be seen that with the voltage climbs the 50V difference in about 1.5 seconds.

4.12 600W Overall Circuit Design

The following section outlines the 600W inverter designed in PSIM.

4.12.1 **Circuit Design**

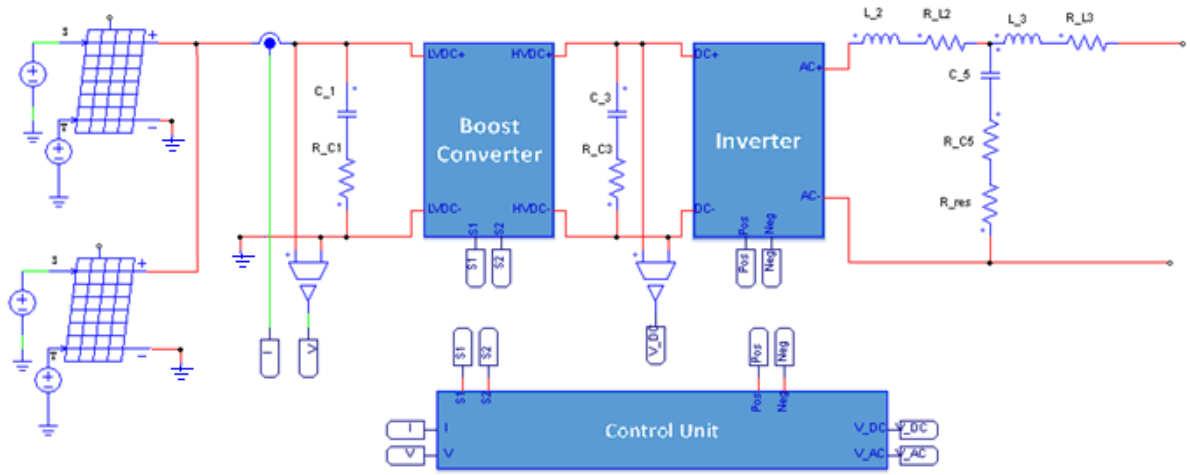

Figure 4-35: 600W Inverter Design

The overall circuit design can be seen in Figure 4-35 above. It is exactly the same as the 300W inverter circuit design, the only difference is the components and firing rates within the circuit. In addition, an extra solar panel is placed in parallel for the input to the inverter. The new list of components can been seen in the bill of materials table below.

4.12.2 **Components**

The following section lists the components needed in order to construct the 600W inverter.

Circuit ID Number	Component Description	Operating Conditions	Component Values	Manufacturer	Maximum Conditions	Amount needed	Cost per unit ($CAN)
C_1	DC link capacitor	0-46V (0-92mA)	4.7µF	Nichicon UDB1H4R7-MPM1TD	0-60V 0-480mA (9.1mΩ)	1	0.39
L_1	Boost inductor	0-210VDC 0-15.98A	30mH	Hammond Manufacturing 195p20-ND	0-250V 0-20A (15mΩ)	1	453.37
C_2	Boost Capacitor	0-195V 0-3.3Arms	3.3mF	TDK B43456A9338M	400VDC 20A (23mΩ)	1	110.26
S1-S6	N-Channel Mosfets	0-195V 0-16A	N/A	Sanken SKP253VR	250V 21A (95mΩ)	6	2.425

C_3	DC link capacitor	0-195V	3.3mF	TDK B43456A9338M	400VDC 20A (23mΩ)	1	110.26
L_2	Filter inductor	0-400V 0-11.5A	1mH	Schurter Inc.	0-15A (10mΩ)	1	33.61
L_3	Filter Inductor	0-120V AC 0-6.7A	50mH	Hammond 195R19	0-5ADC (165mΩ)	1	267.38
C_4	Filter Capacitor	0-220V 0-10A	37µF	TDK (22µF) B4356A2229M	250VDC 34 A AC (ESR 5mΩ)	1	213.12
C_4	Filter Capacitor	0-220V 0-10A	37µF	TDK B4354A2159M (15µF)	250VDC 34 A AC (ESR 7mΩ)	1	191.03
R_res	Filter resistance	0-220V 0-10A	2Ω	Bourns PWR263S-20	2Ω 20W	1	3.51
Control Chip	MPPT + PLL chip	0 - 50V 0-10 120V AC 2.5A AC	N/A	Texas Instruments TMS320 F28027-FPTQ	-0.3-4.6V	1	16.43
Current Sensor (boost)	Boost Converter	0 - 42V 0-8.73A	N/A	Allegro MicroSystems ACS712 ELCTR-20A	20A AC (100mV/A)	1	2.69
Current Sensor	PLL	120V AC 2.5A AC	N/A	Honeywell CSLA2CD	72 A Ac (32.7mV/N)	1	37.03
						Total	1453.7
Extras and Reserve	PCB, wires, resistors, heat sink, Etc.)						+15%
						Estimated Total	1671.7

Table 4-3: 600W Inverter Bill of Materials [55], [56]

The 600W components are listed Table 4-3. As with the 300W inverter, all components data can be found directly on the Mouser and Digikey websites and an extra 15% cost contingency was added to estimate the total cost. This brought the total estimated cost for the 600W inverter to $1,672. This is significantly more expensive than the 300W inverter and is due attributed to the higher cost from high current inductors and capacitors.

4.12.3 **Results**

The following section outlines the simulation results for the 600W micro-inverter.

4.12.3.1.1 Solar Panel Output

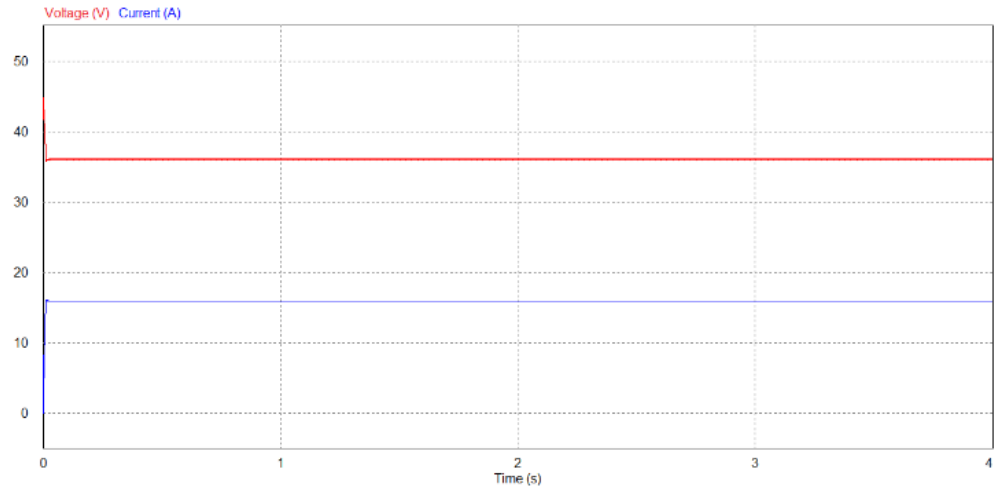

Figure 4-36: 600W Inverter Solar Panel Output

Figure 4-36 shows the steady state operation of the solar panels (two 300W) output power. The blue line shows the solar panels voltage (about 36V) and the red line shows the current (about 16A).

4.12.3.1.2 Boost Converter

The following figure shows the results of the boost converter circuit for the 600W inverter.

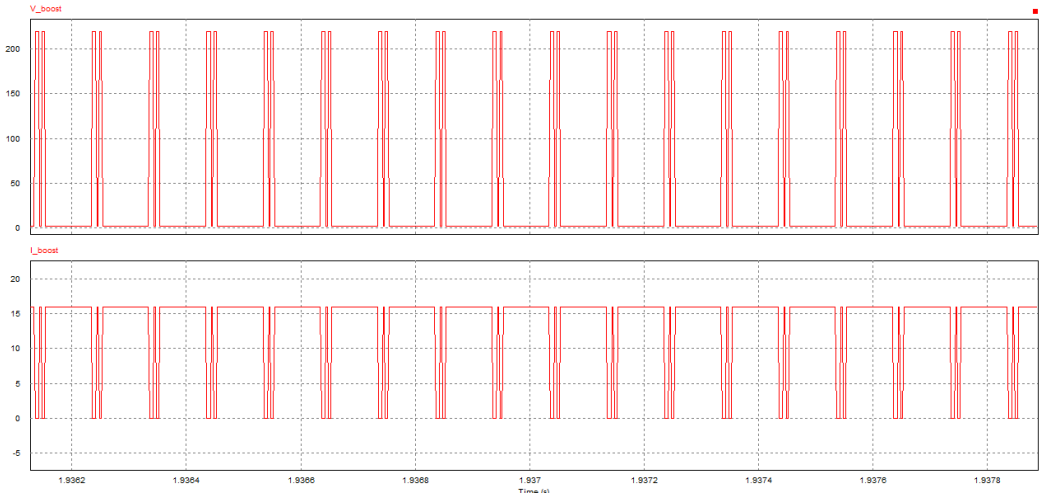

Figure 4-37: 600W Boost Converter

The Figure 4-37 above shows the 600W boost converters output voltage (top figure) and the short circuit current. The output spikes to the DC –Link are at 220V and the current is pulsating the 16A from the solar panels. Below provides the power switching losses within the circuit design.

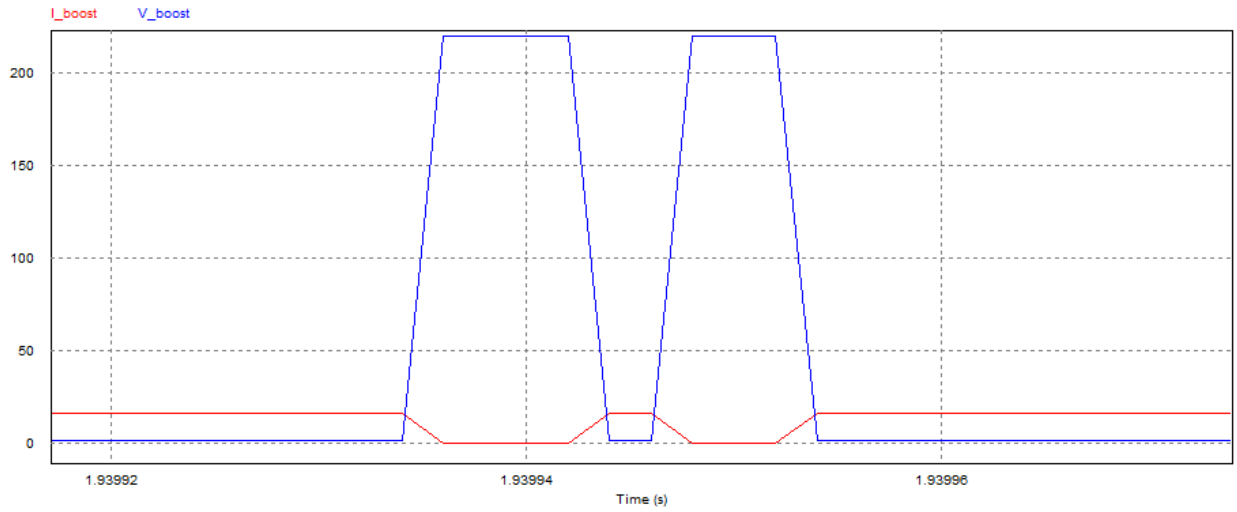

Figure 4-38: 600W Boost Converter Switching losses

The power switching losses are shown in Figure 4-38. Approximately 19W is lost in the primary stage due to the switching losses in the boost converter which contribute to the overall efficiency losses.

4.12.3.1.3 DC Link Voltage

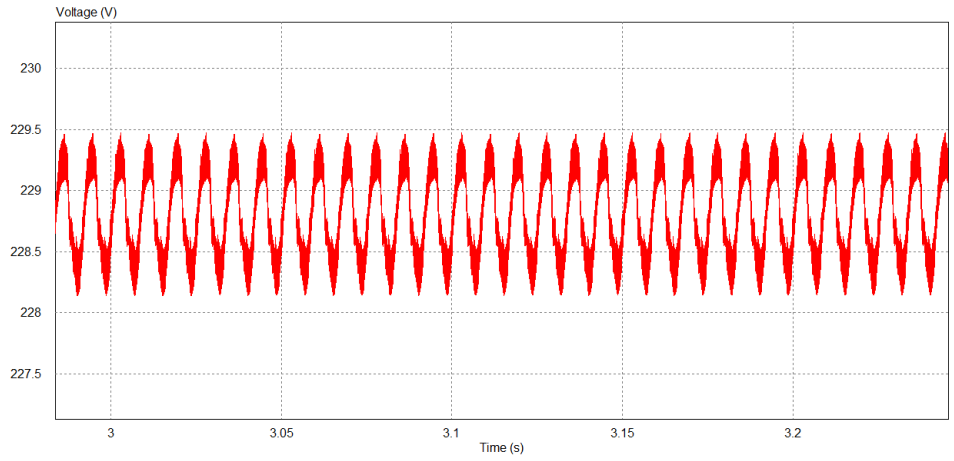

Figure 4-39: 600W DC Link Voltage

Figure 4-39 above shows the voltage across the DC link feeding into the inverter. The fluctuations approximately +/- 0.5V.

4.12.3.1.4 Inverter Output

The output results of the inverter are shown for steady state operation. This can be seen in the figure below.

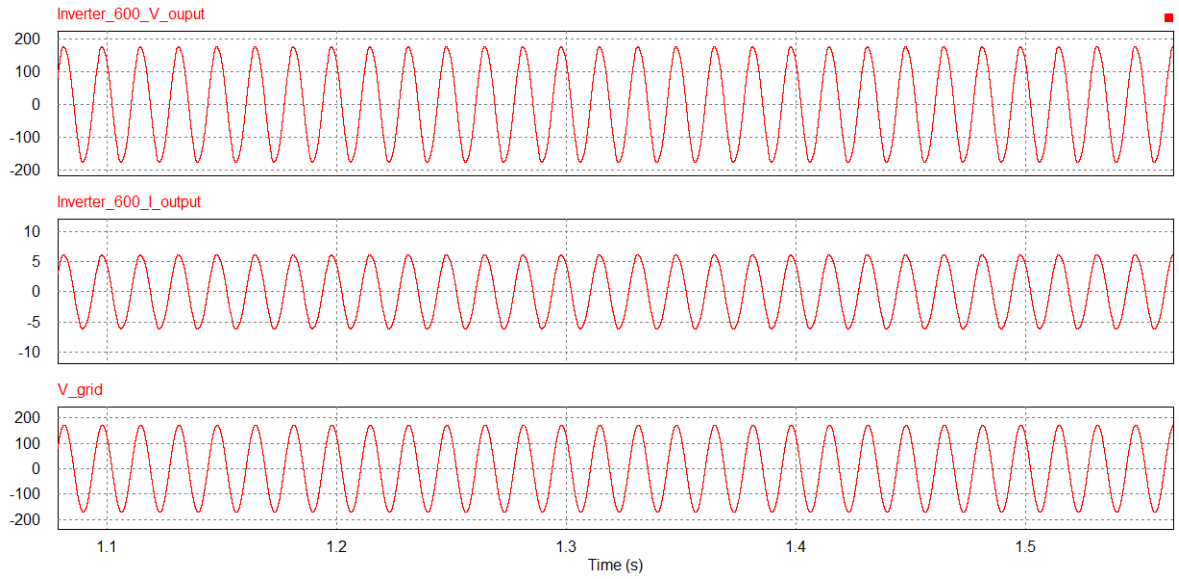

Figure 4-40: 600W Inverter Output

The top most graph of Figure 4-40 shows the 600W inverter output voltage. The middle graphs represents the output current of the inverter system and the bottom most figure shows the grid reference voltage. It can be seen in the figure that the synchronisation has taken place and the system is working in unison. The RMS for the grid is 120Vrms, inverter output is 119.6Vrms and current 4.22Arms.

4.13 Inverter Analysis KPI

The final section outlines the KPI analysis done for the inverters.

4.13.1 **300W**

Key Performance Indicator	**Results**
Operating Efficiency	Pin = 287.44W Pout= 274.44W η= 95.47%
THD	2.11E-002 or 2.11%
PLL synchronisation response time	0^0 Phase Shift = 21.55ms 45^0 Phase Shift = 26.81ms 90^0 Phase Shift = 32.29ms 135^0 Phase Shift = 47.37ms 180^0 Phase Shift = 34.62ms 225^0 Phase Shift = 32.36ms 270^0 Phase Shift = 22.07ms 315^0 Phase Shift = 18.13ms 360^0 Phase Shift = 21.41ms
Over/Under Voltage response time	1.1ms

Initial Cost	$547.4115 (CAN)
PP System	10.18 years

Table 4-4: KPI Analysis 300W micro-inverter

The following Table 4-4 outlines the KPI for the 300W micro inverter. From the analysis it was found that the overall efficiency requirement was met along with the THD requirement. The PP for the system (solar panels, roof mounts, etc.) calculated for Toronto Ontario was found to be 10.2 years given the current price with the micro-fit program offered by the provincial Government of Ontario.

4.13.1.1 Comparison to Equivalent Micro-inverters

The following micro-inverter designed here in has a peak efficiency of 95.5% and a THD of 2.11%. Below a table is provided with a preliminary summary with the designed micro-inverters and ones currently in the market.

Micro-inverter	Power	MPPT	Efficiency	THD	Operating Temp
UOIT	300W	25-50VDC	95.5%	2.11%	N/A
Enecsys UNIV-300GTS-M	300W	22-50VDC	95.2%	2.4%	-40^{0}C - +85^{0}C
Enphase M250	300W	22-48VDC	96.5%	<5%	-40^{0}C - +85^{0}C
Solarbridge Pantheon	250W	18-36VDC	95.5%	<5%	-40^{0}C - +65^{0}C
Siemens SMIINV215R60XX	270W	22-36VDC	96%	3%	-40^{0}C - +65^{0}C

Table 4-5: Micro-inverters in Marketplace

Table 4-5 above provides the specification of the micro-inverters currently available in the market with power ranges around 300W. The summary of the table shows that the preliminary micro-inverter design proposed by this thesis has an efficiency on par with the best micro-inverters currently in market place. In addition, the preliminary design surpasses market ones with a lower THD. Further experimental design (hard ware design) will be needed in order to ensure calculations and simulations data is correct, however this table is meant to provide preliminary comparison between the design 300W micro-inverter to those available in the marketplace. .

4.13.2 **600W**

Key Performance Indicator	Results
Operating Efficiency	Pin = 574.23W Pout= 508.24W η= 88.51%
THD	1.735E-002
PLL synchronisation response time	0^0 Phase Shift = 13.93ms 45^0 Phase Shift = 28.93ms 90^0 Phase Shift = 26.84ms 135^0 Phase Shift = 41.13ms

	180^0 Phase Shift = 35.12ms 225^0 Phase Shift = 24.48ms 270^0 Phase Shift = 21.83ms 315^0 Phase Shift = 12.17ms 360^0 Phase Shift = 14.27ms
Over/Under Voltage response time	1.1ms
Initial Cost Inverter	1,671.8$ (CAN)
Estimated Payback Period	13.89 years

Table 4-6: KPI Analysis 600W inverter

The results of the 600W inverter can be seen in the Table 4-6 above. The inverter is not as efficient as the micro-inverter. This due to the higher internal resistances within the components. In addition this system has a significantly higher cost due to the components needed to handle higher currents.

4.13.2.1 Comparison to Equivalent Micro-inverters

As with the 600W inverter, a preliminary comparison is done with the designed inverter and ones currently available in the marketplace. To re-state, the 600W inverter designed within this paper has a peak efficiency of 88.5% and a THD of 1.74%.

Inverter (600W)		Power	MPPT	Efficiency	THD	Operating Temp
UOIT		600W	25-50VDC	88.5%	1.74%	N/A
Chaomin	cm-tie 600W	600W	10.5-28V	85%	<5%	-25^0C - $+65^0$C
Eco-Worthy	GI600-24120IP65-1	600W	22-50VDC	N/A	<5%	-40^0C - $+65^0$C
i-mesh-bean	SUN-600G	540W	22-60VDC	92%	<5%	-10^0C - $+45^0$C
Power Jack	PSWGT-600-14-28-110	600W	14-28VDC	87%	2%	N/A

Table 4-7: Comparison of 600W Inverters

Comparable to market place inverters, the 600W designed herein provides one of the highest efficiencies compared to those currently available in the market. In addition it surpasses all with a lower THD output. N/A refers to data not given within data sheets online. The temperature range for the inverter designed is not given as this has to be tested in experimental design however parts chosen in the design stage were chosen to operate within IEEE standards for temperature range.

Chapter 5: Micro-Inverter System Resiliency Designs

The following chapter provides an overview of the resiliency phase. First, Case 0 is presented. This is the case all case studies are built upon. Next the need for resiliency is re-stated, along with the assumptions made for both analysing and simulating the different case studies. The resiliency controller is then shown along with the faults used in the simulations. Finally, the case studies are presented. Each case study provides an initial overview of the case, its operational theory, its circuit design and the simulation results.

5.1 Case 0: Micro-Inverter System

In this section the overall system design for a micro-inverter system is shown. This is Case 0 and can be seen in Figure 5-1 below.

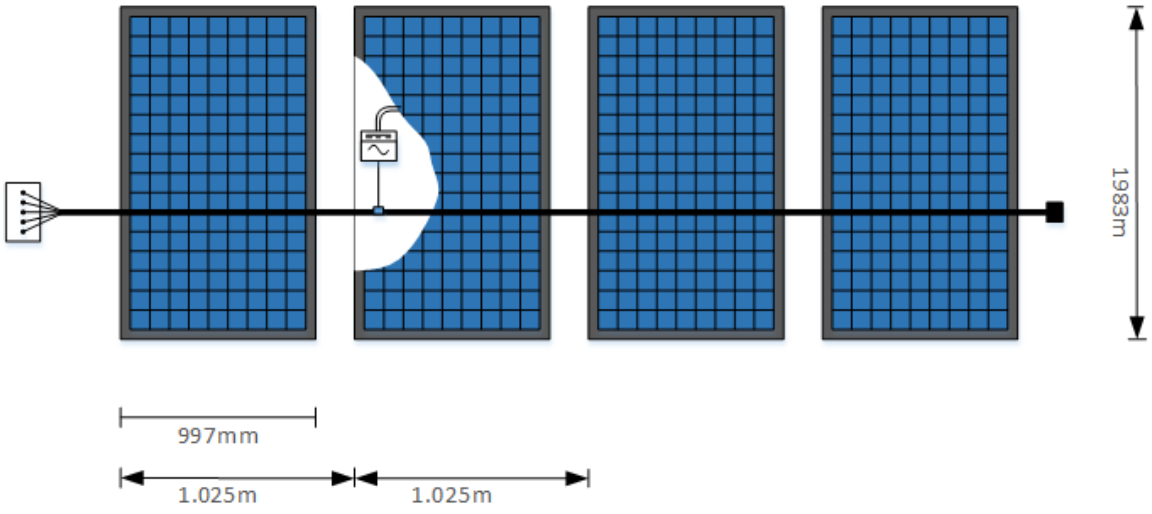

Figure 5-1: Micro Inverter System Design [56]

Case 0 and the system being evaluated consists of four 300W Ecilpsall solar panels (1.2kW total) arranged in the portal method as shown in Figure 5-1. The system was chosen to be 1.2kW for the following reasons. (1) It is easily scalable up to the size of an average PV system. The average installation for residential solar PV in USA is 5kW [57], and Saskatchewan it is 3.5kW [58]. Therefore choosing 1.2kW can be scaled to the average installation sizes quiet easily. (2) A 300W solar panel scales easily up to the 1.2kW system. This makes the analysis easily scalable from a single solar panel up to the full system. (3) In addition, one of the hypothesized resiliency methods was to utilise two solar panels to one inverter (600W). Therefore, using a 1.2kW size provides a good ratio 2 to 1 in order to ensure that the system is adequately supported in case of failure. Increasing the ratio further, would have significantly higher costs of the inverter.

Finally, the portal method of connecting the solar panels was chosen. This method was chosen as it is the recommended method for mounting solar panel from different manufactures installation instructions [59] [60]. This mounting method is recommended, as it is less expensive than the landscape method. This due to the fact that in the landscape mounting the solar panels are turned 90 degrees (compared to Figure 5-1 above) and the main roof mounting support attaches length ways along the solar panel (1.938meter each). For portal method, the roof mounting support attaches width ways along the solar panel (997mm) as shown in the figure above. This results in a need for longer braces, more material (Aluminum) and a higher cost for landscape method.

5.2 Resiliency Methodologies

The following work is to propose and evaluate methods for keeping the micro-inverters in a system working independently. However, the micro-inverter in the system need to be able to link together in a way to improve the overall resiliency of the system should a fault occur.

5.2.1 **Need**

Restating the problem statement, a key factor in the long term success of the photovoltaic industry is the confidence in the reliability of the system [5]. The reliability and resiliency issues have the potential to damage the reputation of the entire industry and hinder the adoption of PV systems [5] [6]. Within deployed systems, the most common failure is caused by the inverters [9]. Despite this, the inverter industry's main focus has been one lowering the price of micro-inverters and improving the overall efficiency [9]. As such, the resiliency of a micro-inverter system has been overlooked.

Restating, resiliency is defined as "the ability of a system to recover from a failure" [37] . Therefore, this work will explore different methods to ensure that the micro-inverter system can recover from an inverter failure within the system.

5.2.2 **Assumptions**

In order to construct and evaluate the case studies the following assumptions have been made.

The system will consists of 1.2kW with 120Vrms for residential grid connected applications. Spacing's for the solar panel installation will be done as per the recommended distances acquired from manufactures datasheets.

The system will be deployed to Toronto, Ontario. Therefore, provincial microFIT prices will apply in addition to the solar irradiation levels for Toronto.

In order to cut down on simulation time and conserve memory, 600W systems will be designed and simulated in PSIM. However, the analysis will be carried out for the full 1.2kW system.

5.3 Resiliency Controller Design

In order for the resiliency circuits to function and desired, a controller is needed. The main tasks for this controller are to first identify if a fault has occurred, then disengage the faulted inverter (if not already done), redirect power flow in the circuit, and then re-engage to the grid. With this in mind a controller was designed which can be easily incorporated into on board micro-controllers and well as software simulations.

5.3.1 **Resiliency Controller Requirements**

The requirements for the controller are listed below:

- Must operate within 0.16 seconds, including time for switches to engage/disengage
- Must be easily be deployed to microcontroller and software simulations
- Must not significantly impact the efficiency of overall system
- Must have minimal impact with THD of system and still meet grid standards

5.3.2 **Resiliency Controller Circuit Design**

In order to accomplish the requirements stated above, the following control circuit was designed in PSIM.

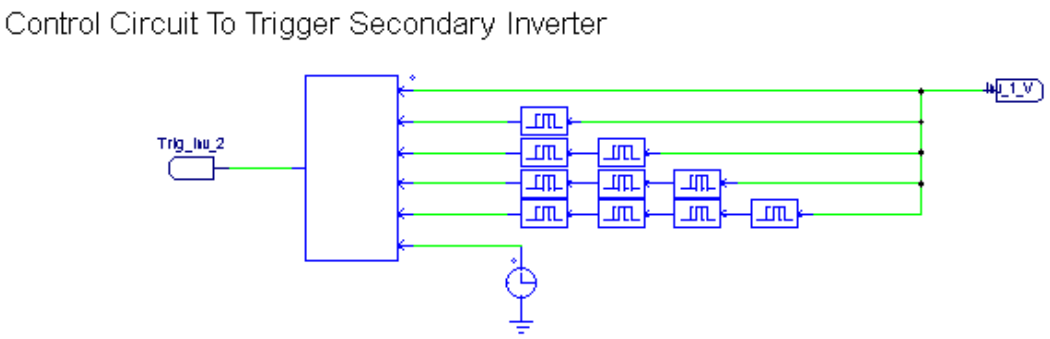

Figure 5-2: Control Circuit for Resiliency

Figure 5-2 shows the control circuit designed in PSIM. The control system was designed using the C-Block function which allows for c-code to be programmed within it. This makes it easy to incorporate into both hardware and simulations. The input for the resiliency controller is the output voltage of a micro-inverter. The time delays are set to 0.01 seconds each and act as memory storage providing the C-block with previous data points in the signal. The operating principle is such that, if all the inputs are zero, the output to the C-block (depicted on the left hand side) becomes 1. For all other cases the output is 0.

The output of the control circuit is then sent to the Mosfets and relays located throughout the system in the case study. Each relay is given its own time delay in order to simulate the switching time as of the device as per its datasheet specifications. The control circuit therefore can recognize a fault occurring and provide

the necessary actions to disconnect and redirect power flow as needed. Thus, with this design the controller can meet the design requirements as specified in the sub-section above.

5.4 Simulation Faults

In order for the resiliency controller to be tested and be evaluated, a fault is needed. This needs to be included into the overall system to test both the resiliency controller and the resiliency case study in question. Two faults were introduced: an open circuit fault and a short shirt fault.

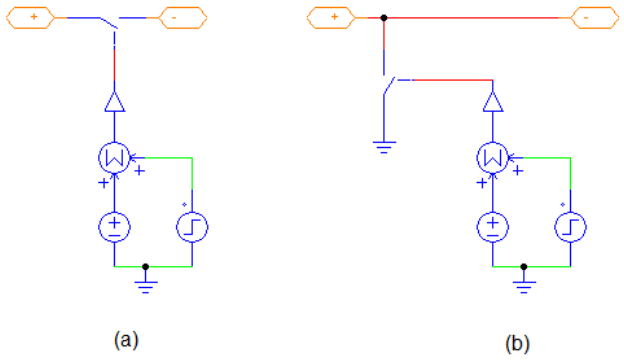

Figure 5-3 PSIM Fault

Figure 5-3 shows the PSIM models for the fault to be triggered within the simulations. Figure 4 (a) shows the sub-circuit design used in order to create an open circuit fault in the inverter. Figure 4(b) shows the short circuit fault created. At the top of both figure (a) and (b) orange lines can be seen with plus and minus symbols. These indicate the connection into the overall circuit design. To place a fault, the sub-circuit is placed into one of the main lead wires for the micro-inverters. The faults times can be adjusted by altering the time step of the step signal source.

5.5 Case 1: Two 300W Inverters Paired Inside Single Inverter Unit

The following section shows the first case study hypothesized in order to increase the residential PV systems resiliency. First, an overview of the resiliency case is shown followed by its operational theory. Next, the circuit design in PSIM is shown along with the simulation results.

5.5.1 **Overview Block Diagram of 1.2kW system**

The following section provides an overview to Case 1 and how the resiliency measure is deployed to the 1.2kW system.

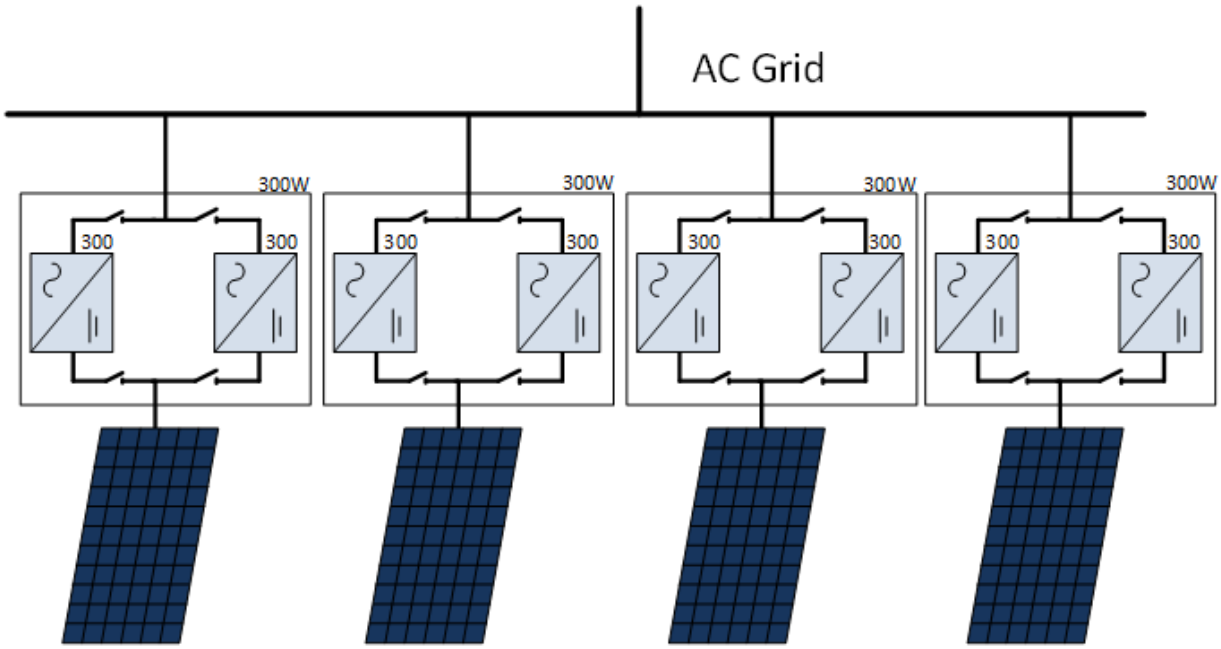

Figure 5-4: Case 1 Overview

For Case 1, each 300W solar panel has two functioning 300W micro-inverters build inside a single box mounted to it. This can be seen in the Figure 5-4 above which shows two 300W micro-inverters inside a black square box coupled together by relays and connected to the grid. This effectively gives one solar panel two possible outputs for grid connection. Each of the micro-inverter offers the fully designed micro-inverter, meaning each has its own individual control system, boost, h-bridge, filter, etc.

5.5.2 **Operational Theory Single 300W Inverter**

The operational theory for Case 1 is provided in the following section. This is done strictly for a single micro-inverter (300W) output.

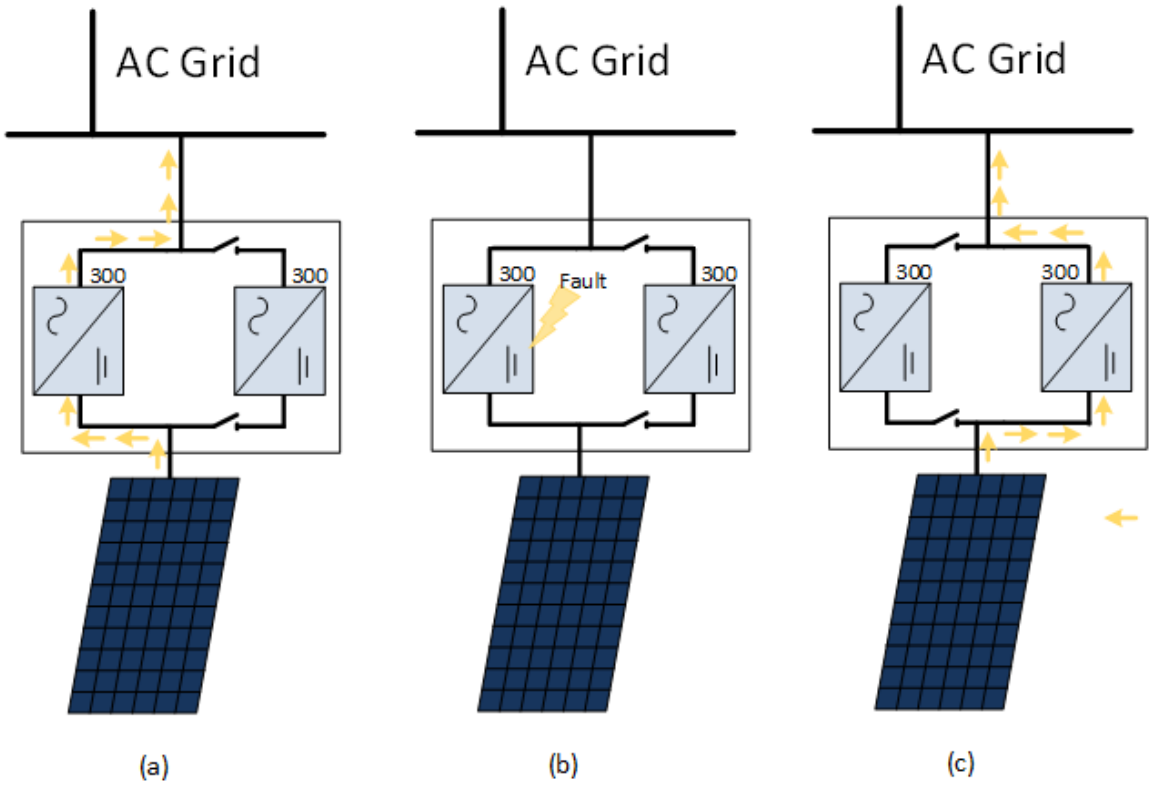

Figure 5-5: Case 1 Operational Theory

The operational theory of Case 1 is depicted in the figure above. Figure 5-5(a) shows the normal operation of the micro-inverter. The switches (a combination of relays and Mosfets) are closed, allowing power to flow through the primary micro-inverter. The switches for the back-up micro-inverter are left open in order to ensure that is not coupled to the grid or solar panel. However, the control system for the back-up micro-inverter is sensing the grid voltage. In case of a fault, this allows the back-up micro-inverter to be able to respond and synchronize quickly. In addition, the back-up micro-inverter is sensing the output voltage of the primary micro-inverter in order to know when to respond.

Figure 5-5 (b) shows a fault occurring in the primary 300W micro-inverter. Once the back-up converter recognizes that a fault has occurred, is opens the switches to the primary micro-inverter disconnecting it from the grid and solar panel. Thus, the faulted micro-inverter is completely isolated. Next, the back-up micro-inverter closes the switches connecting itself to the solar panel and grid. This effectively redirects the power flow for the solar panel in order to ensure that power output is maintained.

5.5.3 **Circuit Design**

The following section outlines how Case 1 model was built, designed and simulated in PSIM. In order to try and keep the overall system operating under high efficiency, Mosfets were desired in the used where ever possible. This is due to their lower internal resistances (95mΩ) and lower costs when compared to relays (100mΩ).

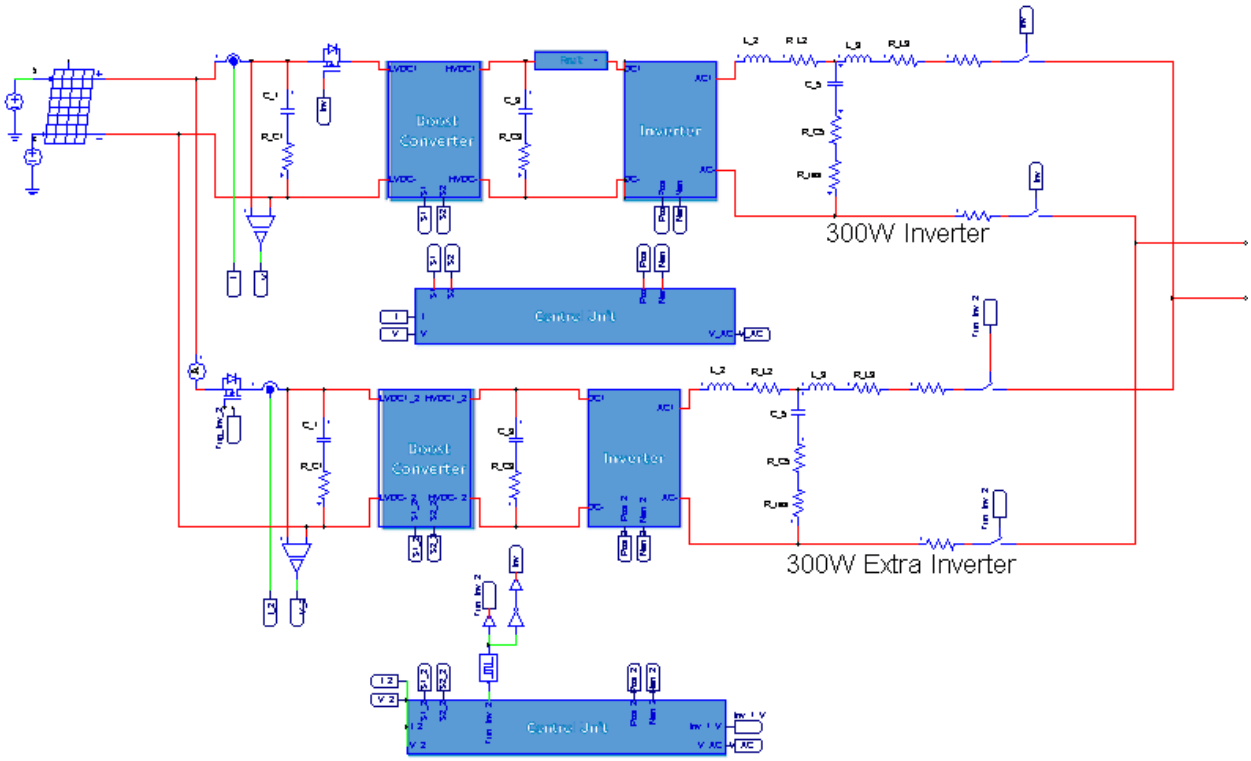

Figure 5-6: Case 1 PSIM Model

Figure 5-6 above shows the PSIM model for Case 1. Inside the figure above the top micro-inverter is the primary micro-inverter, while the bottom being the back-up micro-inverter. Mosfets are placed on the front of end the inverters, operating as switches to control the power flow into the inverters. Relays are used on the output filter side as a means to connect/disconnect to the power grid. Please note that in the top most micro-inverter in the figure there is an extra blue box located by inverter power stage. This extra box contains the faults shown in section 5.4 and is placed in order to provide a fault within the primary micro-inverter during the simulation.

5.5.4 **Results**

The following section outlines the operational results of Case 1 simulated in PSIM. In order converse memory and simulation time for Case 1, a single 300W micro-inverter was simulated along with the back-

up micro-inverter. Since each solar panel making up the 1.2kW system has the same overall design, the results of one simulation can be scaled up to make the full 1.2kW system.

5.5.4.1 Normal Operation

The first portion of the simulation results depicts the normal operational results and can be seen in Figure 5-7 below.

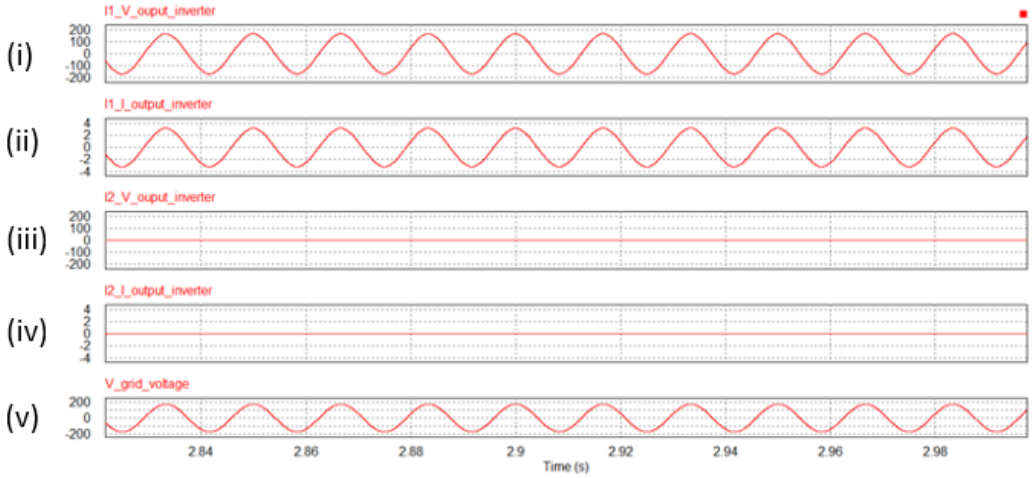

Figure 5-7: Case 1 Results for system working under normal operation

Figure 5-7 above shows the operational results for the Case 1 under normal operating conditions. The top most graph shows the primary micro-inverter output voltage (i), followed by the output current directly underneath (ii). Graph (iii) shows the back-up inverters output voltage, followed underneath by its output current (iv). Finally the bottom most graph shows the grid reference voltage (v). It can be seen that the inverter is outputting a phase locked output voltage and current synchronized with the grid under normal operation.

5.5.4.2 Inverter Failure

The following sections shows the output results for the system in the event of a failure in the primary micro-inverter.

5.5.4.2.1 Inverter 1 Failure

The figure below shows the results of the system with a fault generated in the primary micro-inverter at 5 seconds simulation time.

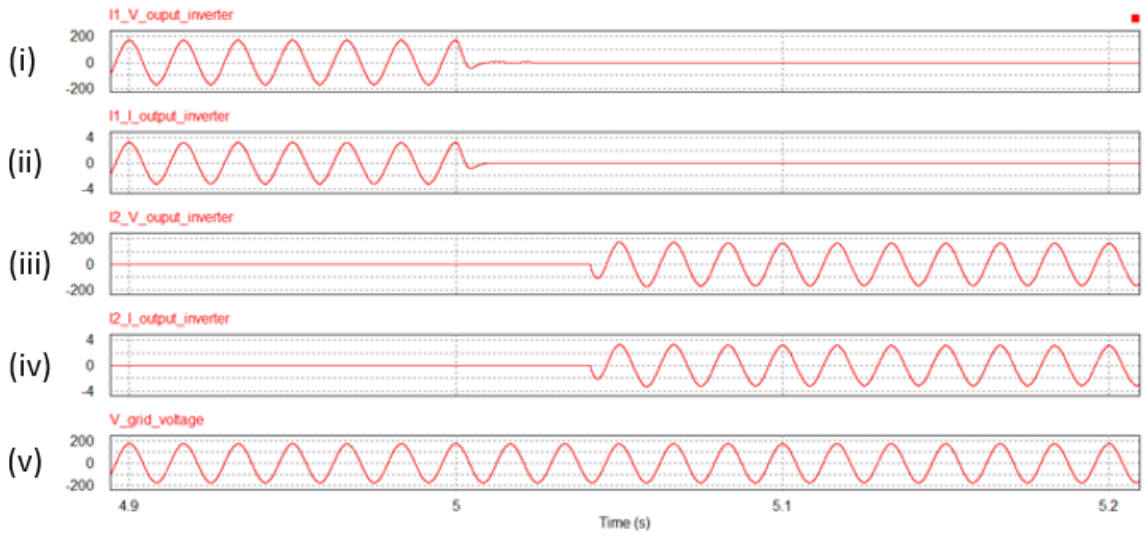

Figure 5-8: Case 1 Micro-inverter 1 Failure

The top most two graphs of Figure 5-8 show the primary micro-inverter's output voltage (i) and output current (ii). The middle graph shows the back-up micro-inverter's output voltage (iii) followed underneath by its output current (iv). The grid reference is on the bottom most graph (v). A fault is triggered at 5 seconds and can be seen in the both the respected graphs [(i) (ii)] as the primary micro-inverter is quickly disconnected from the grid. Graphs (iii) and (iv) provide a time delay as the resiliency controller is recognizing the fault and applying the corrective actions to redirect power flow. Output power resumes and the back-up micro-inverter is outputting at full power in approximately 3 cycles. Upon comparing (iii) and (v) it can be seen that there is no re-synchronization taking place as the back-up inverter's PLL has already been synchronized.

5.5.4.2.2 System Output

The following shows the full system output. At first, the primary inverter is operating until a fault occurs. The control system then engages and redirects the power flow within the system.

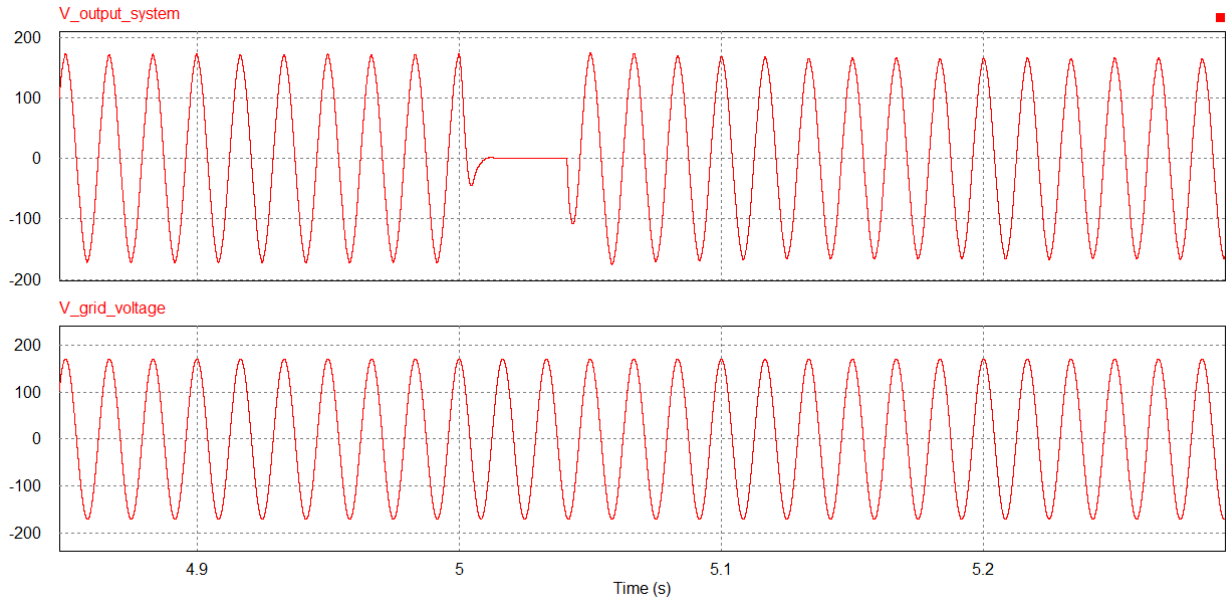

Figure 5-9: Case 1 System Output

Figure 5-9 shows solar panel output voltage on the top most graph. The grid reference voltage is depicted on the bottom graph of Figure 5-9. From the figure, it can be seen that from the initial fault occurring, it takes the system 0.04 seconds before it is outputting at full power again. This meets the initial criteria for system to respond within 0.16 seconds.

5.5.4.3 Additional Components for 1.2kW System

Scaling the simulation up to the full 1.2kW system the following extra components will be needed. This is building on Case 0 to retrofit it into Case 1.

Component Description	Operating Conditions	Manufacturer	Component Maximum Conditions	Amount needed	Cost per unit ($CAN)
Relay	120Vrms 4Arms	Songle srd-05vdc-sl-c	10 A 280VDC 10A 240Vrms (100mΩ)	16	4.99
N-Channel Mosfets	0-36V 0-8.5A	Sanken SKP253VR	250V 21A (95mΩ)	8	2.425
300W inverter	20-50V 0-8.5A	UOIT	20-50V 0-8.5A	4	$548.3

Table 5-1: Case 1 Extra Components [55] [56]

Table 5-1 shows the extra components needed to design the full 1.2kW system with the following resiliency method included into it.

5.5.4.4 KPI Analysis 1.2kW System

The following section provides a brief overview of the KPI results for Case 1.

Key Performance Indicator	Case 1
Peak Operational Efficiency	Pin =287.44W Pout=270.16W η= 93.98% =94%
Peak Operating THD	2.04518E-002
Overall Resiliency Response time	0.03945 sec or 40ms
Resiliency Response Power Output	300W (ideal) Actual is 270.16W
Resiliency Unit Power Output	1
Peak Operational Efficiency Under Fault	Pin =287.44W Pout=270.16W η= 93.98% =94%
Operating THD under fault	2.04518E-002
Overall Cost for 1.2kW system	$6,167.86
Estimated Yearly Income	$382.32
Estimated Payback Period	16.13 years

Table 5-2: Case 1 KPI

A further in depth analysis will be conducted in Chapter 6. This sub-section is meant to provide some closure to the case studies analysis by showing a few KPI for the Case Study. It should be noted that the efficiency has dropped from 95% for a single micro-inverter to 94% with resiliency methods deployed due to the inclusion of extra switches for controlling and directing the power flow within the design.

5.6 Case 2: Extra 300W Micro-inverter in Parallel to Micro-Inverters

Section 5.6 shows the second case study hypothesized in order to increase the PV systems resiliency. This section follows the same format as the previous section: case study overview, operational theory, PSIM model and then simulation results.

5.6.1 **Overview Circuit Block Diagram of 1.2 kW Inverter**

The following section provides an overview of Case study 2 and its resiliency method.

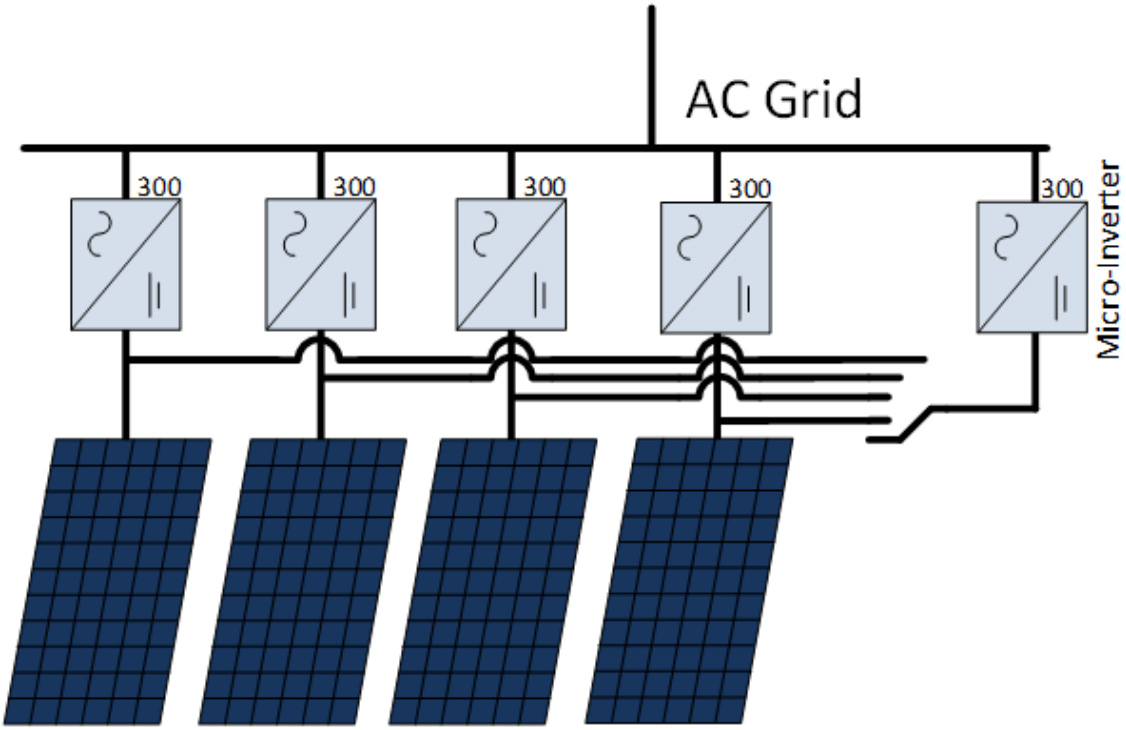

Figure 5-10: Case 2 Overview

Case 2 is shown in Figure 5-10 above. Similar to Case 1, Case 2 is using an extra micro-inverter in order to increase the resiliency of the system. For Case 2, the extra back-up micro-inverter is placed in parallel to the overall 1.2kW system and can be seen in Figure 5-10 above. This back-up micro-inverter is normally disconnected from the grid, although still sensing is the grid voltage in order to be able to respond quickly. In addition, the back-up micro-inverter is sensing the output voltages from all four of the 300W micro-inverters in the system. In the event of a micro-inverter failing, the control system for the back-up micro-inverter disconnects the failed one and isolates from the grid and its solar panel. The back-up micro-inverter then connects to the offline solar panel and grid. Thus power flow is re-directed and the system resumes outing power.

5.6.2 **Operational Theory for 600W system**

The operational theory for Case 2 is described in the following section. For this system, two micro-inverters working in parallel constitute the system design.

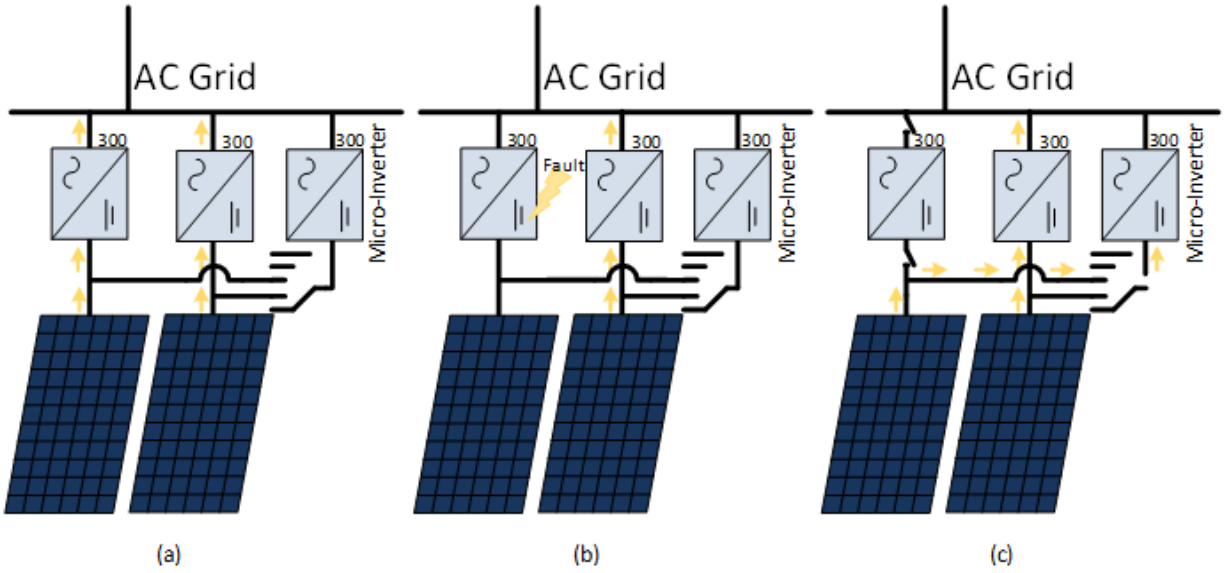

Figure 5-11: Case 2 Operational Theory

Figure 5-11 shows the operational theory of this case. Under normal operation (a), each micro-inverter is connected to its respected solar panel and outputting power to the grid. The isolation switches for all the micro-inverters are closed, except for the back-up micro-inverter which has its open. When a fault occurs, as shown in Figure 5-11 (b), the back-up micro-inverter opens the switches to the faulted inverter, thereby isolating it. Then, the back-up micro-inverter proceeds to close its own switches redirecting power flow through it and to the grid. This allows the system to still have some measurement of resiliency in the event of an inverter failure seen in Figure 5-11 (c).

5.6.3 **Circuit Design**

The following section outlines how Case 2 was built, designed and simulated in PSIM. As with Case 1, Mosfets were desired in the used wherever possible. For Case 2, 2 300W micro-inverters are simulated as the full system in order to reduce simulation time.

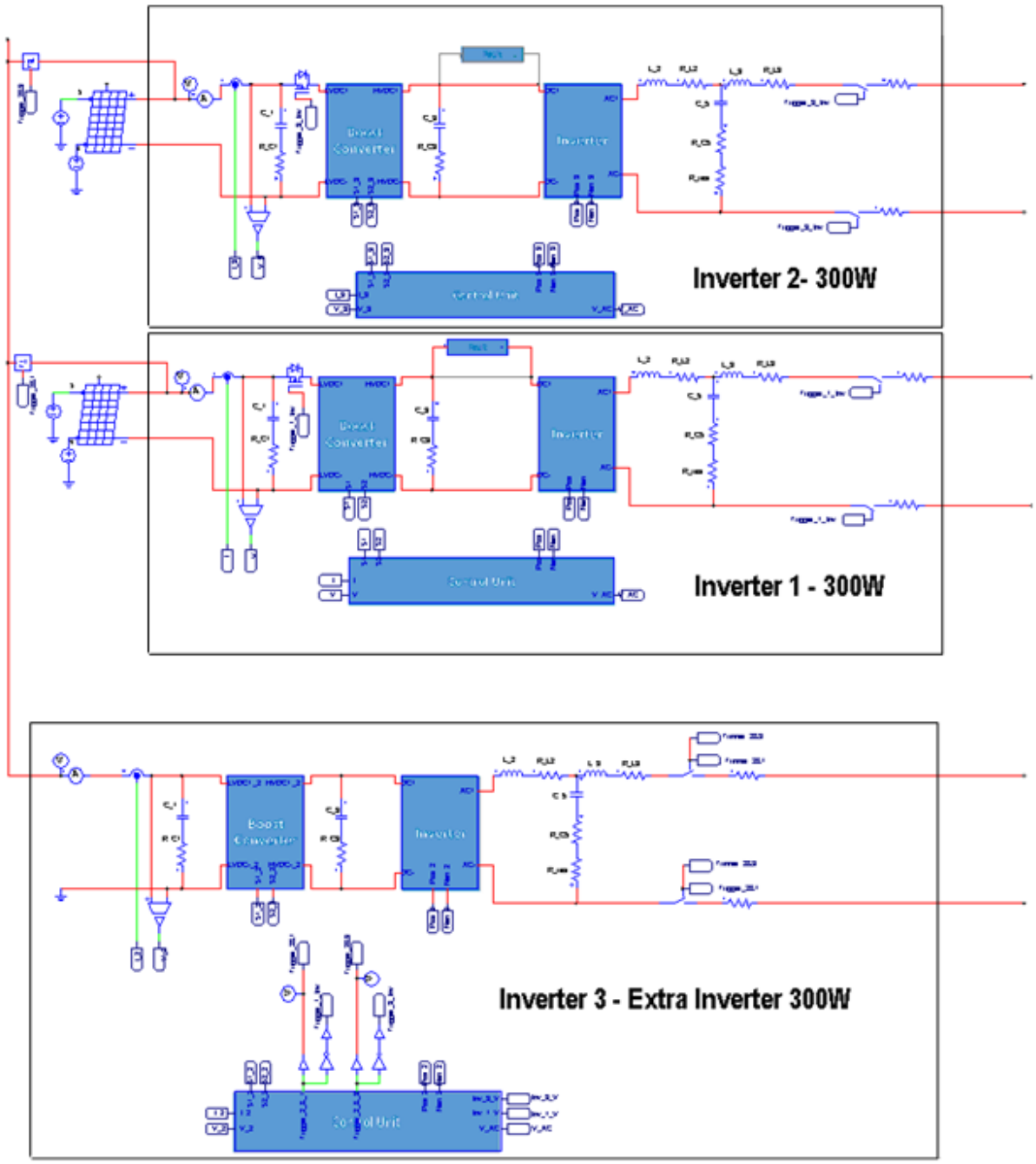

Figure 5-12: Case 2 PSIM Model

Figure 5-12 above shows the PSIM model created in order to simulate the system. Both Inverter 1 and Inverter 2 are primary micro-inverters directly coupled from the solar panel to the grid. Inverter 3 is the back-up/redundancy micro-inverter placed in parallel to the system. Similar to Case 1, Mosfets are used on the inputs and relays the outputs to control power flow within the system.

5.6.4 **Results**

The following section outlines the operational results of the Case 2 in PSIM.

5.6.4.1 Normal Operation

The first portion of the simulation results depicts the normal operational results and can be seen in the figure below.

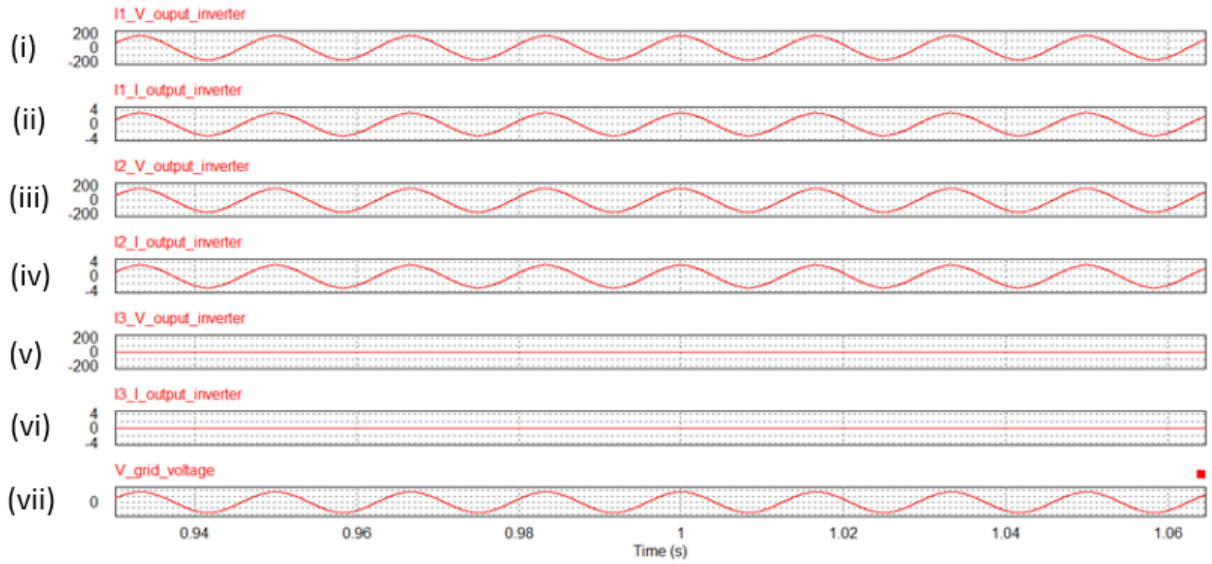

Figure 5-13: Case 2 Results for system working under normal operation

Figure 5-13 shows the normal operation of the micro-inverter system. Micro-inverter 1's output voltage (i) and the then current (ii) are depicted in the top two graphs. Micro-inverter 2's output voltage (iii) and current (iv) are depicted in graphs three and four from the top. Micro-inverter 3 (the back-up/ resiliency micro-inverter) output voltage (v) and current (vi) are depicted in graphs 5 and 6. Finally, the grid reference voltage is shown on the bottom most graph (vii). From the figure it can be seen that the system is operating as expected and both primary micro-inverters are synchronized, outputting with low THD.

5.6.4.2 Inverter Failure

The following sections shows the output results for the system in the event of a failure in one the primary micro-inverters.

5.6.4.2.1 Case 2a: Inverter 1 Failure

The results shown in this section, depict the system in the event of a failure in micro-inverter 1. The fault is triggered at 2 seconds simulation time.

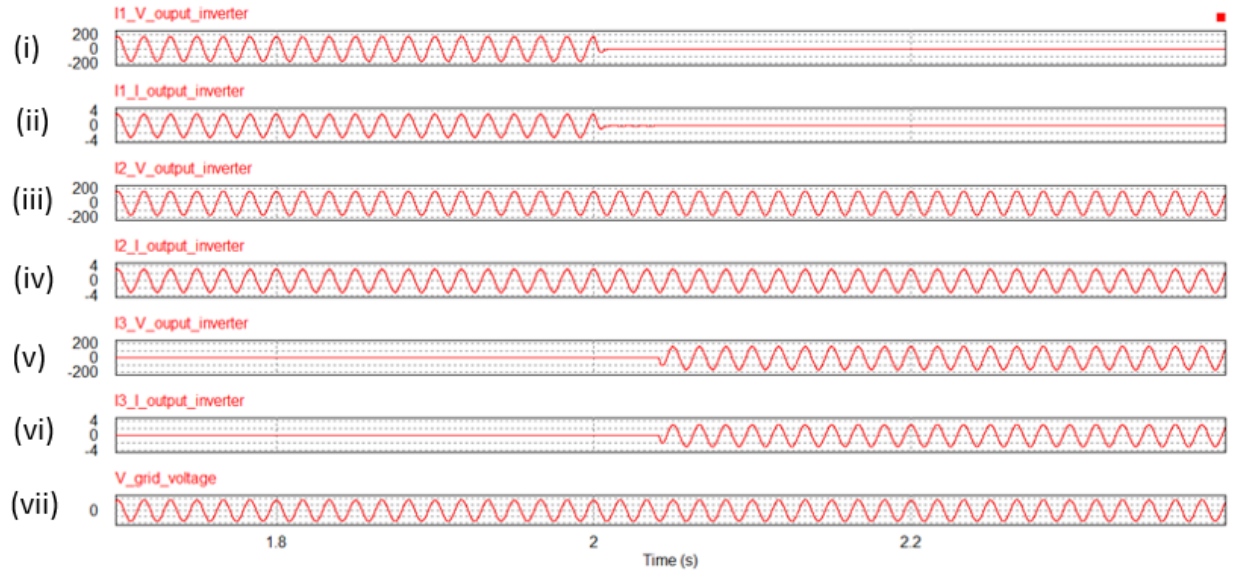

Figure 5-14: Case 2 Micro-inverter 1 Failure

Micro-inverter 1's output voltage (i) and current (ii) graphs are shown in Figure 5-14. These are followed by micro-inverter 2's output voltage (iii) and current (iv). Next, the back-up micro-inverter's output voltage (v) and current (vi) with the grid reference voltage (vii) are shown on the bottom most graph. The fault can be seen by the output of [(i) (ii)] dropping to zero at 2 seconds. Graphs [(iii) (iv)] depict micro-inverter 2's output in which no fault is occurring and it continues operating effectively. Graphs [(v) (vi)] depict micro-inverter 3, the back-up, and its behavior when a fault occurs in the system. It can be seen that after the fault has occurred, micro-inverter 3 begins to recognize and output power is resumed in approximately 3 cycles. This output is synchronized with that of the grid reference voltage (vii).

5.6.4.2.2 Case 2b: Inverter 2 Failure

The following section shows the results while placing a fault in micro-inverter 2 during normal operation.

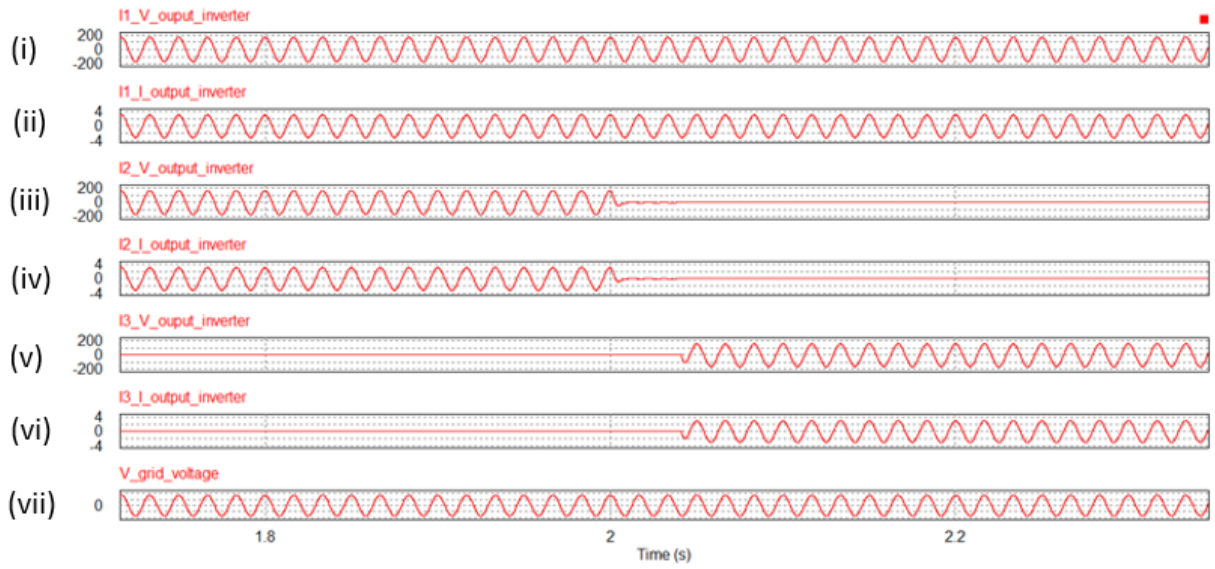

Figure 5-15: Case 2 Micro-inverter 2 Failure

The Figure 5-15 above shows the system results of a fault occurring at 2 seconds in micro-inverter 2. In the figure, it can be seen micro-inverter 1's output voltage (i) and current (ii) are followed underneath by micro-inverter's output 2 voltage (iii) and current (iv). The back-up micro-inverter's output voltage (v) and current (vi) are shown, followed by the grid reference voltage (vii). An open circuit fault occurs at 2 seconds simulation time in micro-inverter 2. The system responds as designed within the roughly the same amount of time as the previous sub-section (3 cycles). It should be noted that for this resiliency strategy, the back-up micro-inverter can only handle 300W. Therefore, if multiple micro-inverters in the system go offline the strategy would not be able to handle the full power capability of the system. Despite this, Case 2 does supply some level of resiliency to the overall system design.

5.6.4.2.3 Switching Time

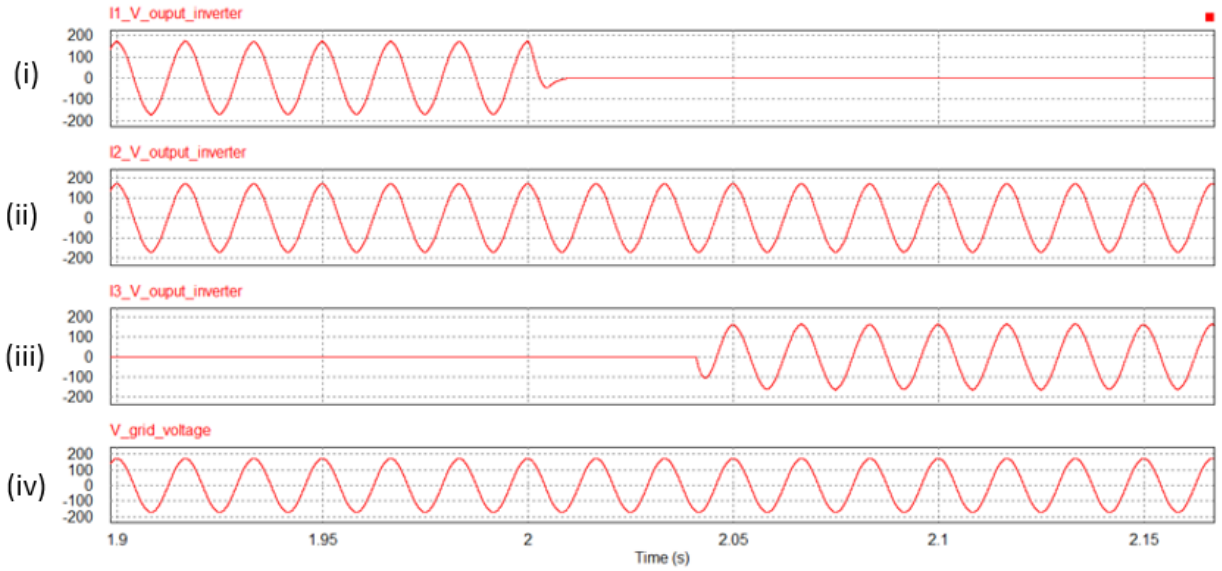

Figure 5-16: Case 2 Switching time

Figure 5-16 above show the switching time for the Case 2. The top most graph depicts micro-inverter 1 output voltage (i), with the fault occurring at 2 second simulation time. The graph second from the top is micro-inverter 2's output voltage (ii) followed by the backup micro-inverter's output voltage (iii). The grid reference voltage on the bottommost graph (iv). From the fault occurring at 2 second, the line is cleared (micro-inverter 2) within ¼ cycle of grid. It takes approximately 0.0446 seconds from the initial fault being detected, until the resynchronization with grid and micro-inverter 3 resuming output.

5.6.4.3 Additional Components 1.2kW System

Scaling the simulation up to the full 1.2kW system the following extra components will be needed. This is building on Case 0 components to retrofit into Case 2.

Component Description	Operating Conditions	Manufacturer	Component Maximum Conditions	Amount needed	Cost per unit ($CAN)
300W inverter	20-50V 0-8.5A	UOIT	20-50V 0-8.5A	1	$548.3
Relay	120Vrms 4Arms	Songle srd-05vdc-sl-c	10 A 280VDC 10A 240Vrms (100mΩ)	14	4.99
Cable	36V	Southwire RHH/RHW-2/USE-2	10AWG 600V	40ft	0.99
Bluetooth	0-5V 0-10m	HC-05	0-5V 0-10m	5	5.48

N-Channel Mosfets	0-195V 0-8.5A	Sanken SKP253VR	250V 21A (95mΩ)	4	2.425

Table 5-3: Case 2 Extra Components [55] [56]

Table 5-3 shows the extra components needed to design the 1.2kW with the following resiliency method included into it for Case study 2. This data will be used further on in the KPI analysis section and is meant to provide an overview of the system with resiliency components added.

5.6.4.4 KPI Analysis for 1.2kW System

Key Performance Indicator	Results
Peak Operational Efficiency	Pin =287.44W Pout=270.16W η= 93.98% =94%
Peak Operating THD	2.04518E-002
Overall Resiliency Response time	0.0446 sec or 45ms
Resiliency Response Power Output	300W (ideal) Actual is 256.6W
Resiliency Unit Power Output	300/1200 = 0.25
Peak Operational Efficiency Under Fault	Pin =276.21W Pout=256.59W η= 92.89% =93%
Operating THD under fault	1.94707E-002
Overall Cost for 1.2kW system	$4,570.22
Estimated Yearly Income	$382.32
Estimated Payback Period	11.954 years

Table 5-4: Case 2 KPI

Table 5-4 above shows the KPI for the system. As with Case 1, a further in depth analysis will be conducted in Chapter 6. This section is meant to provide an overview of results before per unit analysis.

5.7 Case 3: Back up 600W inverter inside Paired Micro-Inverters

The following shows the third design case hypothesized in order to increase the systems resiliency. The format section is follows the same as the previous sections.

5.7.1 **Overview Circuit Block Diagram of 1.2kW system**

The following subsection provides the overview to Case 3.

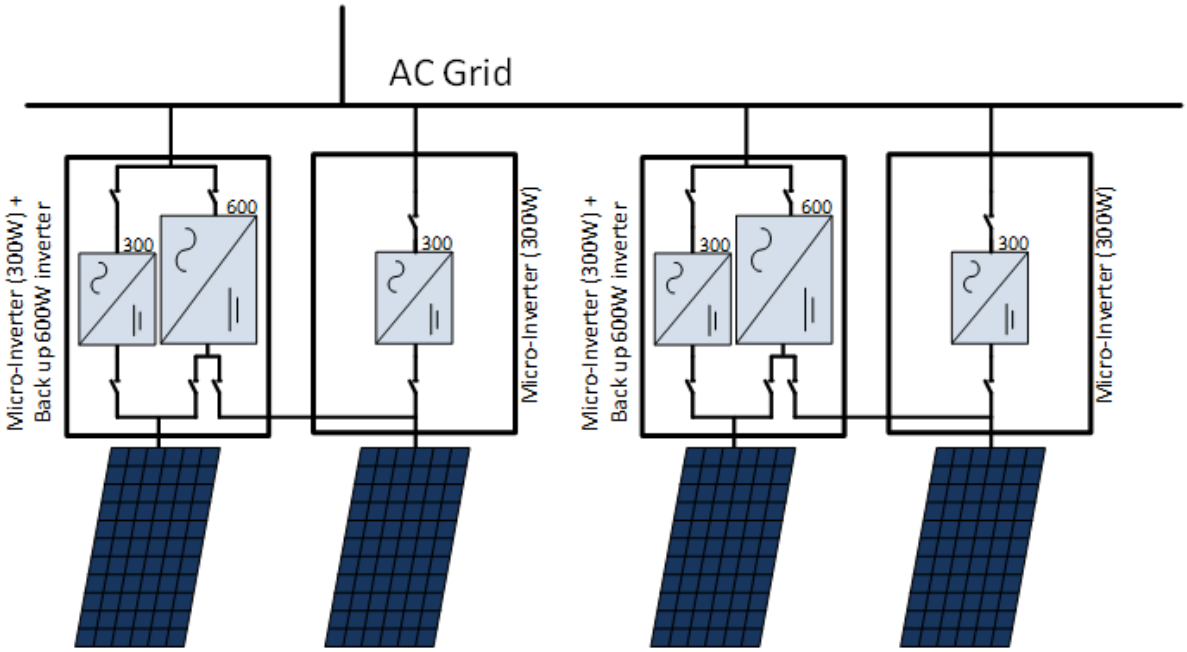

Figure 5-17: Overview Case 3

Case 3 is seen in Figure 5-17 above. For this case, each solar panel is run individually with its own 300W micro-inverter for normal operation. In order to increase the resiliency, an extra back up inverter rated at 600W is placed on the inside of one of the two paired micro-inverters. Similar to the other cases, this back-up inverter is disconnected from the grid. However, its control system is sensing the grid voltage as well as the output from both 300W micro-inverters. In the event of either micro-inverter failing, the control system for the 600W back-up inverter opens all micro-inverter switches. Isolating them both from the grid and their solar panels. Power flow is then redirected from both solar panels through the 600W inverter.

5.7.2 **Operational Theory for 600W system**

The operational theory is described in the following section. This is done strictly for a two micro-inverters working in parallel with a max output power of 600W.

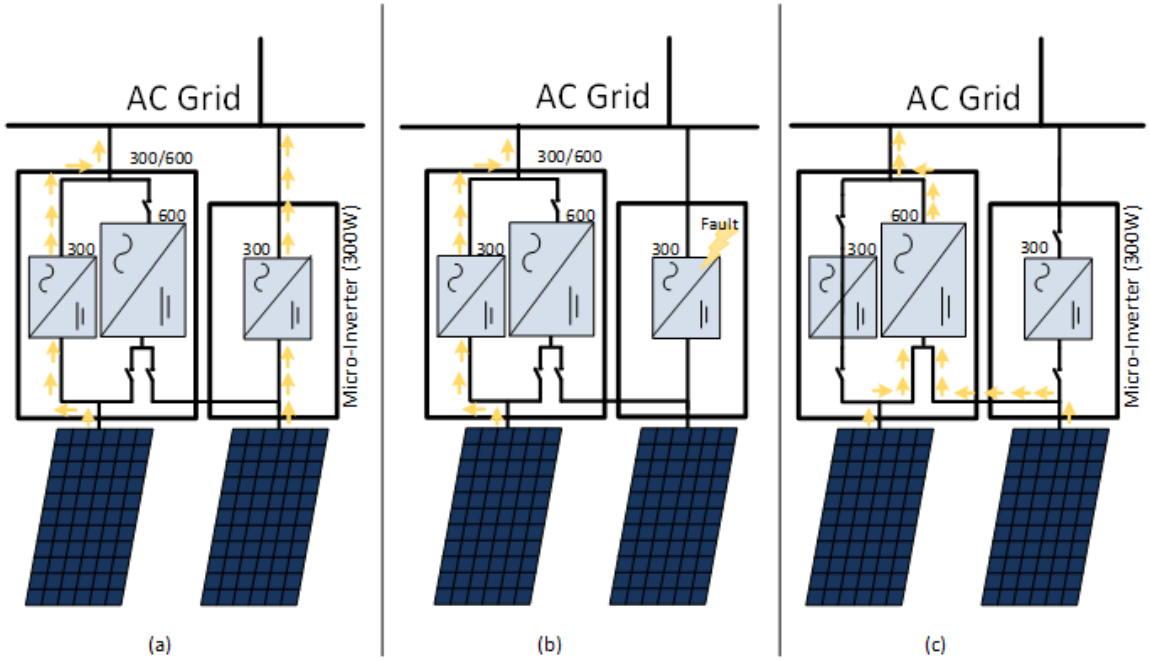

Figure 5-18: Case 3 Operational Theory

Figure 5-18 shows the operation theory of Case 3. Figure 5-18 (a) depicts the two 300W micro-inverters under normal operation. Each is coupled individually to its own solar panel and outputting its power to the grid. Portion (b) of Figure 5-18 shows a fault occurring in one of the micro-inverters. This can occur in either of the two micro-inverters and the resiliency scenario will be deployed. When a fault is sensed by the 600W inverter control system, the control system then opens the switches for the micro-inverters and isolates them from the grid and there respected solar panel. The switches are closed for the 600W inverter connecting it to both solar panels. Power flow is then maintained by redirecting power flow through the 600W inverter as shown in (c) of Figure 5-18.

5.7.3 **Circuit Design**

The following section outlines the Case 3 model designed in PSIM. Similar to the above cases, Mosfets and relays were used in order to control the power flow in the system. Simulation was kept to 600W output to converse memory and cut down on simulation time.

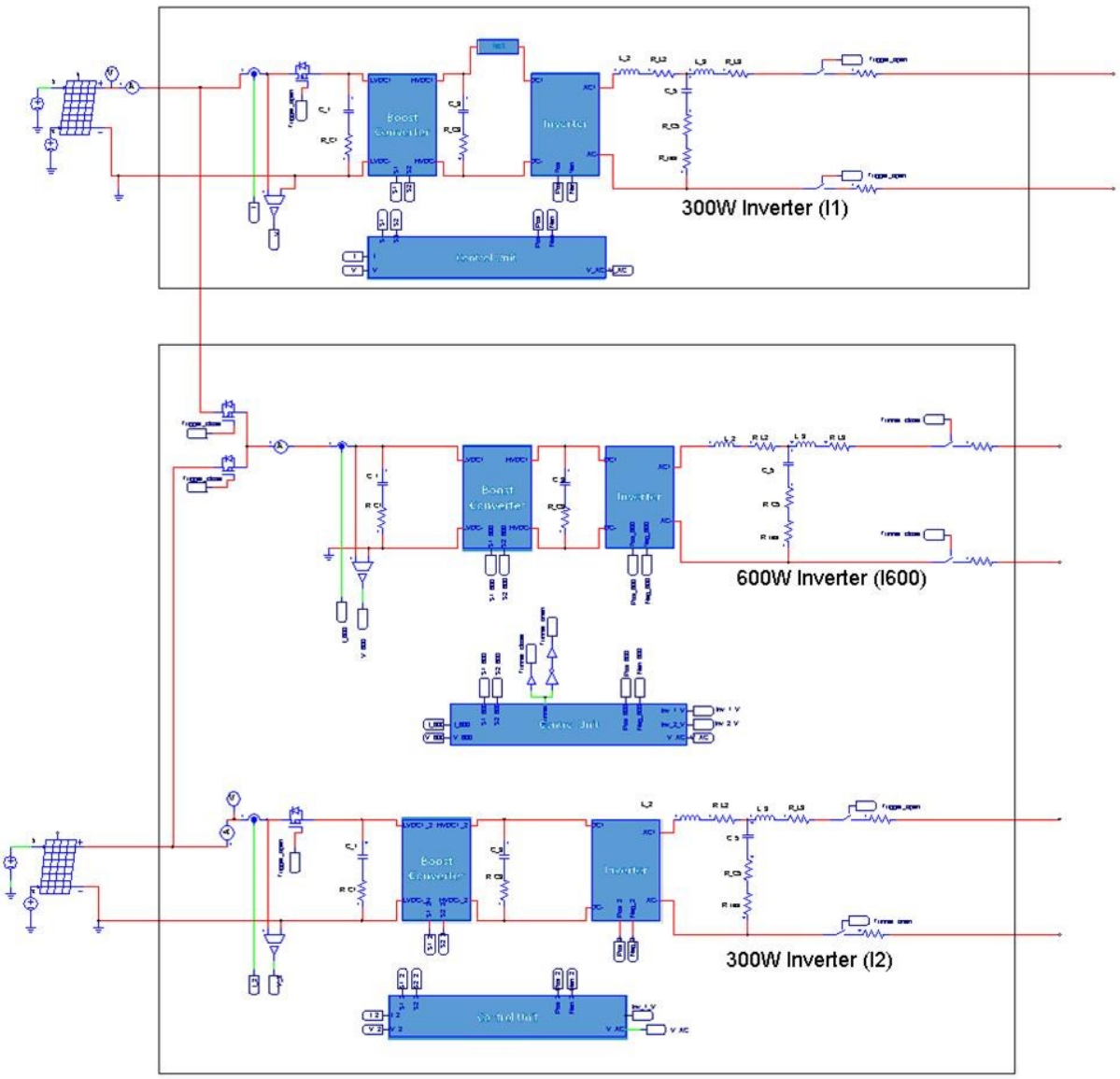

Figure 5-19: Case 3 PSIM Model

Figure 5-19 above shows the PSIM model created for Case 3. The top most square is a primary 300W micro-inverter. The bottom square houses the back-up 600W inverter along with the second primary 300W micro-inverter. The control for the direction of power flow can be seen by the Mosfets and relays located on the inputs and outputs of the inverters.

5.7.4 **Results**

The following section outlines the operational results of the Case 3 in PSIM.

5.7.4.1 Normal Operation

First, the simulation results for the normal operational of Case 3 are shown and can be seen in the figure below.

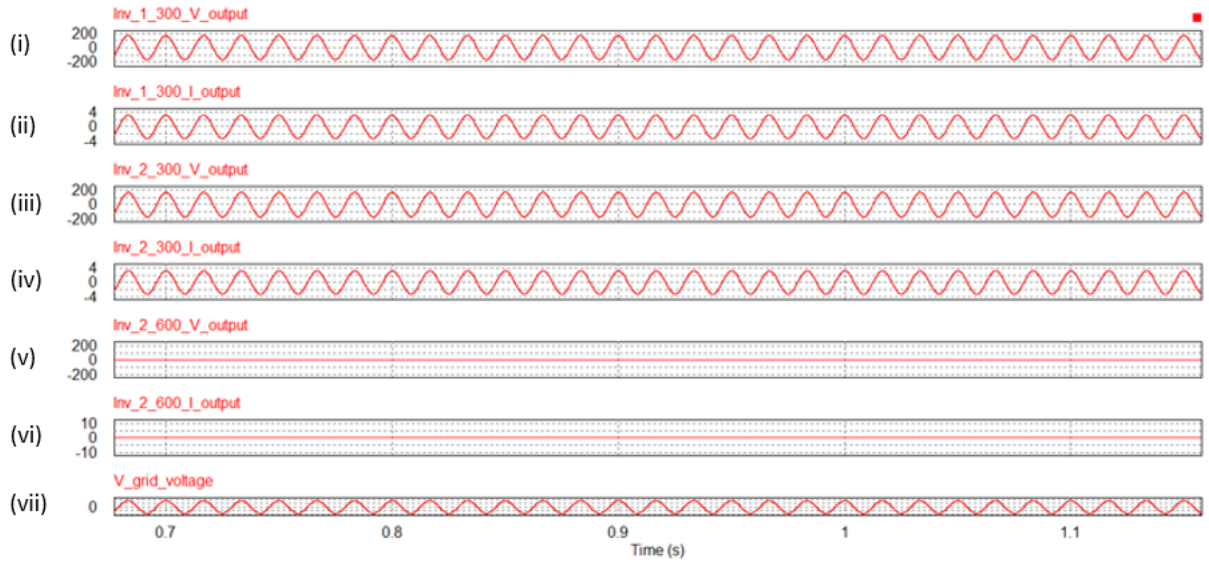

Figure 5-20: Case 3 Normal Operation

Figure 5-20 shows Case 3's normal operation. Beginning from the top; micro-inverter 1's output voltage (i) and current (ii) are shown. This followed by micro-inverter 2's output voltage (iii) and current (iv). Graphs 5 and 6 show the 600W inverter's output voltage (v) and current (vi). Finally the grid reference voltage (vii) is the bottom most graph. It can be seen that the micro-inverters are outputting with a low THD signal in phase with the grid reference voltage. The 600W inverter is outputting no power, which is to be expected under normal operating conditions.

5.7.4.2 Inverter Failure

The following section shows the results in placing a fault in the micro-inverters at 1.5 seconds simulation time.

5.7.4.2.1 Inverter 1 Failure

The results shown in this section, depict the system in the event of a failure in micro-inverter 1. An open circuit fault is triggered at 1.5 seconds simulation time.

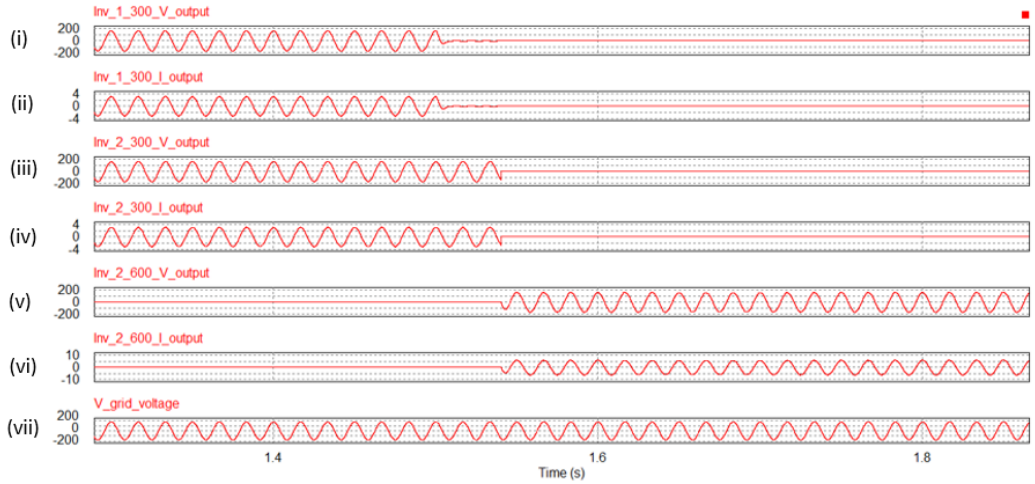

Figure 5-21: Case 3 Micro-inverter 1 Failure

Figure 5-21 above depicts the results of the system with a fault occurring at 1.5 simulation time in micro-inverter 1 [(i) (ii)]. A fault occurs, and the second 300W micro-inverter continues to output its power [(iii) (iv)] as the fault is being recognized by the 600W control system [(v) (vi)]. Once the fault has been recognized, the 600W inverter opens all the switches for the micro-inverters then closes the switches for the 600W inverter. Thus power output is maintained in the system with a small offline period. It can been seen that the outputs are synchronized and meeting grid standards from the figure.

5.7.4.2.2 Inverter 2 Failure

The results shown in this section, depict the system in the event of a failure in micro-inverter 2. As with the previous sub-section, the fault is triggered at 1.5 seconds simulation time.

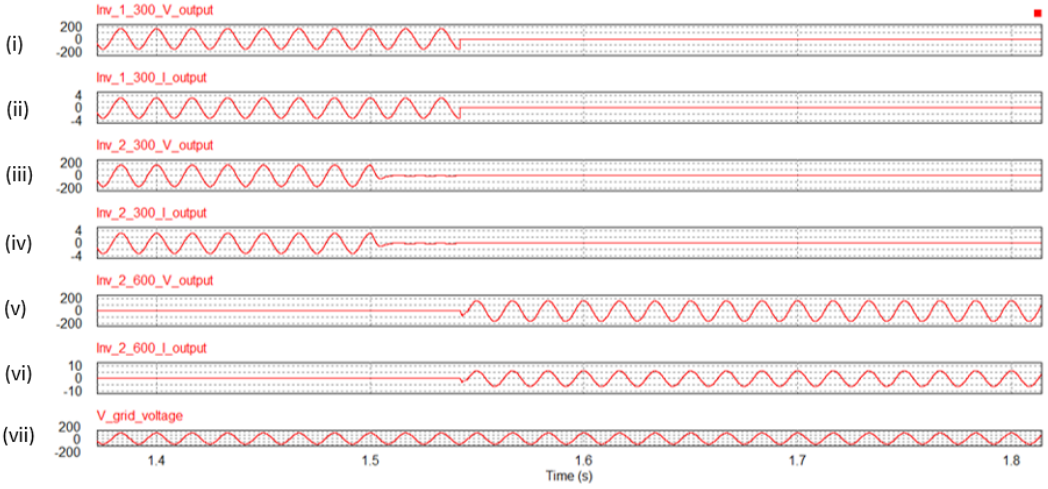

Figure 5-22: Case 3 Micro-inverter 2 Failure

Figure 5-22 above shows the results of a fault occurring in micro-inverter number 2 in the system. Similar results can be seen as that of Figure 5-21. Micro-inverter 2 failure at 1.5 seconds simulation time and disconnection from the grid; Micro-inverter 1 continues to output power until resiliency controller recognizes the failure. After the fault has been recognized, Micro-inverter 2 is disconnected and systems power flow is then redirect through the 600W inverter.

5.7.4.3 Control Time

The following shows the system output for the inverters in case of a fault occurring in on the second 300W micro-inverter.

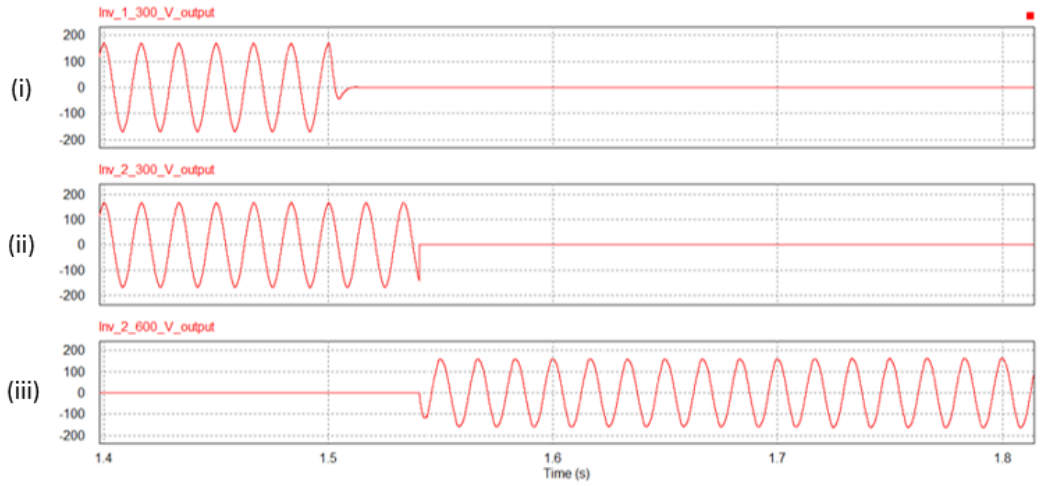

Figure 5-23: Case 3 Control Time

Figure 5-23 above shows the results of the system output. The top most graph shows micro-inverter 1, output voltage (i). Micro-inverter output voltage (ii) is then followed by the 600W inverters output voltage (iii). From the graph it can be seen that once a fault has occurred during the normal operation of the micro-inverter (occurring at 1.5 seconds), it take approximately 0.0467 seconds for the 600W inverter to be outputting power.

5.7.4.4 Additional Components 1.2kW System

Scaling the simulation up to the full 1.2kW system the following extra components will be needed. This is building on Case 0 components in retrofit it into Case 3.

Component Description	Operating Conditions	Manufacturer	Component Maximum Conditions	Amount needed	Cost per unit ($CAN)
Extra Inverter (600W)	20-50V 0-16.5A	UOIT	20-50V 0-16.5A	2	1,671.8
Relay	120Vrms 4Arms	Songle srd-05vdc-sl-c	10 A 280VDC 10A 240Vrms	12	4.99
Cables For Power Transfer	36V	Southwire RHH/RHW-2/USE-2	10AWG 600V	6ft	0.99/ft
Cable For Communication	36V	Southwire RHH/RHW-2/USE-2	10AWG 600V	6ft	0.99/ft
N-Channel Mosfets	0-36V 0-8.5A	Sanken SKP253VR	250V 21A (95mΩ)	8	2.425

Table 5-5: Case 3 Extra Components [55] [56]

Table 5-5 shows the extra components needed to design the 1.2kW with the following resiliency method included into it for Case study 3. As with the similar tables, this data will be used further on in the KPI analysis section and is meant to provide an overview of the system with resiliency components added.

5.7.4.5 KPI Analysis 1.2kW System

Key Performance Indicator	Results
Peak Operational Efficiency	Pin = 287.43W Pout = 269.54W η = 93.77% = 94%
Peak Operating THD	2.03612E-002
Overall Resiliency Response time	0.0467 sec
Resiliency Response Power Output	600W (ideal) Actual is 482.82W
Resiliency Unit Power Output	1200/1200 = 1
Peak Operational Efficiency Under Fault	Pin = 565.4 Pout = 482.82 η = 85.4%
Operating THD under fault	1.7929E-002
Overall Cost for 1.2kW system	$7,320.88
Estimated Yearly Income	$382.32
Estimated Payback Period	19.12 years

Table 5-6: Case 3 KPI

Table 5-6 above shows the KPI for Case 3. A further in depth analysis will be conducted in chapter 6. It should be noted that this resiliency method can cover the entire system (if both micro-inverter fail), however the output efficiency significantly reduces (approximately 10%). The PP of the system has also increase significantly for this case from 11 years for Case 0 to 19 years.

5.8 Case 4: Dual Mode Inverters

Section 5.8 shows the fourth case study hypothesized in order to increase the PV systems resiliency. This section follows the same format as the previous sections.

5.8.1 **Overview Circuit Block Diagram of 1.2kW system**

The following subsection provides the overview to Case 4.

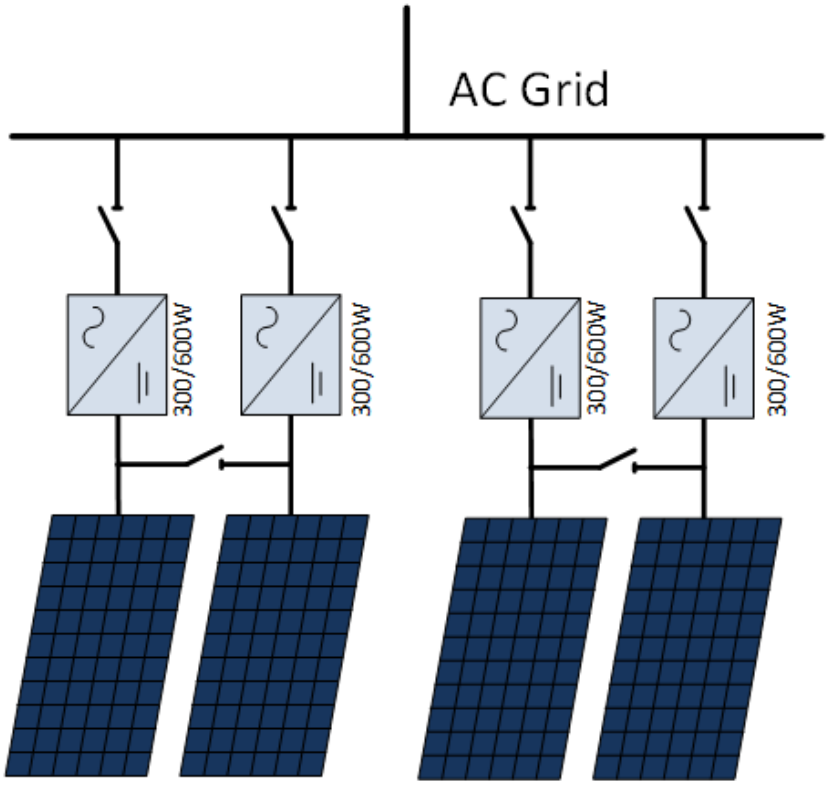

Figure 5-24: Case 4: Overview

Case 4 can be seen in Figure 5-24 above. For this case, each solar panel is connected to a Dual Mode Inverter. This inverter is one which output at two different power levels, 300W and 600W. Under normal operation, each solar panel is run individually and connected to a Dual Mode Inverter which is operating in 300W mode. The panels are isolated from one another and operating individually. In the event of a Dual Mode Inverter failing, the functioning Dual Mode Inverter on the same roof mount (2 solar panels per roof mount), will then modify its internal components and turn itself into a 600W inverter. Both solar panels are paired together and connected to the input of the Dual Mode Inverter and full power output continues.

5.8.2 **Operational Theory for 600W System**

The operational theory is described in the following section. This is done strictly for a two Dual Mode Inverters working in parallel with a max output power of 600W for the system.

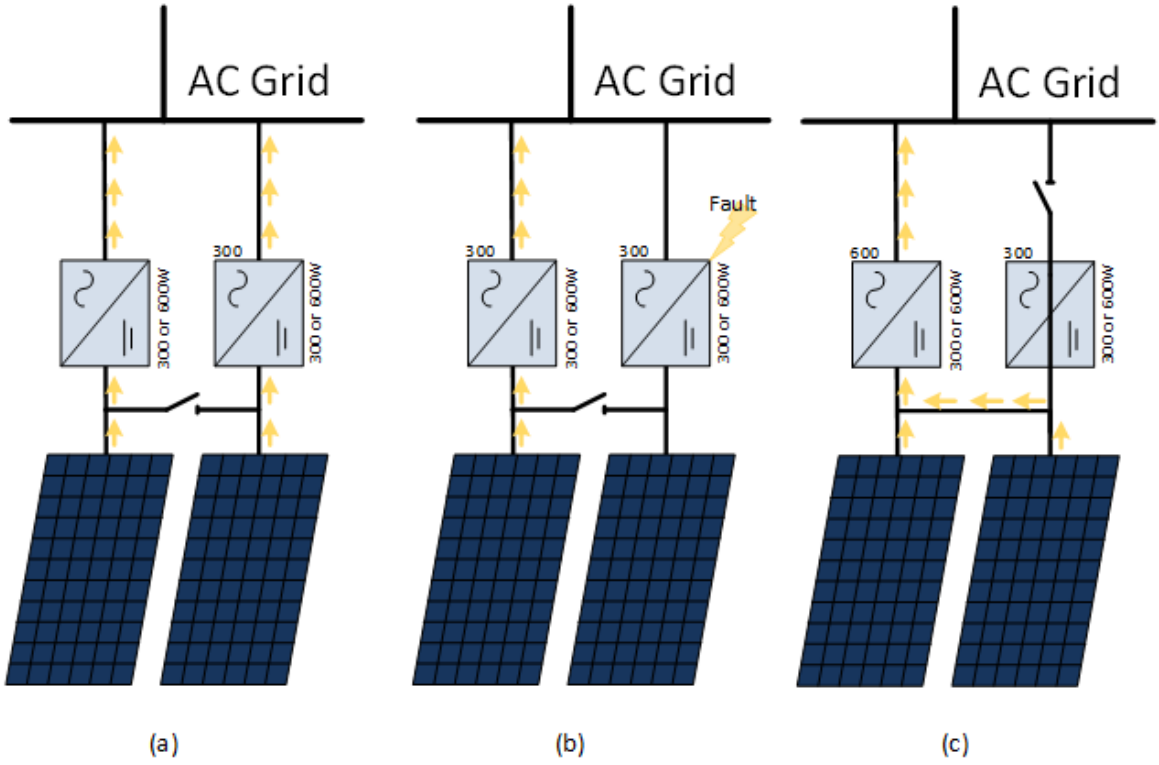

Figure 5-25: Case 4: Operational Theory

Figure 5-25 demonstrates the operational theory for the final resiliency case analyzed. Part (a) shows the normal operation of the design. Both solar panels feed their power directly to their own individual 300W micro-inverter directly coupled to the grid. Under normal operation, both solar panels are not coupled together and are working in isolation from one another. Part (b) of Figure 5-25 shows a fault occurring in a primary micro-inverter. This can occur in either of the micro-inverters. When this occurs, the faulted micro-inverter is disconnected from the grid and its solar panel. Both solar panels are coupled together and the working micro-inverter reconfigures itself in order to produce 600W output power. Before the results are shown, the dual mode inverter will be explained in further detail.

5.8.3 **Dual Mode Inverter Design**

The following section outlines the Dual Mode Inverter designed in PSIM. An overview is provided regarding the modification to the sub-circuits.

5.8.3.1 Boost Controller Sub-Circuit Design

In order for the boost converter to adjust the DC voltage as needed for the different input currents as well as output voltage, a dual purpose boost converter needs to be created.

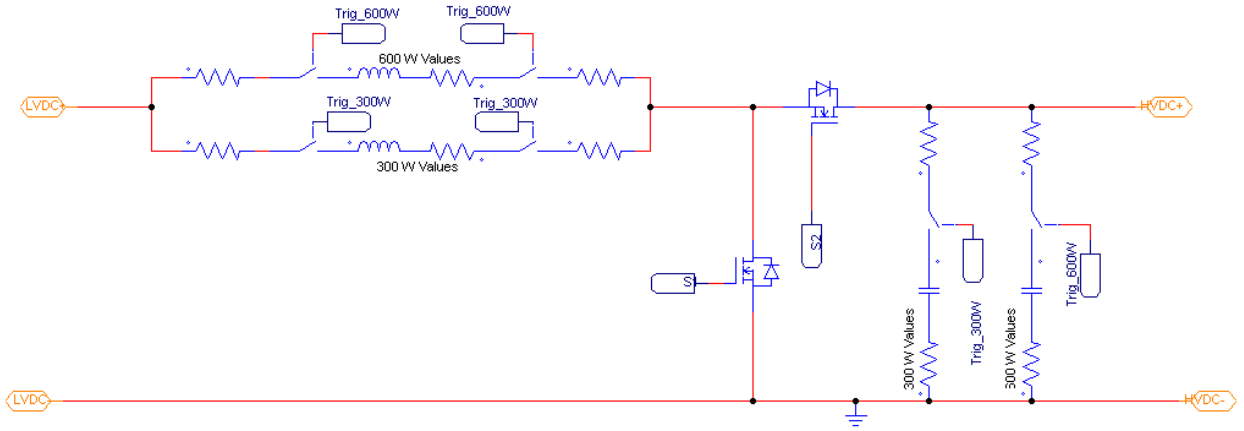

Figure 5-26: Case 4 Boost Converter

Figure 5-26 shows the overall design of the dual mode boost converter. Essentially, both the 300W micro-inverter and the 600W inverter components are placed in parallel with one another connected into the circuit by relays. The opening and closing the relays thus determines which power level the boost converter is operating in. The N-channel Mosfets do not need to be adjusted or changed as they can safely operate at both power levels. The boost converters inductors can be seen on the top left hand side of the figure and the capacitor on the far right hand side. Internal resistances have been included for all the components (inductors, capacitors and relays) within the circuit design. For the inductor, the bottom circuit path holds the value for the 300W micro-inverter, while the top path holds the for the 600W inverter. Thus with this configuration, a boost converter can output at two different power levels.

5.8.3.2 Inverter Sub-circuit Design

The inverter sub-circuit is shown in the figure below. This has not changed as the Mosfets can handle the voltage and currents safely and within margins at both power levels.

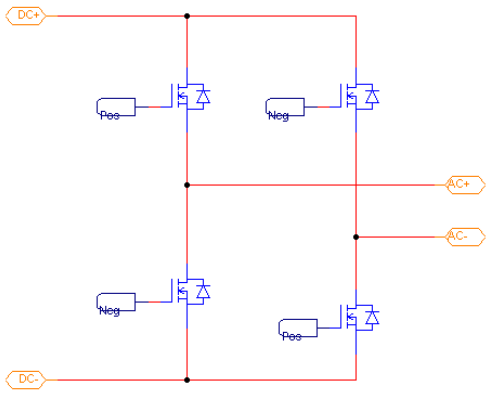

Figure 5-27: Case 4 H-Bridge

The Mosfets chosen, have a low internal resistance (95mΩ) and can handle voltages to approximately 250V and currents of up to 21A [55, 56]. Under normal operating condition, the 300W micro-inverter has a nominal voltage of about 210V and pulses of 5A applied to the H-bridge. While the 600W inverter has approximately 220V and pulses of 10A. As such the Mosfets have a sufficient buffer which can handle the switching stresses at both power levels and therefore it does not require modifications to the sub-circuit.

5.8.3.3 Filter Sub-circuit Design

As with the boost converter, the filters needs to be adjustable to accommodate both power levels. Therefore, relays were used to connect the two different LCL filters designed: the 300W LCL filter and the 600W LCL filter. Relays are placed on the inputs and outputs to the filter, in order to connect/disconnect them to the inverter power stage and grid.

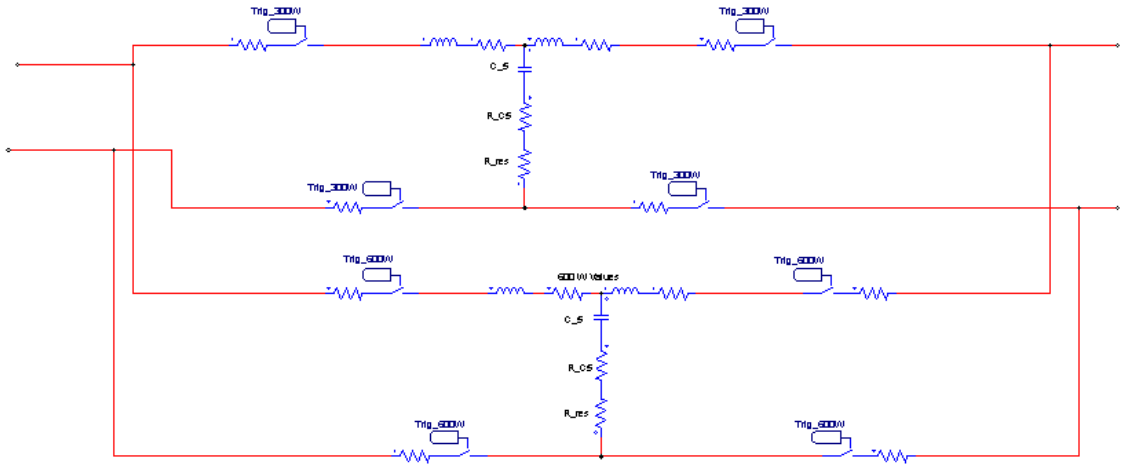

Figure 5-28: Case 4 Filter

Figure 5-28 shows the dual filter circuit designed. It is essentially two filters are placed in parallel with one another and all input and outputs are given their own relay in order to completely isolate/connect them as needed by the control circuit.

5.8.3.4 Components Dual Mode Inverter

In creating a dual mode inverter the following components are needed.

300 Watt Inverter							
Circuit ID Number	**Component Description**	**Operating Conditions**	**Component Values**	**Manufacturer**	**Maximum Conditions**	**Amount needed**	**Cost per unit ($CAN)**
C_1	DC link capacitor	0-46V 0-62.8mA	4.7µF	Panasonic ECA2CM4R7	0-160V 0-78mA (9.1mΩ)	1	0.49
L_1	Boost inductor	0-210V 0-8.3A	9mH	Wurth Elektronik	0-250V 0-13A (15mOhm)	1	34.98
C_2	Boost Capacitor	0-210V	10mF	Electronicon E50.R29-505NTO	600VDC 100A (0.72mΩ)	2	70.65
S1-S6	Boost + Inverter N Channel	0-195V 0-8.5A	N/A	Sanken SKP253VR	250V 21A (95mOhm)	6	2.425
C_3	DC link capacitor (high voltage)	0-210V 0-6A	5mF	Electronicon E50.R29-505NTO	600VDC 100A (0.72mΩ)	1	70.65
L_2	Filter inductor	0-400V 0-7.5A	390µH	J.W.Miller 1140-391K-RC	0-9A (0.082Ω)	1	10.82
L_3	Filter Inductor	0-120V 0-3.48A	100mH	Hammond 195T5	0-5ADC (0.64Ω)	1	135.44
C_4	Filter Capacitor	0-205V 0-5A	18.3µF	TDK B32794D3205 (3.3µF)	300Vrms 630VDC (ESR 9.7mΩ)	1	1.45
C_4	Filter Capacitor	0-205V 0-5A	18.3µF	TDK B32794D2156 (15µF)	250Vrms 700VDC ESR 3.1mΩ)	1	6.67
R_res	Filter resistance	0-11V 0-5A	2Ω	Bourns PWR263S-20	2Ω 20W	1	3.51
Control Chip	MPPT + PLL chip	0 - 42V	N/A	Texas Instruments c2000 Piccolo Micro controller	-0.3-4.6V	1	16.43
Current Sensor	Boost Converter	0 - 42V 0-8.73A	N/A	Allegro MicroSystems	20Arms (100mV/A)	1	2.69

	current sensor			ACS712 ELCTR-20A			
Current Sensor	PLL grid current sensor	120Vrms 2.5Arms	N/A	Honeywell CSLA2CD	72 Arms (32.7mV/N)	1	37.03
600 Watt Components							
L_1	Boost inductor	0-210VDC pulse 0-15.98A pulse	30mH	Hammond Manufacturing 195p20-ND	0-250V 0-20A (15mΩ)	1	453.37
C_2	Boost Capacitor	0-195V 0-11A pulse	3.3mF	TDK B43456A9338M	400VDC 20A (23mΩ)	1	110.26
L_2	Filter inductor	0-400V 0-11.5A	1mH	Schurter Inc.	0-15A (10mΩ)	1	33.61
L_3	Filter Inductor	0-120V AC 0-6.7A	50mH	Hammond 195R19	0-5ADC (165mΩ)	1	267.38
C_4	Filter Capacitor	0-350VAC 0-10AAC	37µF	TDK (22µF) B4356A2229M	250VDC 34 A AC (ESR 5mΩ)	1	213.12
C_4	Filter Capacitor	0-350VAC 0-10AAC	37µF	TDK B4354A2159M (15µF)	250VDC 34 A AC (ESR 7mΩ)	1	191.03
R_res	Filter resistance	0-350VAC 0-10AAC	2Ω	Bourns PWR263S-20	2Ω 20W	1	3.51
Relays	Boost, Filter , DC Link	0-220V 0-16.5A	N/A	TE PB1014-ND	240VAC 30A (100mΩ)	14	6.19
						Total	1834.95
Extras and Reserve	PCB, wires, resistors, heat sink. etc.						15%
						Estimated Total	2110.2

Table 5-7: Dual Mode Inverter Components [55] [56]

Table 5-7 above shows the results of the dual mode inverter. As with the other inverters, an additional 15% was added to compensate for unknowns. This brought the total to $2,091 which is comparable to adding the two inverters together in cost. The biggest cost within the system is attributed to the indicators and the capacitors needed for higher current and voltage applications.

5.8.4 **Circuit Design**

Figure 5-29 shows the PSIM model of Case 4 with two Dual Mode Inverters deployed. As with the other cases, the limit for the simulation will be a 600W output power to cut down on simulation time.

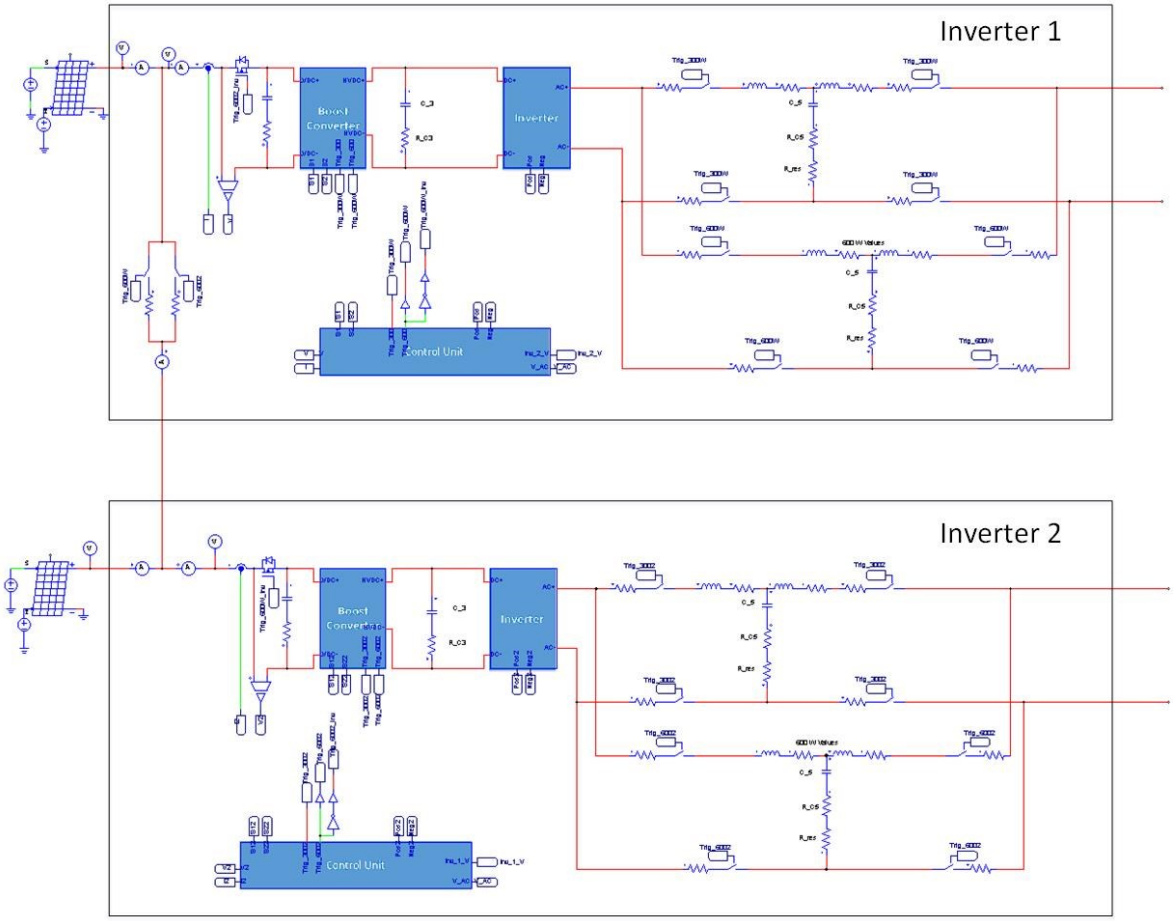

Figure 5-29: Case 4 PSIM Model

As stated previous, both inverters have the ability to modify their internal components to different power levels and have the ability control power flow within the system. The two solar panels can be paired together with closing the relay connected to each panel. Power flow into the inverters is controlled by Mosfets. The output filters are connected and disconnected with relays in order to allow for two direction flow of voltage and current. Inverter 1 is the top most inverter, while Inverter 2 is the bottom most inverter for this simulation. The results of the system will be explored in the following sections below.

5.8.5 **Results**

The following section outlines the operational results of Case 4 in PSIM.

5.8.5.1 Normal Operation

The first section shows the simulation results for normal operation of the inverters. Both Dual Mode Inverters are operating in 300W mode and directly coupled to its own individual solar panel.

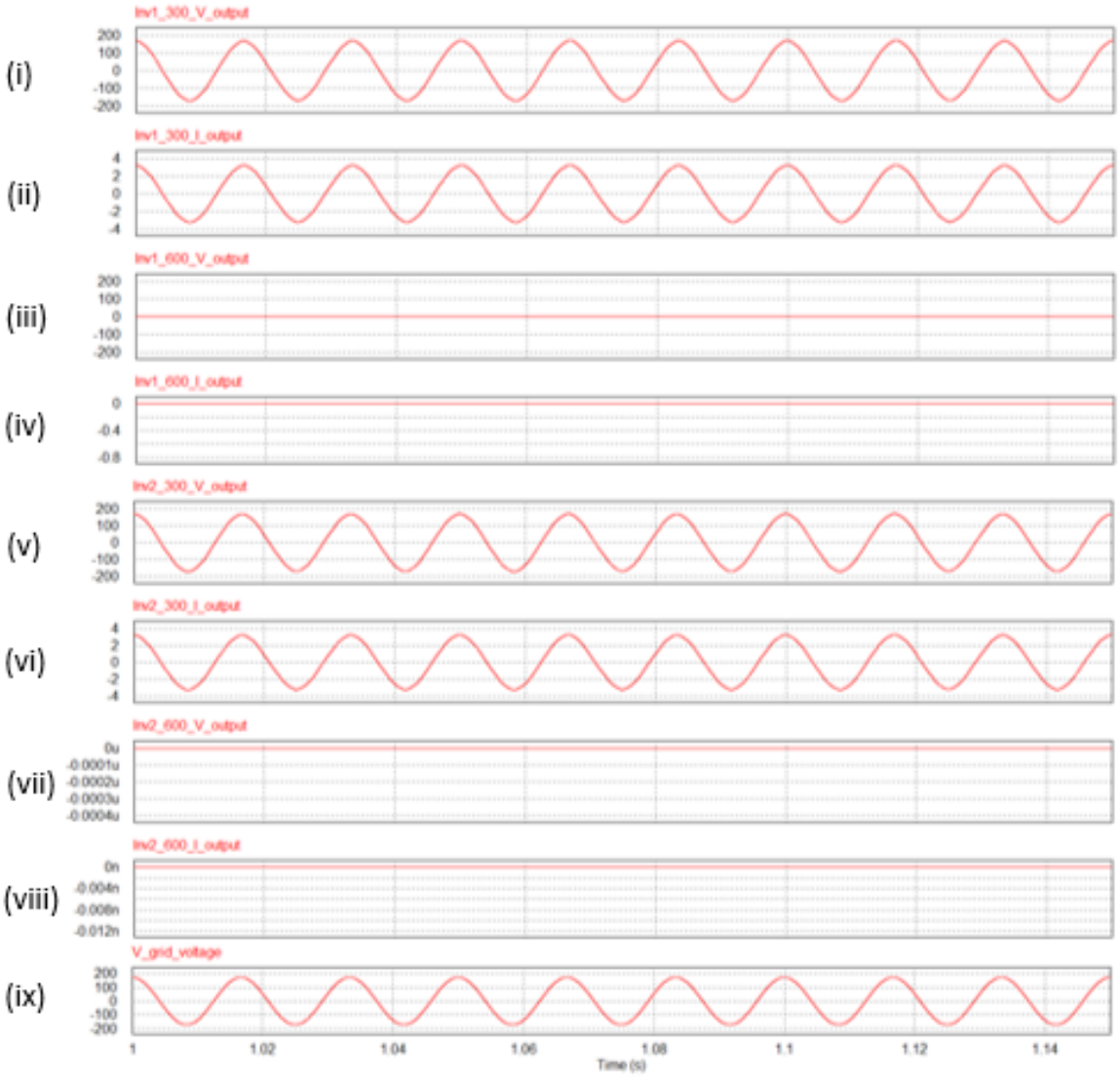

Figure 5-30: Case 4 Normal Operation

Figure 5-30 shows the results for the simulation run in PSIM. Dual Mode Inverter 1's 300W mode output voltage (i) and current (ii) are followed by its 600W mode output voltage (iii) and current (iv). Dual mode Inverter 2's 300W mode output voltage (v) and current (vi) followed by its 600W modes output voltage (vii) and current (viii). Finally the bottom most graph shows the grid reference voltage (ix). From Figure

5-30 it can be seen that the system is operating as expected, both Dual Mode Inverters are operating in 300W mode and synchronized to the grid with low THD.

5.8.5.2 Inverter Failure

The following sections provides an overview of the results when a fault is placed into one of the inverters at 2 seconds simulation time. In order to save space within the thesis, only voltages will be displayed for the resiliency results in this sub-section.

5.8.5.2.1 Inverter 1 Failure: Inverter 2 Turns Into 600W

The resiliency testing beings with placing a fault in Dual Mode Inverter 1.

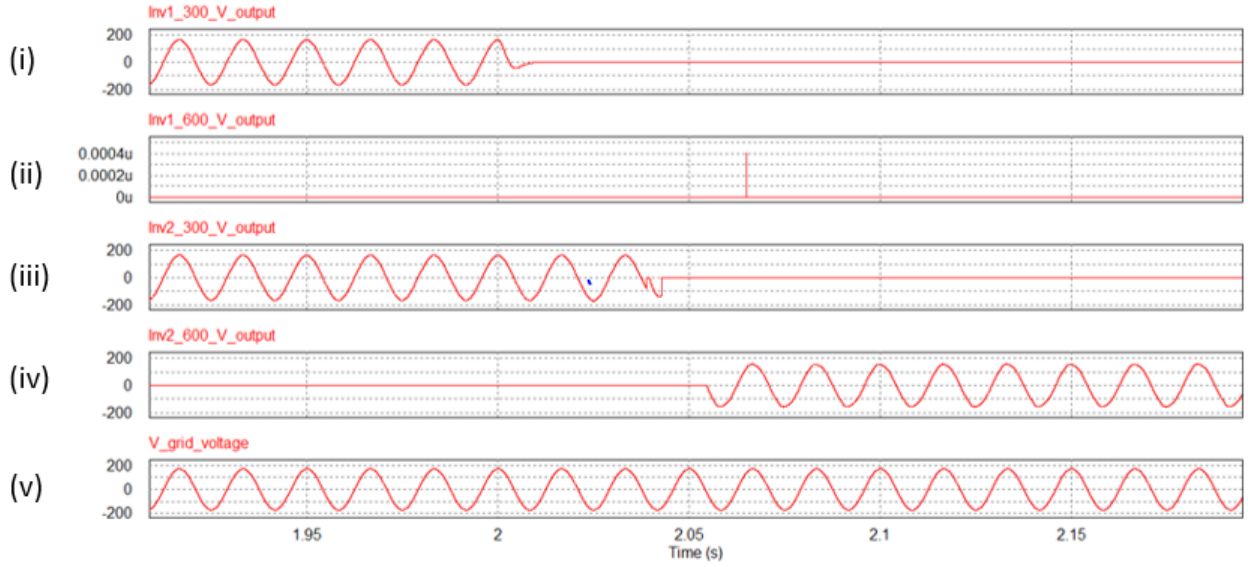

Figure 5-31: Case 4 Inverter 1 Failure

A fault was placed at 2 seconds simulation time. From top to bottom, the graphs are: Dual Mode Inverter 1 300W mode (i) followed by its 600W mode (ii). Dual Mode Inverter 2 300W mode output voltage (iii) followed by its 600W output voltage (iv). Finally grid reference voltage (v) is the bottom most graph. The open circuit fault was placed within Dual Mode Inverter 1 on the DC link side of the inverter stage. Dual Mode Inverter 2 continues to operate in the 300W mode. Once its control system recognizes that a fault has occurred, the necessary switches are opened isolating Dual Mode Inverter 1. The internal components for Dual Mode Inverter 2 are then adjusted in order to output 600W. Dual Mode Inverter 2 then pairs both solar panels and reconnects to the grid to resume outputting power. It can be seen that the dual mode inverter operates effectively and within the 160ms target.

5.8.5.2.2 Inverter 2 Failure: Inverter 1 Turns Into 600W

The resiliency then beings with placing a fault in Dual Mode Inverter 2, the results of the simulation which can be seen in the Figure 5-32 below.

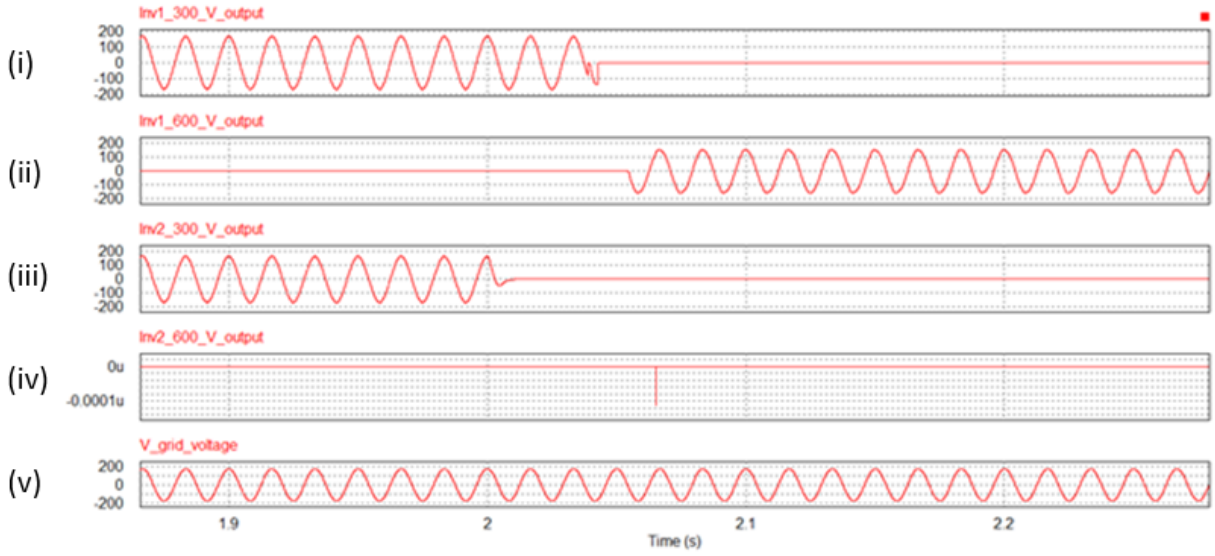

Figure 5-32: Case 4 Inverter 2 Failure

Similar to the previous simulation, the open circuit fault was placed a 2 second simulation time. The graphs of Figure 5-32 are as follows: Dual Mode Inverter 1 300W mode voltage (i) followed by its 600W mode (ii). Dual Mode Inverters 2's 300W output (iii) is then followed by its 600W output (iv). The grid reference occurs in the bottom most figure (v). The fault occurs in Dual Mode Inverter 2 at 2 seconds and it is disconnected from the grid. Dual Mode Inverter 1 continues to output as its control system is recognizing the failure in Dual Mode Inverter 2. Once the control system has recognized the fault, it modifies the switches throughout the circuit accordingly and power output to continues.

5.8.5.3 Control Time

The following shows the system output in case of a fault occurring in one of the Dual Mode Inverters.

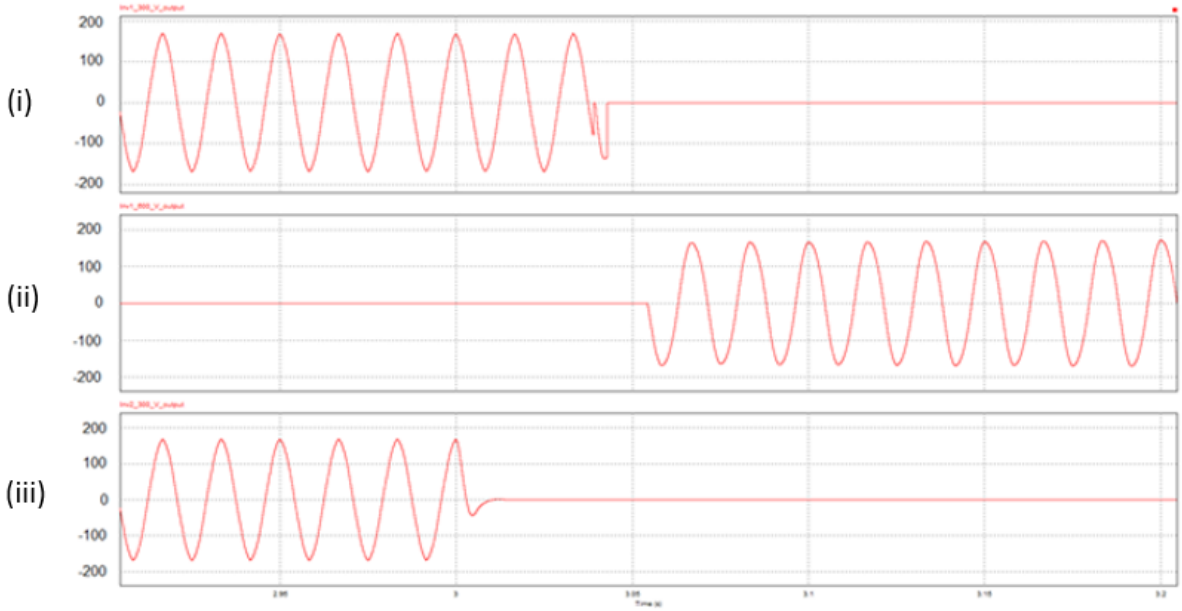

Figure 5-33: Case 4 Control Time

Figure 5-33 (i) shows Dual Mode Inverter 1 300W voltage, (ii) Dual Mode Inverter 1 600W voltage, (iii) Dual Mode Inverter 2 300W output voltage. The fault occurs in the secondary dual mode inverter as the system operates under normal conditions. From Figure 5-33 above, it can been seen that the system takes approximately 0.0541 seconds from the initial fault occurs before the system is resuming full power output.

5.8.5.4 Extra Components 1.2 kW System

Scaling the simulation up to the full 1.2kW system the following extra components will be needed. This is building on Case 0 components in retrofit it into Case 4.

Component Description	Operating Conditions	Manufacturer	Component Maximum Conditions	Amount needed	Cost per unit ($CAN)
Relay	120Vrms 4Arms	Songle srd-05vdc-sl-c	10 A 280VDC 10A 240Vrms	4	4.99
Cables (Power)	36V	Southwire RHH/RHW-2/USE-2	10AWG 600V	10ft	0.99/ft
Cables (Communication	5V	Southwire RHH/RHW-2/USE-2	10AWG 600V	10ft	0.99/ft
Mosfets	0-36V 0-8.5A	Sanken SKP253VR	250V 21A (95mΩ)	4	2.54

Table 5-8: Case 4 Extra Components [55] [56]

Table 5-8 shows the extra components needed to design the 1.2kW system with the following resiliency method included proposed for Case Study 4. As with the similar tables, this data will be used further on in the PU-KPI analysis section and is meant to provide an overview of the systems extra components needed.

5.8.5.5 KPI Analysis 1.2kW System

Key Performance Indicator	Results
Peak Operational Efficiency	Pin = 287.43W Pout 255.3W η =88.82% = 88.8%
Peak Operating THD	2.14E-002
Overall Resiliency Response time	0.054817
Resiliency Response Power Output	600W (ideal) Actual is 489.29W
Resiliency Unit Power Output	1200/1200=1
Peak Operational Efficiency Under Fault	Pin = 559.7W Pout = 415.3W η = 74.2%
Operating THD under fault	1.3556-002
Overall Cost for 1.2kW system	$10,172.34
Estimated Yearly Income	$361.08
Estimated Payback Period	28.18 years

Table 5-9: Case 4 KPI

Table 5-9 above shows the KPI for the system for this case. A further in depth analysis will be conducted in Chapter 6. Note the high PP of 28.2 years. As with some of the previous case, this method can cover the entire system in the event of micro-inverter failure. The output efficiency for this case has significantly reduced. Under normal operation the output system is now 88% efficient. When a fault has occurred, the system operates at 74.2% efficiency. This significant reduction in efficiency is due to the addition of relays located throughout the circuit for both creating the Dual Mode Inverter as well as controlling power flow within the system.

Chapter 6: Results

6.1 Motivation

The following section provides an overview of the results for the different cases studies. In addition this section applies the proposed system evaluation methodology created to identify which case study is best suited.

6.2 Assigning Weights

The first step in the methodology, is to generate Case 0 and calculate the KPI results for it. This has already been achieved and therefore the process will proceed to the second step in the evaluation methodology. This portion consists of assigning weights to the PU-KPI performance characteristics.

PU-KPI	Equation Number	a_j weight
$PU\_KPI_{Resnse\ Time}$	2-14	1
$PU\_KPI_{Res\ Power\ Coverage}$	2-15	1
$PU\_KPI_{E\ N\ to\ F}$	2-16	1
$PU\_KPI_{E\ Case\ to\ Case}$	2-17	1
PU_KPI_{THD}	2-18	1
$PU\_KPI_{THD\ Case\ to\ Case}$	2-19	1
$PU\_KPI_{Initial\ Cost}$	2-20	3
PU_KPI_{PPI}	2-21	4

Table 6-1: Weights

Table 6-1 above shows the results of the weights assigned. The stakeholders were asked the individual PU-KPI and asked to rate their preferences on them based on their needs. Rating was done on a scale from 1 to 5, with 1 being not a major concern and 5 being a major concern. It can be seen from the table, that the stakeholders requested a system which will have a low initial cost and fast PP. Recall, that the higher the summation, the better the choice.

6.3 Summary of Resiliency KPU

The third step in the methodology is to summarize the KPI for analysis. Prior to this, a couple of the KPI will be shown for the case studies.

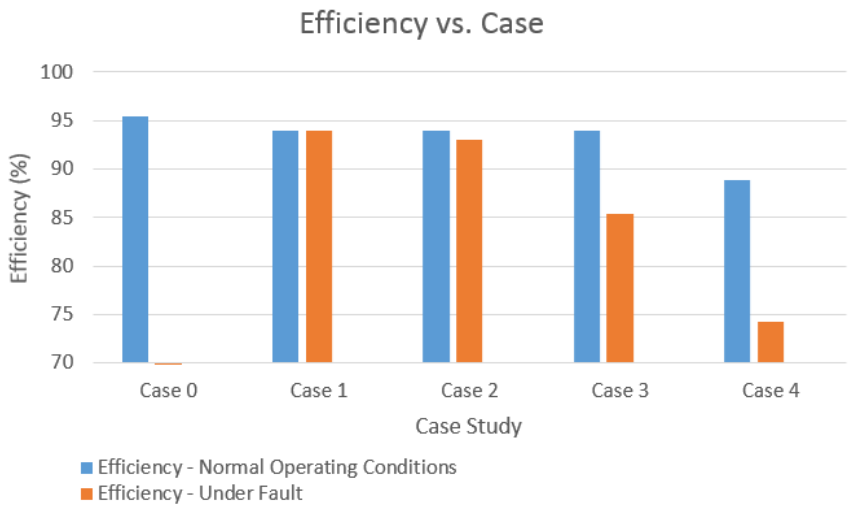

Figure 6-1: KPI Efficiency vs. Case

Figure 6-1 above shows the efficiencies for the different case studies. The blue graphs indicate the efficiency under normal operating conditions, or rather, when the systems are operating as isolated micro-inverters. The orange graphs show the efficiency of the system when operating under resiliency scenarios. Case 0, the normal micro-inverter case contains no resiliency scenarios, therefore no orange graph is show for that case. Case 1 has the highest operating efficiencies within both modes of operation, followed closely by Case 2. Case 4, the Dual Mode Inverters has the lowest efficiencies under both operating conditions. As stated earlier, this is due to the extra losses located throughout the system from the relays and Mosfets.

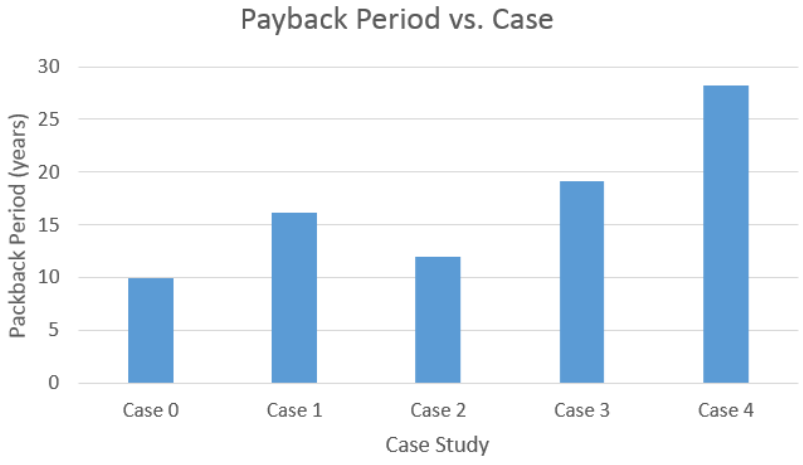

Figure 6-2: KPI PP vs. Case

Figure 6-2 above shows the PP for each of the scenarios. Case 0 has the minimum PP, and that is because it is the base scenario all the case studies are building upon. Of all the resiliency cases, Case 2 (300W micro-inverter in Parallel) has the lowest PP with Case 4 having the largest. Summarizing all the KPI for the case studies:

Key Performance Indicator	Case 0: No Resiliency added	Case 1 : Two 300W inverter Inside	Case 2: 300W inverter in Parallel	Case 3: 600W inverter inside	Case 4: Dual Mode Inverter
Peak Operational Efficiency	Pin = 287.44W Pout= 274.44W η= 95.47%	Pin =287.44W Pout=270.16W η=94%	Pin =287.44W Pout=270.16W η=94%	Pin= 287.43W Pout = 269.5W η = 94%	Pin = 255.3W Pout 287.43 η= 88.8%
Peak Operating THD	2.11E-002	2.04518E-002	2.04518E-002	2.03612E-002	2.4E-002
Overall Resiliency Response time	N/A	0.03945 sec	0.0446 sec	0.0467 sec	0.05417 sec
Resiliency Response Power Output	N/A	300W (ideal) Actual is 270.16W	300W (ideal) Actual is 256.6W	600W (ideal) Actual is 482.82W	600W (ideal) Actual is 415.3W
Peak Operational Efficiency Under Fault	N/A	Pin =287.44W Pout=270.16W η= 93.98% =94%	Pin =276.21W Pout=256.59W η= 92.89% =93%	Pin = 565.4 Pout = 482.82 η = 85.4%	Pin = 559.7W Pout= 415.3W η = 74.2%
Operating THD under fault	N/A	2.04518E-002	1.94707E-002	1.7929E-002	1.3556E-002
Overall Cost for 1.2kW system	$3,871.64	$6,168.56	$4,560.62	$7,320.88	$10,172.34
Estimated Yearly Income	$387.98	$382.32	$382.32	$382.32	$361.1
Estimated Payback Period	9.98 years	16.13 years	11.92 years	19.12 years	28.2 years

Table 6-2: KPI Summary Table

Table 6-2 above shows the summary of the KPI for Cases 0 to 4. Overall all the systems show relatively good performance results such as efficiency and low THD. The annual income is relatively the same across the case studies due to the fact that operating efficiency are relatively consistent among all the cases. Slight variation are seen in the resiliency response times. The biggest differences between the systems can be seen in the initial cost and PP results of the systems.

6.4 Calculating and Mapping of PU-KPI

The following section provides an overview of the results and compares the cases studies to one another based on the PU-KPI methodology proposed. Recall the objective of this was to standardise the KPI which

consists of different units (years, $, W, etc.) into unit less values. The results of the PU-KPI should typically range around 1 in value.

6.4.1 **Resiliency Power Coverage**

The following refers to the resiliency power coverage.

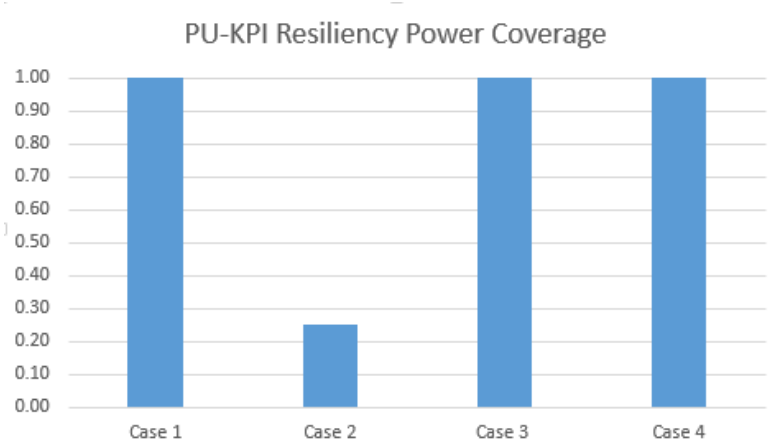

Figure 6-3: PU-KPI Resiliency Power Coverage

Figure 6-3 shows the results from the PU-KPI calculation throughout the cases studies. This graph essentially demonstrates, that all case studies have 1.2kw back up capacity expect for Case 2. Therefore for Cases 1, 3 and 4 the micro-inverter system were to fail and go offline, full power output can still be maintained. In Case 2, only 25% of the solar panels capacity can be maintained.

6.4.2 **Efficiencies**

The following Figure 6-4 below shows the results of the efficiencies of the systems.

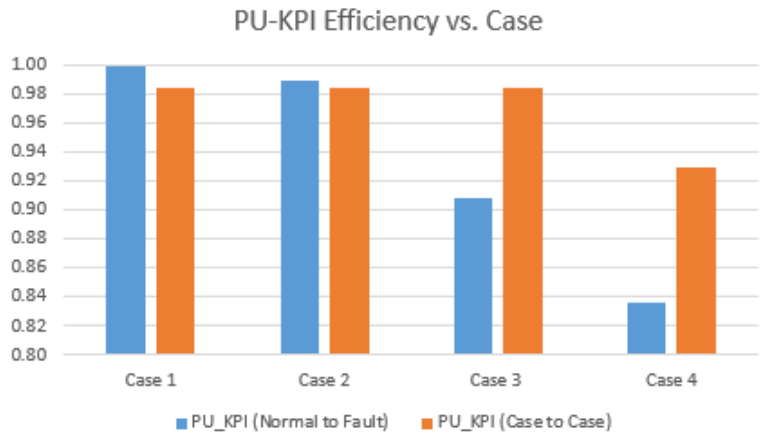

Figure 6-4: PU-KPI Efficiency

The blue graphs of Figure 6-4 shows the relation of efficiencies changes from normal operation to operation under fault. The highest value 1, indicates that no efficiency change has occurred. Case 4, which has the least value, demonstrates that the system has undergone a large drop in efficiency from normal operation to operation under fault. This is useful measurement as it can help system designers understand power losses in the system and capabilities of the system under different modes of operations. In addition it provides an understanding of sizing thermal management in order to ensure proper cooling is given during different modes of operation. The orange graphs of Figure 6-4 shows the relations of efficiency deviation from Case 0 to Case j. The higher the value, the closer the specific case study is to the highest preforming system.

6.4.3 **Response Time**

The following section shows the results of the response times of the case studies.

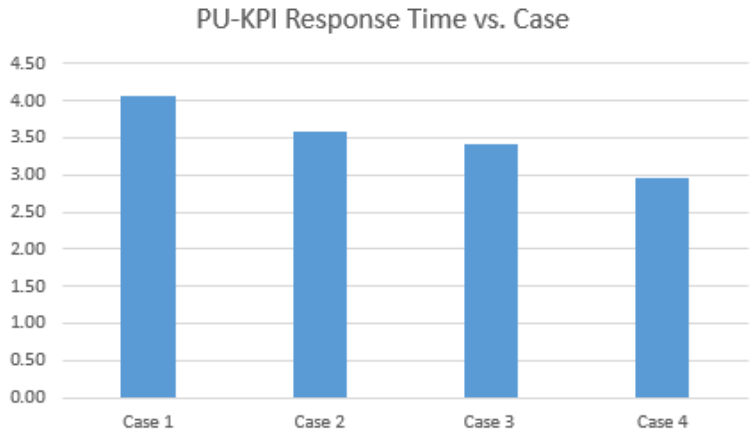

Figure 6-5: PU-KPI Response time

Figure 6-5 depicts the PU-KPI results for the response time for the different case studies. This PU-KPI essentially describes how much quicker/slower the control system for resiliency is verses the grid standard. The quickest case, Case 1 has a response time 4 times faster than the grid requirements of 0.16 seconds. The case studies differ in response time due to the placement and type of switches applied to direct the power flow. This can be seen in Case 4, which has a lot of extra relays and Mosfets (when compared to the rest of the cases).

6.4.4 **THD**

This section shows the THD results for the case studies.

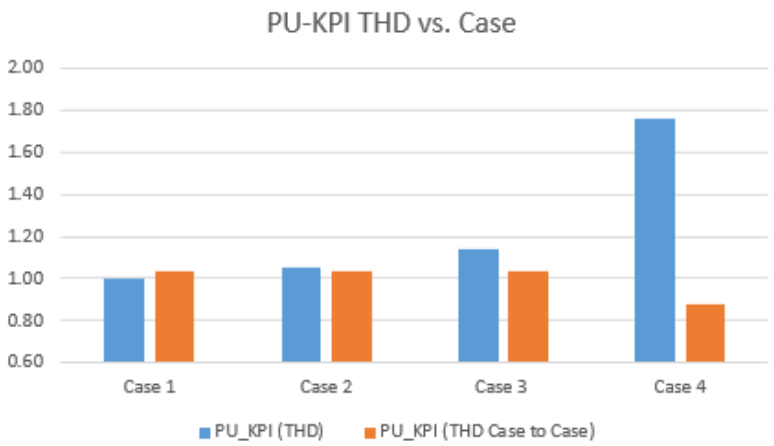

Figure 6-6: PU-KPI THD

Figure 6-6 shows the results for the PU-KPI THD of the systems. The blue graph shows the THD changes from normal operation to operation under fault. A result greater than value, the better the THD of the resiliency scenario. This can be seen by Case 2 and Case 3 in blue graphs of Figure 6-6. A result equal to 1 indicates the system is operating at the same THD (as with Case 1). A result of less than one indicates that the system has a higher THD once the resiliency has been deployed. This PU-KPI designers know how in fact the THD changes depending on mode of operation and plan accordingly. The orange graph of Figure 6-6 shows the relation of the THD of the inverters from Case 0 to Case j. Similar to the efficiency, a designer might wish to know how the THD is being modified by the deployment of the resiliency cases. A result of this PU-KPI greater than 1 indicates that the system has better THD than Case 0.

6.4.5 **Economics**

The final PU-KPI shown is in relation to the economics of the cases.

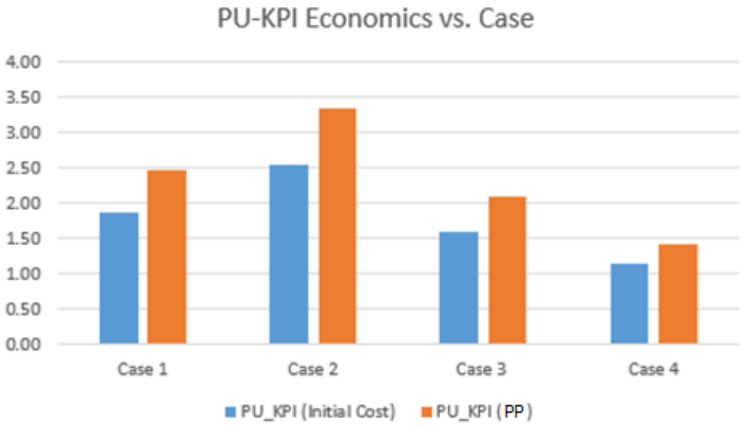

Figure 6-7: PU-KPI Economics

The blue graph of Figure 6-7 above shows the deviation of the initial cost from Case 0 to Case j. The closer the value is to 1, the lower the initial cost of the case study. Reversely, the lower the value on the graph, the higher initial cost of the case study. This helps designers see the deviation in the initial cost.

The orange graph in Figure 6-7 shows the deviation of PP from Case 0 to Case j. The higher the value, the closer to the case 0. This can be seen in Case 2 which had a PP of 11.92 years in relation to case 0 which has a PP of 9.98years. This helps show the relation of how the PP changes from the deployment of resiliency scenarios and its effect on the PP of the systems.

6.5 Governing Equation and Design Choice

Once, all the KPI have been standardised, the final step of the methodology is applied. The governing equation is used in order to identify the best method summarizing the PU-KPI performance characteristics.

PU-KPI	a_j weight	Case 1	Case 2	Case 3	Case 4
$PU\_KPI_{Resnse\ Time}$	1	4.06	3.59	3.43	2.95
$PU\_KPI_{Res\ Power\ Coverage}$	1	1.00	0.25	1.00	1.00
$PU\_KPI_{E\ N\ to\ F}$	1	1.00	0.99	0.91	0.84
$PU\_KPI_{E\ Case\ to\ Case}$	1	0.98	0.98	0.98	0.93
PU_KPI_{THD}	1	1.00	1.05	1.14	1.76
$PU\_KPI_{THD\ Case\ to\ Case}$	1	1.03	1.03	1.04	0.88
$PU\_KPI_{Initial\ Cost}$	3	1.88	2.55	1.59	1.14
PU_KPI_{PP}	4	2.47	3.35	2.09	1.42
	$\sum_{j=1}^{n} a_j * PU\ KPI_j$	13.43	13.79	12.17	10.91

Table 6-3: PU-KPI Summation

Table 6-3 above shows the results of the PU-KPI. In addition the weights are shown. The two values are multiplied by one another and then summed for each case which can be seen on the bottom row.

The Case which best suits the stakeholders request is Case 2: 300W micro-inverter in parallel. This case is the clear choice due to its high performance characteristic (such as excellent efficiency, quick response time and satisfactory coverage amount) and beneficial economics characteristics. It should be noted, that if more power coverage is requested, and a higher emphasis put on that PU-KPI, then Case 1 would have been the best method in order to deploy resiliency as the two final values are very close to one another.

Chapter 7: Applications

In addition for micro-inverter for residential homes, there are other potential applications as well. The following section provides an overview of a couple extra applications for resilient micro-inverters.

7.1 Micro Energy Grid

The Micro Energy Grid (MEG) is a laboratory device used to simulate a variety of real world scenarios. Developed inside of the ESCL lab, the device consists of two main voltage lines: an AC bus line (2kVA, 120Vrms) and a DC bus line (1.5kW, 48VDC). DC programmable sources is the main supply for the DC line, simulating wind, solar, and other DC generation sources. On the same line, the programmable DC loads exists which can be programmed to output certain power consumption patterns. Similar to the DC side, the AC side contains both programmable AC sources and loads. Connection between the two buses lines are done through and 1.5kW inverter and a 1.5kW rectifier. This allows for the full hardware simulation of a complete AC and DC system with variable sources, loads and means to exchange power between lines.

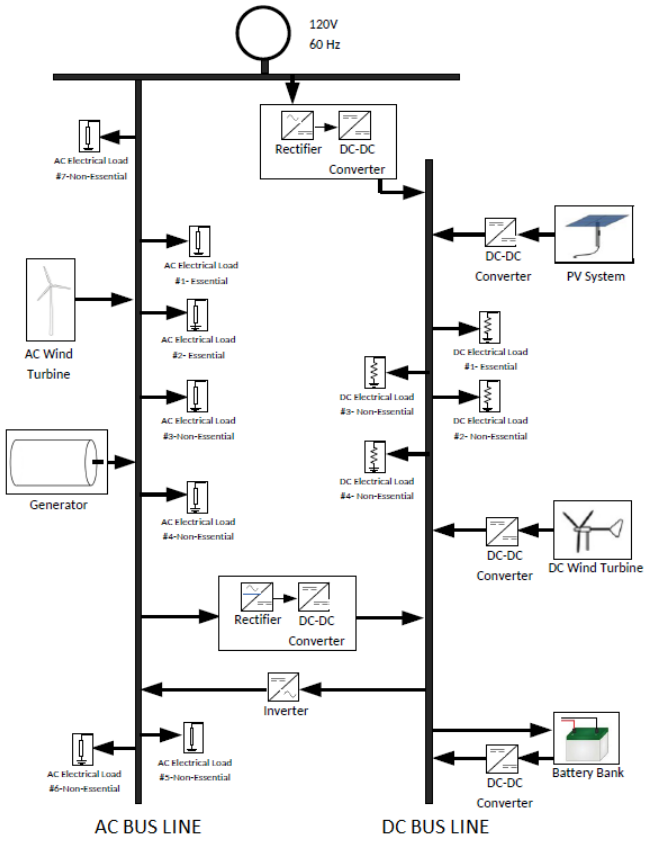

Figure 7-1: MEG

The Figure 7-1 above shows the MEGSM schematic. The inverter system is a 1.5kW synchronized inverter in order to transfer the power from the DC bus to the AC bus. This inverter can be replaced with the 1.2kW system (with a few minor modifications) described with the resiliency methods deployed. This can firstly be used to provide the hardware proof of concept from the thesis. But after, the resiliency scenarios could also be used as a part of the tool in order to maintain power output between lines.

7.2 Solar Panel Windows

A novel application to the resiliency micro-inverter system is for solar panel windows to be deployed to large buildings. New advances in solar panels are bringing new technologies forth. One of the most promising technologies is the thin-film and transparent solar cells which can be directly printed onto glass or silicon. These new cells, provides a semi-transparent coating and can be easily integrated onto building windows.

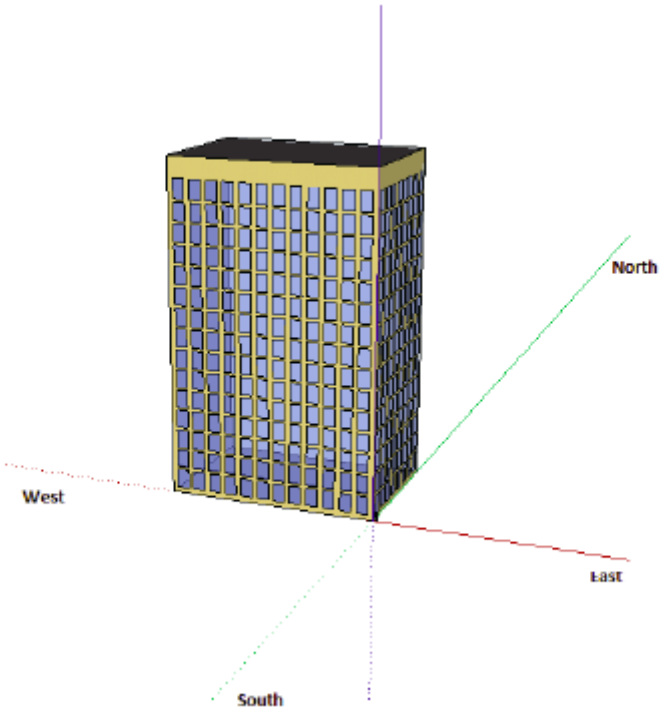

Figure 7-2: Building in Toronto

Figure 7-2 above shows an apartment in Toronto with a southern facing wall. This building, could be one of many in cities around the world which could deploy the solar windows to its structure. Thereby turning the southern facing side of the building into a distributed renewable power source. There are a few companies actively doing research and bring these technology to market. Sharp is one of them, which

produces transparent film with an 8.5% efficiency [61]. Sharp utilize silicon based cells, however they are 1/100 the size of the normal ones and transparent [61]. Another company and one of the most promising is coming out from Oxford PV in the UK. This technology utilises semi-transparent perovskite technology and has had recent significant increases in efficiency from 4% in 2010 to 20.1% in 2014 [62].

With each window, now consider a solar panel, each can be connected to its own independent micro-inverter turning the whole building in a inverter based system utilising the resiliency measures proposed in this thesis to ensure performance. The applications for resilient micro-inverter systems are not limited to the ones described above, and can find applications in a wide variety of different fields as well. Such examples in electric vehicles, airplanes and telecommunications.

Chapter 8: Conclusions and Future Work

8.1 Motivation

There is growing demand for clean and renewable energy systems as a result of the growing implications of climate change. Photovoltaics provide an excellent means to help generate energy with no operating emissions. However, there are issues faced by the photovoltaics industry of unreliable and low product life spans in the system. This is mainly attribute to inverters failing when deployed to the field. These issues have the possibility to hinder the future growth of the industry. The aim of this research was therefore to design a micro-inverter system with improved resiliency strategies. This system is meant for PV integration within buildings.

8.2 Summary and Conclusions

In this thesis, the practicalities of increasing the resiliency are shown along with their analysis. A detailed literature survey was conducted to summarize the state of the art and identify problems and gaps within the field. After this had been completed, the thesis was broken into the inverter phase and the resiliency phase.

The Inverter phase of the research work started with the design of a 300W micro-inverter using the iterative methodology described in sub-section 3.2.1. Following the design of a 300W micro-inverter, a 600W inverter was designed following the same methodology. All inverters were modeled using readily available components in the marketplace. In addition, the internal resistances of the components were added. At the end of each model, a few KPI were used to evaluate the inverters in order to ensure that the components were not stressed and design had met the requirements. Upon successful completion of both inverter designs, a performance analysis was done analysing KPI.

The Resiliency phase of the thesis consisted of improving the resiliency of a micro-inverter system. First, a state of the art was done. Data was collected in order to provide a standard micro-inverter system platform to improve upon. This system was chosen to be a 1.2kW system located in Toronto, Ontario. Next, a method to evaluate residential micro-inverter systems against each other was desired. However, no current methods were found and a novel method was created based on PU-KPI performance criteria. Next, a resiliency controller was designed which could easily be deployed across each case study and easily implemented into hardware. The next portion consisted of designing and creating the case studies. Each resiliency case study was designed using the design methodology shown in 3.2.2. The case studies were designed, built and then simulated in PSIM. Upon completion of the specific case study, the results were given a preliminary KPI analysis ensuring engineering requirements had been met. The final step consisted of a full in-depth analysis based on the PU-KPI evaluation method proposed. From applying the proposed system evaluation

method, it was found that Case 2: Extra Micro-Inverter in Parallel was the best system. This was because this system provided adequate coverage, has high performance and was the most economical to deploy.

8.3 Innovative Contributions for the Thesis Work

The aim of this research work was to make advancements of the resiliency of micro-inverter systems for PV grid connected applications. In order to determine which method was the most applicable, different case studies were simulated and analysed. The main contributions of the thesis are summarized as follows:

8.3.1 **Literature Review**

(1) A literature review was conducted to study the history, market, and state of the art.

8.3.2 **Inverter Design**

(1) A 300W micro-inverter was designed and tested in software. This was designed with components readily available in the marketplace and from reputable manufactures. The designed micro-inverter exhibits good performance characteristics such as high efficiency and low THD.

(2) A 600W inverter was designed and tested in software also with readily available components. The designed inverter exhibits good performance characteristics comparable to marketplace inverters of similar output wattage and a very low THD.

(3) A novel type of inverter was designed which can modify its internal components in order to output at two different power levels 300W to 600W. This was coined the Dual Mode Inverter.

8.3.3 **Micro-Inverter System**

(1) A novel method for evaluating micro-inverters systems as a whole based was created. This was based off of PU-KPI characteristic. This method can help designers and manufacturers alike as it can help demonstrate which system design is best suited for certain applications.

(2) A simple, easy to deploy control system was developed for resiliency purposes. This control system can easily be incorporated into most commercially available micro-inverter which already utilise micro-controllers. The code is simple, does not take a lot of lines of code, and does not need to include extra libraries which cuts down on memory use, processing speed and power consumption.

(3) Four different case studies were proposed in order to increase the resiliency of a residential micro-system. The developed case studies have successfully been tested to micro-inverter systems under different conditions and each shows promising results.

(4) Finally, the resiliency method best suited for PV grid connection applications was found. This helps provide a cost effective solution for increasing the resiliency of a micro-inverter system. In addition this helps manufactures add additional sales, increasing their profitability. In addition, this helps grid operators by having a more constant and steady supply or power from renewable energy sources.

8.4 Future Work

In the framework of future design, we propose the following tasks:

8.4.1 **Experimental Design within MEG**

In this research work, software models for the inverter were designed in Chapter 4 and micro-inverter systems in Chapter 5. These were simulated in PSIM in order to provide results. This was the only option due to time and budget constraints. Therefore, present research work lacks the experimental results. Further investigation is needed in order to develop the hardware circuit design and provide a physical proof of concept.

8.4.2 **Reliability improvements to micro-inverter**

This thesis mentions current reliability issues being faced by the industry in Chapter 1 and 4. The main culprit being the DC link capacitor, which can be swapped out for thin film capacitors. Future work can include improving the reliability of the micro-inverter, minimizing the DC-Link capacitor, utilising high reliability switches, and new novel methods to improve the reliability in cost effective ways.

8.4.3 **KPI Improvements**

This thesis presented models for the micro-inverter and a micro-inverter system. Improvements and further refinement of the designs can be explored in order to improve upon certain KPI. For example, trying to further improve the efficiency of the inverter through soft switching circuits, or lower internal resistance Mosfets can be achieved. The reduction of response time by utilizing fast recovery semiconductors is another aspect with can be explored further. Increasing the resiliency methods, or reducing the resiliency costs are all viable improvements which can be explored further in the future.

Bibliography

[1] International Energy Angency , "Technology Roadmap: Solar Photovoltaic Energy - 2014 edition," 1 September 2014. [Online]. Available: https://www.iea.org/publications/freepublications/publication/technology-roadmap-solar-photovoltaic-energy---2014-edition.html. [Accessed 30 September 2015].

[2] National Resources Canada, "Improving Energy Performance in Canada – Report to Parliament Under the Energy Efficiency Act," 1 December 2014. [Online]. Available: http://oee.nrcan.gc.ca/publications/statistics/parliament10-11/chapter5.cfm?attr=0. [Accessed 12 March 2015].

[3] The Government of Ontatio Ministry of Energy, "Ontario's Long Term Energy Plan," The Government of Ontatio Ministry of Energy, 7 July 2013. [Online]. Available: http://www.energy.gov.on.ca/en/ltep/. [Accessed 10 July 2015].

[4] Government of Canada, "National Resources Canada: Photovoltaic Technology Status and Prospects: Canadian Annual Report 2014," 1 Janruary 2015. [Online]. Available: http://www.nrcan.gc.ca/energy/publications/sciences-technology/renewable/solar-photovoltaic/16384. [Accessed 30 Sepetember 2015].

[5] National Renewable Energy Laboratory, "A Review of PV Inverter Technology Cost and Performance Projections," US. Department of Energy, Battelle, 2006.

[6] Sandia National Laboratories, "Utility-Scale Grid Tied PV Inverter Reliability Workshop Summary Report," U.S. Department of Commerce, Springfield, 2011.

[7] N. Mohan, T. Undeland and W. Robbins, Power Electronics, Converters, Applications and Design, New Jersey: Joh Wiley & Sons, 2003.

[8] E. Owen, "History [origin of the inverter]," *IEEE Industry Applications Magazine,* pp. 64-66, 1996.

[9] M. Rashid, Power Electronics Handbook, Oxford: Elsevier Inc. , 2001.

[10] S. Kjaer and J. B. F. Pedersen, "A Review of Single-Phase Grid Connected Inverters for Photovoltaic Modules," *IEEE Transactions on Industry Applicationcs,* vol. 41, no. 5, pp. 1292- 1306, 2005.

[11] IEEE, "Standard for Interconnecting Distributed Resources with Electric Power Systems," IEEE, Piscataway, 2003.

[12] S. Ayob, Z. Salam, A. Azli and M. Elbuluk, "Control of A Single Phase Inverter Using Fuzzy Logic," in *Industry Application Society Annual Meeting*, Houston , 2009.

[13] R. Bhatnagar, M. Anwer and A. Arora, "Modeling of PWM Inverter for Harmonic Reduction under various load conditions using Fuzzy Controller," *International Journal of Computer Applications,* vol. 55, no. 8, pp. 990-996, 2012.

[14] C. Cheng, "Design of Output Filter for Inverters using Fuzzy Logic," *Expert Systems with Applications,* vol. 38, no. 7, pp. 8639-8647, 2011.

[15] M. Sivagmasundari and P. Melba Mary, "Sinusoidal PWM Based Cascaded H-Bridge Five Level Inverter Using Fuzzy Logic Controller," *Journal of Applied Sciences,* vol. 14, no. 24, pp. 3486-3492, 2014.

[16] Y. Lai, J. Wang, Z. Lin, M. Wang and S. Tien, "Internet-Based Monitoring and Control of Fuzzy-Controlled Inverter System," in *Industrial Electronics Society*, Sevilla, 2002.

[17] B.-R. Lin and C. Hua, "Buck/Boost Converter Control With Fuzzy Logic Approach," in *International Conference on Industrial Electronics, Control, and Instrumentation*, Maui, 1993.

[18] R. Ahuja and R. Kumar, "Desing and Simulation of Fuzzy Logic Controller based Switch-Mode Power Supply," *International Journal of Electrical Engineering,* vol. 2, no. 5, pp. 16-21, 2014.

[19] A. Abubakkar Siddik and M. Shangeetha, "Implementation of Fuzzy Logic controller in Photovoltaic Power generation using Boost Converter and Boost Inverter," *International Journal of Power Electronics and Drive Systems,* vol. 2, no. 3, pp. 249-256, 2012.

[20] S. Singh and K. Nair, "Intelligent Controller for Reduction of Total Harmonics in Single Phase Inverters," *American Journal of Applied Science,* vol. 10, no. 11, pp. 1378-1385, 2013.

[21] Floyd, Electronic Devices: Conventionals Current Version, Upper Saddle River: Prentice Hall, 2007.

[22] Floyd, Principles of Electric Circuit: Conventional Current Version, Upper Saddle River: Prentice Hall, 2006.

[23] A. Nambodiri and H. Wani, "Unipolar and Biopolar PWM Inverters," *International Journal for Innovative Research in Science and Technology,* vol. 1, no. 7, pp. 237-243, 2014.

[24] J. Baskaran, S. Thamizharasan and R. Rajtilak, "GA Based Optimization and Critical Evaluation SHE Methods for Three-level Inverter," *International Journal of Soft Computing and Engineering,* vol. 2, no. 3, pp. 321-326, 2012.

[25] L. Bo, X. Guo-Chun and W. Lu, "Comparison of performance between bipolar and unipolar double-frequency sinusoidal pulse width modulation in a digitally controlled H-bridge inverter system," *Chinese Physics B,* vol. 22, no. 6, pp. 1-8, 2013.

[26] X. Guo, W. Wu and H. Gu, "Phase lock loop and synchronization methods for grid interfaced converters: a review," *Przeglad Elektrotechniczny,* vol. 87, no. 4, pp. 182-188, 2011.

[27] V. Kroupa, Phase Lock Loops and Frequency Synthesis, Toronto : Wiley, 2003.

[28] O. Carranza, C. Trujillo, R. Ortega and J. Rodrigueze, "Synchronizationto the grid using linear kalman filter applied to single phase inverters," in *Calidad de la Energia Electrica*, Medellin, 2013.

[29] T. Brasil, "Comparative study of single-phase PLLs and fuzzy based synrchronism algorithm," in *IEEE Industrial Electronics*, Istanbul, 2014.

[30] T. Thacker, R. Wang, D. Dong, R. W. Burgos and D. Boroyevich, "Phase-Locked Loops using State Variable Feedback for Single-Phase Converter Systems," in *Applied Power Electronics Conference and Exposition*, Washington, 2009.

[31] N. Guerrero-Rodriguez, A. Rey-Boue, A. Rigas and V. Kleftakis, "Review of Synchronization Algorithms used in Grid-Connected Renewable Agents," in *International Conference on Renewable Energies and Power Quality*, Cordoba , 2014.

[32] M. Karimi-Ghartemani, "A Unifying Approach to Single-Phase Synchronous Reference Frame PLLs," *IEEE Transaction on Power Electronics,* vol. 28, no. 10, pp. 4550 - 4556 , 2012.

[33] M. Antchev, I. Pandiev, M. Petkova, E. Stoimenov, A. Tomova and H. Antchev, "PLL For Single Phase Grid Connected Inverters," *International Journal of Electrical Engineering and Technology,* vol. 4, no. 5, pp. 56-77, 2013.

[34] A. Tomova, M. Petkova, M. Antchev and H. Antchev, "Computer investigation of a sine and cosine based phased-locked loop for single phase grid connected inverter," *International Journal of Engineering Research and Applications,* pp. 726-728, 2013.

[35] J. Duffie and W. Beckman, Solar Engineering of Thermal Processes, Hoboken: John Wiley and Sons Inc., 2006.

[36] IESO, "microFit," IESO, 1 September 2015. [Online]. Available: http://microfit.powerauthority.on.ca/types-renewable-technology-types. [Accessed 1 September 2015].

[37] E. Hollnagel and C. Nemeth, Resilience Engineering Perspectives, Volume 2: Preparation and Restoration, Boca Raton: CRC Press, 2009.

[38] Eclipsall Energy Group , "Products," Eclipsall Energy Group , 5 Janruary 2015. [Online]. Available: http://www.eclipsall.com/. [Accessed 5 Janruary 2015].

[39] R. Muhammad, Power Electronics Handbook, San Diego: Elseviser, 2007.

[40] M. Salcone and J. Bond, "Selecting film bus link capacitors for high performance inverter applications," in *Electric Machine and Drives Conference*, Miami, 2009.

[41] L. Zhang, X. Ruan and X. Ren, "Second-Harmonic Current Reduction and Dynamic Performance Improvement in the Two-Stage inverters: An Output Impedance Perspective," *IEEE Transactions on Industrial Electronics,* vol. 62, no. 1, pp. 394- 404, 2015.

[42] G. Ruan and L. W. X. Zhang, "On the Reduction of Second Harmonic Current and Improvement of Dynamic Response for Two-Stage Single-Phase Inverters," *IEEE Transactions on Power Electronics,* vol. 30, no. 2, pp. 1028-1041, 2015.

[43] R. Chen, Y. Liu and F. Peng, "DC Capacitor-Less Inverter for Single-Phase Power Conversion With Minimum Voltage and Current Stress," *IEEE Transactions Power Electronics,* vol. 30, no. 10, pp. 5499-5507, 2014.

[44] F. Schimpf and L. Norum, "Effective use of film capacitors in single-phase PV-inverters by active power decoupling," in *Annual Conference on IEEE Electronics Society*, Glendale, 2010.

[45] H. Jong, G. Kim and K. Lee, "Second-order Harmonic Reduction Technique for Photovoltaic Power Conditioning Systems Using a PR Controller," *Energies,* vol. 6, no. 1, pp. 79-96, 2013.

[46] E. Jung and S. Sul, "Implementation of grid-connected single phase inverter based on fpga," in *Applied Power Electronics Conference and Exposition*, Washington, 2009.

[47] K. Ogata, Modern Control Engineering, Upper Saddle River: Prentice Hall, 2010.

[48] H. Cha and T. Vu, "Comparative Analysis of Low-Pass Output Filter for Single-phase Grid-connected Photovoltaic Inverter," in *Applied Power Electronics Conference and Exposition (APEC)*, Palm Springs, 2010.

[49] Y. Lang, D. Xu, S. Hadianamrei and H. Ma, "A Novel Method of LCL Type Utility Interfance for Three-Phase Voltage Source Rectifier," in *Power Electronic Specialists Conference*, Recife, 2005.

[50] W. Wu, M. Huang and F. Blaabjerg, "Efficiency comparison between the LLCL-and LCL filters based single phase grid tied inverters," *Archives of Electrical Engineering,* vol. 63, no. 1, pp. 63-79, 2014.

[51] M. Eltawil and Z. Zhao, "MPPT Techniques for Photovoltaic Applications," *Renewable and Sustainable Energy Reviews,* vol. 25, no. 1, pp. 793-813, 2013.

[52] M. Gomes de Brito, L. Galotto, L. Sampaio, G. Azevedo e Melo and C. Cansin, "Evaluation of the Main MPPT Techniques for Photovoltaic Applications," *IEEE Transactions on Industrial Electronics,* vol. 60, no. 3, pp. 1156-1167, 2013.

[53] S. Beydaghi, B. Vahidi, Y. Ankouti, G. Babmalek and G. Gharenpetian, "Simulation of Improved Perturb and Observe MPPT Using SEPIC Converter," *Science International,* vol. 27, no. 3, p. 186901873, 2015.

[54] A. Dolara, R. Faranda and S. Leva, "Energy Comparison of Seven MPPT techniques for PV Systems," *Journal of Electromagnetic Analysis and Applications,* vol. 1, no. 3, pp. 152-162, 2009.

[55] Digikey, "Parts," Digikey, 20 September 2015. [Online]. Available: http://www.digikey.ca/. [Accessed 20 Spetember 2015].

[56] Mouser Electronics, "Parts," Mouser Electronics, 20 September 2015. [Online]. Available: http://ca.mouser.com/. [Accessed 20 September 2015].

[57] Solar Energy Industries Association, "Solar Photovoltaic Technology," Solar Energy Industries Association, 1 November 2015. [Online]. Available: http://www.seia.org/research-resources/solar-photovoltaic-technology. [Accessed 1 November 2015].

[58] S. White, "Is this solar-power program a money-saver?," The Globe and Mail, 30 November 2011. [Online]. Available: http://www.theglobeandmail.com/globe-investor/personal-finance/household-finances/is-this-solar-power-program-a-money-saver/article4180338/. [Accessed 2 November 2015].

[59] Enphase Energy, "Installation and Operations Manual," Enphase, Petaluma, 2015.

[60] Siemens, "Siemens Micro-Inverter System: Selection and application guide," Siemens, Oakville, 2011.

[61] Sharp, "Thin-film PV," Sharp, 10 August 2014. [Online]. Available: http://www.sharpusa.com/SolarElectricity.aspx. [Accessed 30 June 2014].

[62] Oxford PV, "http://www.oxfordpv.com/Technology," Oxford PV, 1 December 2015. [Online]. Available: http://www.oxfordpv.com/Technology. [Accessed 1 December 2015].